The Dissertation Committee for Chi Hung Tang Certifies that this is the approved version of the following Dissertation:

The Environmental Influences on the Growth and Grazing of Marine Protists

Committee:

Edward J. Buskey, Supervisor

Deana L. Erdner

Zhanfei Liu

Diane K Stoecker

The Environmental Influences on the Growth and Grazing of Marine Protists

by

Chi Hung Tang

Dissertation

Presented to the Faculty of the Graduate School of

The University of Texas at Austin

in Partial Fulfillment

of the Requirements

for the Degree of

Doctor of Philosophy

The University of Texas at Austin

December 2020

Acknowledgements

I am thankful to many people and organizations who provided support for me to finish my dissertation. I thank Dr. Edward Buskey for his supervision on my projects and constructive comments on my dissertation Chapters. My gratitude goes to Cammie Hyatt, Dr. Sarah Cosgrove, Dr. Maud Moison and Tracy Weatherall for their assistance to my experiments in Chapters 3 and 4. I am also grateful for the opinions by Dr. Diane Stoecker that inspired me to improve the experimental design of the project in Chapter 2. I am thankful to Dr. Deana Erdner and Dr. Paul Zimba who provided access to their laboratories and use of their equipment. I thank for the comments from all the dissertation committee members that helped improved this dissertation. Last but not least, I thank my families who provided unlimited support for me to pursue my research interest and career.

These projects are funded by the DROPPS consortium of the Gulf of Mexico Research Initiative. I am also thankful for the financial support provided by the Graduate School Summer Fellowship of The University of Texas at Austin and the E.J. Lund Founder Fellowship for Graduate Students of Exceptional Merit of the Department of Marine Science of The University of Texas at Austin.

Abstract

The Environmental Influences on the Growth and Grazing of Marine Protists

Chi Hung Tang, Ph.D.

The University of Texas at Austin, 2020

Supervisor: Edward J. Buskey

Marine protists are important components at the base of the marine food web. The growth and grazing of protistan organisms in response to the toxicity of petroleum hydrocarbons and elevated seawater temperature at the community and species levels were investigated. In exposure to 10 μL L^{-1} of chemically dispersed crude oil in the mesocosms, the grazing impacts of microzooplankton (20-200 μm) on phytoplankton were reduced. While the microzooplankton grazing accounted for ~50% of the phytoplankton' population growth in the control treatment, there was a de-coupling between these two parameters in the oil-loaded treatment. The de-coupling could potentially lead to algal blooms in the natural environment under certain conditions. In contrast, in exposure to chemically dispersed crude oil in the microcosms, the grazing impacts of nanoplankton (2-20 μm) on bacteria did not differ among the treatments of control and low (2 μL L^{-1}) and high (8 μL L^{-1}) concentrations. The tight couplings between the nanoplankton grazing and bacterial population growth in the control and oil-loaded treatments could have kept the abundance of bacterial cells steady. The community compositions of bacteria in the low and high dose crude oil treatments

became increasing similar and different from those in the control treatment. It is believed to be related to the availability of carbon and inorganic nutrients. The relatively high abundance of hydrocarbon-degrading bacteria *Cycloclasticus and Alcanivorax* in the oil-loaded treatments indicated the presence of biodegradation. Exposure experiments were conducted to investigate the responses of marine protistan species to the toxicity of soluble petroleum hydrocarbon and elevated seawater temperature. In exposure to increasing concentrations of the water accommodated fraction (WAF) of crude oil, the heterotrophic dinoflagellates *Oxyrrhis marina* and *Protoperidinium* sp. and ciliates *Euplotes* sp. and *Metacylis* sp. showed species- specific vulnerabilities to oil toxicity, as reflected by their specific growth rates. When compared to the control treatment, their population grazing impacts and *per capita* ingestion rates were reduced with exposure to the WAF of crude oil alone and the mixture of crude oil and dispersant at the same concentration. In exposure to elevated seawater temperature, the Florida strain of mixotrophic dinoflagellate *Fragilidium subglobosum* obtained a specific growth rate of ~0.3 d^{-1} at both 19°C and 23°C in mono-specific culture but zero or negative growth rates in cultures with added prey dinoflagellate *Tripos tripos*. *F. subglobosum* grown at 19°C showed higher maximum photosynthetic efficiency than at 23°C but did not differ in cellular chlorophyll-*a* content or cell size. This strain of *F. subglobosum* is believed to be non-mixotrophic and therefore the hypothesis that this dinoflagellate species becomes more heterotrophic at elevated temperature was not proved or disapproved.

Table of Contents

List of Tables

List of Figures

Chapter 1: General Introduction

MARINE PROTISTS AND THEIR TROPHIC ROLES IN MARINE ECOSYSTEMS

Marine protists, the unicellular eukaryotes

Marine protists are unicellular eukaryotes that include ciliates, flagellates, diatoms, amoeba, foraminifera, and fungi. They can be categorized based on their modes of nutrition. Photoautotrophic protists are generally referred to as phytoplankton as they are capable of photosynthesis. Chemoorganotrophic protists (i.e. protozoa) are essentially heterotrophs that consume bacteria, algae, smaller zooplankton or particulate organic matters. Mixotrophic protists are believed to be capable of exploiting both the nutrition modes. Marine protists can also be categorized by size ranges: Pico- and nano-sized protists fall within the size ranges of 0.2-2 μm and 2-20 μm, respectively. Micro-sized protists range from 20-200 μm while some protists can be larger than 200 μm (Sieburth *et al.*, 1978).

Predators and prey in marine protists

The interactions of organisms in the planktonic food web is complex. The simple Nutrient-Phytoplankton-Zooplankton (N-P-Z) food chain depicts that nutrient supplies control the abundance of phytoplankton from the bottom-up, while zooplankton consumption keeps phytoplankton population in check from the top-down. Pomeroy (1974) and Azam *et al.* (1983) introduced the importance of microbes and protists in the food chains. They described the consumption of dissolved organic matter from phytoplankton by bacterial cells within the microbial loop of the Bacteria-Flagellates-Microzooplankton food chain. Sherr & Sherr (1988) further incorporated the pivotal role of nanoflagellates and ciliates as grazers of both bacteria and small algae in the microbial loop, and as prey for larger zooplankton.

Calbet (2008) pointed out that the percentage of primary production consumed daily by microzooplankton, composed of mainly heterotrophic dinoflagellates and ciliates, is usually > 60% in habitats including open oceans, coastal regions and estuaries. Comparatively, the relative importance of mesozooplankton (200-2000 μm) herbivory declines with increasing primary production. Microzooplankton are thought to be capable of coupling with the changes in phytoplankton abundance since they have similar growth rate to that of phytoplankton (Strom, 2002; Stoecker *et al.*, 2008; Chen *et al.*, 2009). Meanwhile, micro-sized grazers such as ciliates and dinoflagellates constitute a large component of copepod diets, particularly in less productive systems (Saiz & Calbet, 2011). Calbet & Saiz (2005) showed that the percentage of ciliates in copepods' diet in terms of carbon could be approximately 50% in non-productive systems.

Smaller protists, typically < 20 μm, are known to substantially consume bacterioplankton. Boenigk & Arndt (2002) estimated that heterotrophic nanoflagellates (HNF) generally have a specific clearance rate of 5-10 bacteria protist^{-1} h^{-1} at a food concentration of 10^6 bacteria mL^{-1}. It is argued that HNF could consume 25-100% of the daily production of bacterioplankton (reviewed in Sherr & Sherr, 1994), while ciliates can contribute substantially to the total bacterivory (Sherr & Sherr, 1987). Mixotrophic phytoflagellates are important bacteria grazers as well (Stibor & Sommer, 2003; Unrein *et al.*, 2007; Zubkov & Tarran, 2008). Bacterivory is thought to cause changes in the bacterial abundance and shape their community composition (Jurgens & Matz, 2002). Hahn & Hofle (2001) pointed out that bacterial cells of 0.4-1.6 μm belong to the most grazing-vulnerable group while smaller or larger cells get refuge from predation. Apart from cell size, selective grazing by bacterivorous protists based on prey motility, shape and cell surface characteristics can also structure the bacterial population (Jurgens & Massana, 2008).

Mixotrophy in marine protists

Mixotrophy, the capability of being photosynthetic and phagotrophic within a single organism, can be found in many marine dinoflagellates and ciliates. The ubiquity

of mixotrophs is thought to be because of an evolutionary pressure towards mixotrophy that allows the organisms to adapt to various environmental gradients (Selosse *et al.*, 2017). Given the common occurrence of mixotrophic plankton, suggestions to revise the misused phytoplankton-zooplankton dichotomy were proposed (Flynn *et al.*, 2013). The functional group classification of mixotrophic protists by Mitra *et al.* (2016) defines that phagotrophic protozoan constitutively capable of carbon fixation belong to constitutive mixotrophs (CM) while those can acquire C-fixation capability from phototrophic prey are non-constitutive mixotrophs (NCM). Within the NCM category, C-fixation could be mediated either by symbionts (i.e. endosymbiotic NCM such as green *Noctiluca* sp.) or by the sequestered chloroplasts from prey (i.e. plastidic NCM such as *Dinophysis* sp. and *Mesodinium* sp.).

Many phytoplankton species previously thought to be obligately photosynthetic are now considered heterotrophic or mixotrophic. Gaines & Elbrachter (1987) argued that ~50% of the known 2000 living dinoflagellates species do not contain chloroplasts and thus depend on feeding on particulate food for nutrients. Jeong *et al.* (2005) demonstrated that many bloom-forming dinoflagellates are mixotrophic species. Consumption of prey and intraguild predation on competitors or potential grazers could have contributed to the abundance of heterotrophic or mixotrophic dinoflagellates (Stoecker *et al.*, 2006), particularly in coastal and estuarine waters that experience chronic eutrophication (Burkholder *et al.*, 2008). Flynn *et al.* (2018) argued that, within the annual cycle of marine ecosystems, the plankton community is likely be dominated by mixotrophs when the system becomes mature, even though the traditional phytoplankton-zooplankton structure is still the predominating condition before the transition to the more mature state.

MARINE PROTISTS' RESPONSES TO ENVIRONMENTAL FACTORS

Marine protists in a warmer environment

It is well documented that protists are influenced by various abiotic variables including temperature, irradiance, nutrients, pH, pCO_2, and salinity of the aquatic environments (e.g. Lomas & Glibert, 1999; Dickman *et al.*, 2006; Matsubara *et al.*, 2007; Smith & Hansen, 2007; Beaufort *et al.*, 2011; Edwards *et al.*, 2016). Among these variables, the projected rising sea surface temperature has been one of the major concerns (Alexander *et al.*, 2018; IPCC, 2018). Temperature has been shown to cause changes to protists at both the individual and the community levels. These changes affect the cell size (Atkinson *et al.*, 2003), growth (Raven & Geider, 1988), feeding (Heinze *et al.*, 2013), food digestion (Sherr *et al.*, 1988), community grazing (Franze & Lavrentyve, 2014), community structure (Marinov *et al.*, 2010; Hinder *et al.*, 2012), and functions of the pelagic food webs (Muren *et al.*, 2005).

By extending the metabolic theory of ecology (Brown *et al.*, 2004), which states that there are universal linear relationships between metabolic rates and body size or temperature, Allen *et al.* (2005) extrapolate that, over the temperature range of 0-30°C, there will be a 16-fold increase in rates controlled by respiration due to the temperature dependence of respiratory protein complexes and a 4-fold increase in rates controlled by photosynthesis due to the temperature dependence of chemical reactions in chloroplasts. These predictions imply that heterotrophs must increase their food consumption to meet for the elevated respiratory needs in a warmer environment. Supporting evidence is mounting from studies on heterotrophic ciliate *Tetrahymena pyriformes* feeding on bacterial prey (Fussmann *et al.*, 2017), ciliate *Condylostoma spatiosum* feeding on dinoflagellate (Li *et al.*, 2011), and at the community level of microzooplankton that graze on phytoplankton under the warming conditions (Liu *et al.*, 2019). In the context of plankton mixotrophy, protistan mixotrophs have been shown to become more heterotrophic and ingested more prey items at increased temperatures (Heinze *et al.*, 2013; Wilken *et al.*, 2013; Jeong *et al.*, 2018).

Oil pollution and its effects on marine protists

It is estimated there are > 1.2 million metric tons (~360 million gallons) of crude oil enter the marine environment annually (NRC, 2003). Natural seepage accounts for 47% of the amount and the remaining 53% results from leaks and spills (Kvenvolden & Cooper, 2003). Crude oil contains different proportions of petroleum hydrocarbons, including saturated and unsaturated aliphatic hydrocarbons, aromatic hydrocarbons (monocyclic and polycyclic aromatic hydrocarbons (PAHs)), resins, and asphaltenes. These components can get into marine systems through processes such as dissolution, dispersion, emulsification, and sedimentation (NRC, 2005). Components of low molecular weight are readily evaporated and removed due to their high volatility and fast degradation in water. Compounds with higher molecular weight are more persistent and some of them are soluble in water (NRC, 2005). Dispersants, substances usually used in the remediation of oil spills, help enhance the process of natural dispersion through formation of oil droplets and increase the solubility of crude oil in seawater (Fiocco & Lewis, 1999).

Components of crude oil are toxic to aquatic life. Among the aromatic components of crude oil, benzene hydrocarbons and low-ring PAHs are highly soluble in water and are assumed to be the most toxic fractions that causes mortality or adverse physiological effects to marine protists. These effects include inhibition of growth, and changes in cell size, cellular contents of chlorophyll, protein, and nucleic acid (Karydis & Fogg, 1980; El-Sheekh *et al.*, 2000; Bonnet *et al.*, 2005). Chemically dispersed crude oil is thought to be more toxic than crude oil alone to marine protists (Hook & Osborn, 2012; Jung *et al.*, 2012; Ozhan *et al.*, 2014), and dispersants alone are toxic to aquatic organisms as well (Rogerson & Berger, 1981; George-Ares & Clark, 2000; Cohen *et al.*, 2014). Consequentially, the water accommodated fraction (WAF) of crude oil, a laboratory-prepared medium essentially free of particles of the bulk material (Singer *et al.*, 2000), has been used for toxicity tests of aquatic organisms (Singer *et al.*, 2001; Saco-Alvarez *et al.*, 2008; Forth *et al.*, 2017a) due to its standardized method in preparation of the medium and high comparability of toxicity across studies. On the other hand,

insoluble components of crude oil form particulate droplets when mixed with seawater and dispersants and remain suspended in the water column. Ingestion of oil droplets has been shown in marine protists (Andrews & Floodgate, 1974; Almeda *et al.*, 2014a), which could potentially lead to lethal or sub-lethal effects on aquatic organisms.

Biodegradation of crude oil by prokaryotic microbes

Apart from abiotic weathering, most of the crude oil remaining in the marine environment is removed eventually by microbial degradation. The biodegradation process of crude oil involves chemical transformation of hydrocarbon molecules into simpler products by microorganisms, especially prokaryotic microbes. There are more than 320 genera of Eubacteria and 12 genera of Archaea capable of hydrocarbon metabolism (Prince *et al.*, 2018). Some typical examples of hydrocarbon-degrading bacteria genera include *Alcanivorax*, *Cycloclasticus*, *Pseudomons* and *Marinobacter*. Hydrocarbon-degrading bacteria are thought to exist in most aquatic environments, even in pristine waters that have not been polluted (Margesin *et al.*, 2003). Influxes of hydrocarbons from crude oil spills, leaks or seepages likely increase the relative abundance of these types of bacteria in the environment due to stimulated proliferation. Nutrients (nitrogen, phosphorus, and iron) and oxygen availability are believed to be the most crucial limiting factors for the biodegradation process (Hassanshahian & Cappello, 2013). Biodegradation of saturated hydrocarbons (e.g. alkanes) is quantitatively the most important process in the removal of crude oil due to the large relative quantity of them in crude oil by mass. The biodegradations of PAHs and other less abundant compounds are of importance as well due to their high toxicity. The use of dispersants can enhance the rate of biodegradation since it increases the exposed surface area of crude oil droplets for biological attack (Hassanshahian & Cappello, 2013).

SUMMARY

Marine protists are eukaryotic microbes consisting of producers and consumers at the base of food web. Increased recognition of mixotrophy in marine protists has brought

new insights and complexity to the understanding of the marine ecosystems. Increases in the seawater temperature due to climate change has inspired ecologists to test the prediction that planktonic mixotrophs become more heterotrophic in a warmer environment. Apart from temperature, environmental pollutants such as petroleum hydrocarbons have been shown to cause adverse effects on marine protists from the sub-cellular level to the community level. A large proportion of these hydrocarbon pollutants is eventually metabolized by marine microbes, especially by oil-degrading bacteria. Bacterivory by small protozoa can affect the abundance and community composition of the bacteria and can potentially influence the processes of biodegradation of the hydrocarbon pollutants. This dissertation focuses on the trophic interaction of marine protists in response to environmental factors including increased seawater temperature and influx of petroleum hydrocarbon pollutants.

Chapter 2: Effects of Temperature on the Growth and Grazing of the Mixotrophic Dinoflagellate *Fragilidium subglobosum*

ABSTRACT

Great concern related to climate change and global warming have been the inspiration of marine ecologists to study the ecological implications of elevated seawater temperature in the planktonic food web. Mixotrophic protists play pivotal roles at the base of the food web in a warming environment. Incubation experiments were conducted to test the hypothesis that the mixotrophic dinoflagellate *Fragilidium subglobosum* becomes more heterotrophic at increased temperatures. The cell densities of *F. subglobosum* and its prey *Tripos tripos* in mono-specific and mixed cultures at 19°C and 23°C were monitored for 20 days. The specific growth rate *F. subglobosum* in autotrophic growth did not differ between 19°C and 23°C, with a range between 0.30-0.32 d^{-1}. Contrary to previous reports, the dinoflagellate *F. subglobosum* did not grow well in mixed cultures with potential prey at both temperatures tested. An incubation experiment with a shorter period revealed near zero or negative *per capita* ingestion rate of *T. tripos* by *F. subglobosum* at both temperatures, suggesting the dinoflagellate cultures used may not be mixotrophic. The maximum photosynthetic efficiency (Fv/Fm) of *F. subglobosum* was approximately 0.4 at 19°C for both the mono-specific and mixed cultures. These ratios were significantly higher than those at 23°C. With the observation that the *F. subglobosum* cultures used may not be mixotrophic, the hypothesis that this mixotroph species becomes more heterotrophic at elevated temperature was not proved or disapproved.

INTRODUCTION

Climate change has been an important issue globally and sea surface temperatures are projected to keep rising (Alexander *et al.*, 2018). Ecological models predict a greater increase in rates of consumption by heterotrophs than synthesis of cellular organic carbon

by autotrophs in various organisms over a certain increase in temperature range (Allen *et al.*, 2005). In the perspective of predator-prey interactions, this prediction implies strengthened consumer control on primary production with rising temperature, which is evident in studies on planktonic organisms (O'Connor *et al.*, 2009; Yang *et al.*, 2016; Liu *et al.*, 2019). Mixotrophy in plankton, a combination of autotrophic and heterotrophic nutrition modes within an organism, is now recognized as a norm rather than an exception in aquatic ecosystems for protists (Stoecker *et al.*, 1989; Jacobson & Anderson, 1996; Jeong *et al.*, 2005). The incorporation of planktonic mixotrophs into the food chain is thought to increase the trophic transfer efficiency and enhance the sequestration of oceanic carbon (Ward & Follows, 2016; Stoecker *et al.*, 2017). Mixotrophs being both primary producers and consumers simultaneously leads to changes in their ecological functions in aquatic food webs in warmer environments that have just started to be discovered. For instance, in cultures of the freshwater mixotrophic chrysophyte *Dinobryan sociale*, Princiotta *et al.* (2016) found increases in photosynthesis and bacteria ingestion rates with increasing temperatures from 8-16°C. By comparing the difference in the activation energy of the metabolic processes associated with the growth and grazing as a function of temperature, Wilken *et al.* (2013) concluded that the mixotrophic chrysophyte *Ochromonas* sp. shifted the balance between phototrophy and phagotrophy towards the latter with increased temperatures.

Protistan mixotrophs are thought to be favored in mature ecosystems over other protistan groups (Flynn *et al.*, 2018) and many harmful algae species that form blooms in eutrophic waters are thought to be mixotrophs (Stoecker *et al.*, 2006; Burkholder *et al.*, 2008). Phagotrophic phytoplankton could have higher growth rates than those growing autotrophically in nutrient-rich habitats. They are therefore also potential consumers of primary production. Particularly, mixotrophic flagellates were shown to be substantial grazers of bacteria and other protists in both field and laboratory studies (Safi & Hall, 1999; Zubkov & Tarran, 2008; Glibert *et al.*, 2009; Hansen, 2011). Given their widespread prevalence and ecological significance, there is a greater need to understand

the balance between autotrophy and heterotrophy within planktonic mixotrophs in response to increased temperature.

Fragilidium subglobosum, a facultative mixotrophic dinoflagellate species previously thought to be an obligate phototroph, has been shown to feed exclusively on marine *Tripos* spp. (previously known as *Ceratium* spp., later proposed to be named under the genus name *Tripos* Gomez (2013)) by engulfment (Skovgaard, 1996a). *F. subglobosum* could therefore be a biological control of the *Tripos* spp. that form blooms in various regions of the oceans (Nielson, 1991; Carstensen *et al*., 2004; Pitcher & Probyn, 2011). Being a constitutive mixotroph, *F. subglobosum* is thought to be able to form bloom and increase the cumulative C-fixation in computer simulations (Mitra *et al*., 2016). Previous studies showed that heterotrophic activity of *F. subglobosum* was affected by light intensity, prey species and prey concentration (Hansen & Nielsen, 1997; Skovgaard *et al.*, 2000). However, the effect of rising seawater temperatures on the phagotrophy of *F. subglobosum* and their contribution to the trophic transfer of carbon has not been studied. In this study, we conducted incubation experiments to examine the changes in the autotrophy and heterotrophy of *F. subglobosum* at increased temperatures, with the goal of understanding the general ecological roles of planktonic mixotrophs in a warmer environment.

METHODOLOGY

Preparation and maintenance of dinoflagellate cultures

A culture of the dinoflagellate *Fragilidium subglobosum* (CCMP-3029) was obtained from National Center for Marin Algae and Microbiota (NCMA) at Bigelow Laboratory for Ocean Sciences. It was isolated from the seawater near Florida (U.S.A.) in 2005 and reported to have a temperature range between 18-24°C. *Tripos tripos* cultures were initiated from cells obtained from local waters (Port Aransas, Texas) by isolating single cells in droplets of autoclaved 0.2 µm filtered seawater (AFSW) that were rinsed several times. The two dinoflagellate species were maintained in AFSW (28-32 PSU)

with modified F/2-Si enrichment (Guillard, 1975) and unilateral illumination at ~60 µE m^{-2} s^{-1} (measured with LICOR LI250 light meter) with a light:dark cycle of 12:12 in incubator conditioned at 20±1°C until experiments. The light intensity was chosen based on previous study that *F. subglobosum* showed a highest ingestion rate on *T. lineatum* at approximately 60 µE m^{-2} s^{-1} (Skovgaard, 1996b).

Physiological temperature range of autotrophic growth

To determine the autotrophic growth rate of *F. subglobosum* at various temperatures, cultures of the dinoflagellate originally maintained at 20°C were acclimated for 4-5 days separately at temperatures of 18°C, 20°C, 22°C, 24°C, and 27°C with the same light regime (~60 µE m^{-2} s^{-1}) before incubation experiments. Cultures acclimated to the temperatures were separately incubated in 72 mL tissue-culture flasks in triplicate. At different time points, subsamples (2mL) from each flask were collected and preserved with acidic Lugol's solution (~2% final concentration) for microscopic cell enumeration (Olympus BX60). Specific growth rate (SGR) was determined for the exponential growth phase of cultures as:

$$\mathrm{SGR} = \ln\left(\frac{N_t}{N_0}\right)/t \qquad \text{Eqn 2.1}$$

where N_t is the cell density at time t, N_0 is the initial cell density at the previous time point, and t is the time duration of the incubation in days.

Growth and ingestion at different temperatures

Population dynamics in mono-specific and mixed cultures

Mono-specific stock cultures of *F. subglobosum* and *T. tripos* in F/2-Si enriched AFSW were acclimated at temperatures of 19±1°C and 23±1°C separately for ≥ 7 days at a light intensity of ~60 µE m^{-2} s^{-1} with a 12:12 light:dark cycle. These two temperatures were chosen based on the results from the physiological temperature range of *F. subglobosum* during autotrophic growth (Fig. 2.1). Within this temperature range of 19-

23°C, *F. subglobosum* was shown to have an increasing growth rate with increasing temperature. The light intensity was chosen based on a study of *F. subglobosum* which showed the highest *per capita* ingestion rate of prey occurred at this light intensity (Skovgaard, 1996b). Triplicates of mono-specific and mixed cultures of *F. subglobosum* and *T. tripos* were prepared with fresh enriched medium in 72 mL tissue-culture flasks with the initial cell densities of *F. subglobosum* and *T. tripos* of 0-1 cells mL^{-1} and 35-46 cells mL^{-1} (*F. subglobosum:T. tripos* ratio at ~1:110), respectively, and incubated at the corresponding temperatures. The incubation experiment lasted for 20 days and sampling was conducted every other day. During sampling, duplicate 2 mL subsamples from each flask were taken, preserved with acidic Lugol's solution (~2% final concentration), and enumerated under the microscope. Meanwhile, fresh enriched medium acclimated at the corresponding temperatures were added into the flasks to replenish the withdrawn volume (totally 4 mL each sampling). The determination of cell densities of the dinoflagellates was adjusted to account for the dilution effect from the added fresh medium. The SGRs of *F. subglobosum* and *T. tripos* in the different treatments (i.e. 19Mono: mono-specific culture at 19°C; 19Mixed: mixed culture at 19°C; 23Mono: mono-specific culture at 23°C; and 23Mixed: mixed culture at 23°C) were determined for the exponential growth phase of cultures according to Eqn 2.1.

Per capita ingestion rate

In a 6-day experiment, another set of mono-specific and mixed cultures of *F. subglobosum* and *T. tripos* were prepared in triplicate in 72 mL tissue-culture flasks using the temperature-acclimated stock cultures. Given the observation that *F. subglobosum* in mixed cultures tend to decrease in cell density, the initial cell density of *F. subglobosum* was increased to ~7 cells mL^{-1} and the ratio of *F. subglobosum:T. tripos* was increased to approximately 1:5. On days 0 and 3, triplicate subsamples from each flask were collected, preserved with acidic Lugol's solution (~2% final concentration), and enumerated under the microscope. Again, the SGRs of *F. subglobosum* and *T. tripos* at the different treatments were determined according to Eqn 2.1 assuming the cultures were in

exponential growth phase. The ingestion rate (IR) of *F. subglobosum* in the mixed cultures at the corresponding temperature was also determined according to Frost (1972) and Heinbokel (1978) as

$$IR = \frac{(\mu_c - \mu_g) \cdot N_P}{N_G} \qquad \text{Eqn 2.2}$$

where μ_c is the specific growth rate of *T. tripos* in mono-specific cultures and μ_g is the specific growth rate of *T. tripos* in mixed cultures. N_P and N_G represent the geometric mean density (Gallegos *et al.*, 1996) of *T. tripos* and *F. subglobosum*, respectively, in mixed cultures during incubation.

Photosynthetic performance

On the last day of the 6-day incubation, ~350-510 live cells (except for cultures in the 23Mixed treatment that only ~130 cells were collected due to low cell abundance), including both motile cells and non-motile division cysts, of *F. subglobosum* from each culture flask were picked using a glass micropipette (Stoecker *et al.*, 1988) under a dissecting microscope (Olympus SZ61). The cells were temporarily stored in a 2 mL tube and acclimated in darkness at the corresponding temperature for ≥ 30 minutes. They were then transferred into the sample-holding tube of the FASTact system (Chelsea Technologies) and measured with the fast repetition rate fluorometry (FRRF) using a single-turnover (ST) acquisition protocol with 12 sequences. The sequence protocol consists of 100 flashes (1 µs duration) with 1µs interval at a saturation level, followed by 50 relaxation flashes (1 µs flash duration and 49 µs interval). The fluorescence of replicates of 2 mL AFSW were also measured as fluorescence blanks. The readings of fluorescence from all samples were corrected by subtracting the values of the fluorescence blanks. The blank-corrected maximal photochemical efficiency (Fv/Fm) of the photosystem II (PSII) of dark-adapted cells was calculated as

$$Fv/Fm = (Fm-Fo)/Fm, \qquad \text{Eqn 2.3}$$

where Fo and Fm are the minimal and maximum fluorescence yield, respectively, of the cells. The Fv/Fm ratio generally represents the overall availability of functional PSII reaction centers of the cells.

The chlorophyll-*a* levels (Chl-*a*) of the picked live cells in the sample-holding tube were also measured by the FRRF method. The cellular Chl-*a* content of *F. subglobosum* in the treatments (i.e. 19Mono, 19Mixed, 23Mono, and 23Mixed) were determined and corrected for by using the fluorescence blanks. After measurement, the cells were preserved with acidic Lugol's solution (2% final concentration). Images of the preserved cells were captured with a digital camera and analyzed with the image processing software ImageJ (1.52h, N.I.H.) to measure the cross-sectional area. The estimated equivalent spherical diameter (ESD) of cells were computed based on the area measurements of 50-70 imaged cells for each treatment.

Statistical analysis

All statistical analyses and graphical presentations were conducted using R version 3.6.1 (R Core Team, 2019) and packages *emmeans* version 1.4.6 (Length, 2020) and *ggplot2* version 3.2.1 (Wickham, 2016). One-way ANOVA with *post-hoc* Tukey's test were conducted to test for significant difference ($\alpha = 0.05$) of the measurements among the 4 treatments.

RESULTS

Physiological temperature range of mono-specific cultures

Within the tested temperature range of 18-27°C, the mean specific growth rates of *F. subglobosum* in mono-specific cultures were -0.62 d^{-1} at 18°C and 0.09 d^{-1} at 20°C. Specific growth rate increased with temperature and peaked at 0.21 d^{-1} at 24°C. It then dropped to 0.10 d^{-1} at 27°C (Fig. 2.1). The physiological temperature range of *F. subglobosum*, which is defined as the sub-optimal temperature range that the cells can maintain an increasing trend of growth rate, is therefore > 18°C and < 24°C.

Population dynamics in mono-specific and mixed cultures

Throughout the 20-day experiment, the mono-specific cultures of *F. subglobosum* maintained an exponential growth and reached a mean cell density of ~8 cells mL^{-1} and ~13 cells mL^{-1} at 19°C and 23°C, respectively, on day 20. However, *F. subglobosum* in mixed cultures did not grow well and decreased to 0 cells mL^{-1} at the end of experiment for both temperatures (Fig. 2.2). The mean specific growth rate of *F. subglobosum*, determined by the change in cell densities between days 8 and 20, in the 19Mono and 23 Mono treatments were 0.30 d^{-1} and 0.32 d^{-1}, respectively while those in the 19Mixed and 23Mixed treatments were significantly ($P < 0.05$) lower, at 0 d^{-1} and -0.09 d^{-1}, respectively (Fig. 2.3).

The cell densities of *T. tripos* increased exponentially within the first 10 days and remained steady in the days onwards in all the 4 treatments. *T. tripos* reached the peak mean cell densities of ~260 cells mL^{-1} on day 14 in the 19Mono treatment and of ~272 cells mL^{-1} on day 18 in the 19Mixed treatment (Fig. 2.2). Similarly, the peak mean cell densities were ~367 cells mL^{-1} on day 10 and ~413 cells mL^{-1} on day 10 in the 23Mono and 23Mixed treatments, respectively (Fig. 2.2). The mean specific growth rates of *T. tripos* in the 4 treatments, determined by the change in cell densities between days 0 and 8, ranged from 0.21 d^{-1} to 0.23 d^{-1} and did not differ significantly ($P > 0.05$) (Fig. 2.3).

Photosynthetic performance, cellular Chl-*a* content and cell size of *F. subglobosum*

On the last day of the 6-day incubation, the maximal photochemical efficiency (Fv/Fm) of *F. subglobosum* differed significantly ($P < 0.05$) between 19°C and 23°C. At 19°C, the mean Fv/Fm ratios were 0.42 and 0.41, respectively, in the mono-specific and mixed cultures. At 23°C, those ratios were 0.27 and 0.28, respectively, in the mono-specific and mixed cultures (Fig. 2.4).

The mean cellular Chl-*a* content of *F. subglobosum* did not differ significantly ($P > 0.05$) in the 19Mono, 19Mixed, and 23Mono treatments, with a range between 36.2 pg

cell^{-1} and 38.0 pg cell^{-1}. The mean Chl-*a* level in the 23Mixed treatment was significantly ($P < 0.05$) higher than the others, at 43.1 pg cell^{-1} (Fig. 2.4).

The mean estimated equivalent spherical diameters (ESDs) of *F. subglobosum* were 40.4 µm and 41.1 µm in the 19Mono and 19Mixed treatments. Those in the 23Mono and 23Mixed treatments were 36.1 µm and 37.9 µm, respectively (Fig. 2.4). The ESD in the 19Mixed was significantly ($P < 0.05$) higher than that in the 23Mixed treatments.

Per capita ingestion rate

The estimated *per capita* ingestion rate of *T. tripos* by *F. subglobosum* was -0.13 cells grazer^{-1} d^{-1} at 19°C and 0.03 cells grazer^{-1} d^{-1} at 23°C (Fig. 2.5), indicating no obvious prey ingestion by the dinoflagellate at both temperatures.

DISCUSSION

Population growth, prey ingestion and mixotrophic capacity of *F. subglobosum*

This strain of *F. subglobosum* (CCMP-3029) from NCMA was reported to originate from western Florida, in Gulf of Mexico waters, and have a temperature tolerance range between 18°C and 24°C. The results of the physiological temperature range experiment confirmed the reported temperature tolerance. The dinoflagellates did not growth well at 18°C and obtained a lower than optimal growth at temperature higher than 24°C in mono-specific cultures (Fig. 2.1).

Previous study showed that, at ~60 µE m^{-2} s^{-1}, *F. subglobosum* obtained growth rates at ~0.2 d^{-1} and ~0.45 d^{-1} in phototrophic and mixotrophic growth, respectively (Skovgaard, 1996b). Contrary to previous reports (Skovgaard 1996a; Skovgaard, 1996b; Hansen & Neilsen, 1997), *F. subglobosum* did not grow in cultures with added prey *T. tripos* at 19°C and 23°C. The cell densities of *F. subglobosum* decreased to 0 cells mL^{-1} near the end of experiment in both the 19Mixed and 23Mixed treatments (Fig. 2.2). The cell densities of the prey, *T. tripos*, in the mixed cultures seemed not affected by the

presence of the mixotroph *F. subglobosum* (Fig. 2.2). Hansen *et al*. (2000) showed a rapid decrease in cell density of *T. tripos* and a complete depletion of them after 7 days in mixed cultures with *F. subglobosum*. However, this was not the case in our results. While *F. subglobosum* grew well and maintained specific growth rates 0.30 d^{-1} and 0.32 d^{-1} in the 19Mono and 23Mono treatments, respectively (Fig. 2.3), the population in the 19Mixed and 23Mixed cultures died off (Fig 2.2). This contradicts other studies that reported the growth rates in mixotrophic culture were higher than those in phototrophic cultures at the same light intensities (Skovgaard, 1996b; Hansen & Nielson, 1997). It suggests that the presence of *T. tripos* could have an adverse effect on *F. subglobosum* in our experiments.

F. subglobosum was reported to be mixotrophic and feed solely on *Tripos* spp. (Skovgaard, 1996a; Hansen & Neilsen, 1997; Rodriguez *et al.*, 2014), the reversal of the roles of predator and prey has not been reported for this species. However, such reversal in the predator-prey interaction was observed in a close relative species, *Fragilidium* cf. *mexicanum* (Jeong *et al*., 1997). The authors reported that when the initial concentration ratio of *F*. cf. *mexicanum*: *Protoperidinium* cf. *divergens* was ≤ 0.4, both species prey on each other and when the ratio was > 0.8, *P*. cf. *divergens* was readily preyed upon by *F*. cf. *mexicanum*. Aware of the effect of initial cell density ratio on the predator-prey interaction, in our 20-day incubation experiment, the ratio of the initial cell density of *F. subglobosum:T. tripos* was tried to be kept at 1:10, but not successfully. In another set of experiments that lasted 6 days, the initial density ratio was kept at ~1:5 with the cell density of *F. subglobosum* at ~7 cells mL^{-1}. Similar ratios were used in previous studies (Skovgaard, 1996b; Hansen *et al*. 2000) that showed obvious ingestion on *Tripos* spp. by *F. subglobosum*. However, *F. subglobosum* in our experiment did not show obvious ingestion of prey cells at either 19°C or 23°C even with the increased initial predator:prey ratio (Fig. 2.5). Results from both sets of experiments suggest that the *F. subglobosum* culture that we used is not mixotrophic on the prey we offered.

Assuming there were not misidentifications of both *F. subglobosum* and *T. tripos*, the lack of prey ingestion by *F. subglobosum* in our experiments could be related to prey

selectivity, the triggering of phagotrophy, or the intraspecific strain variation in mixotrophic capacity of this mixotrophic dinoflagellate.

F. subglobosum was reported to be a facultative mixotroph that can survive autotrophically in light, and heterotrophically when in the dark (Skovgaard, 1996b). It was shown to prey on several *Tripos* spp. and with a selectivity towards *T. tripos* and *T. lineatum*, where *T. tripos* was the maximum prey size that the mixotroph can handle (Skovgaard, 1996a). Though *F. subglobosum* needs approximately 24 hours to transit from phototrophic to phagotrophic growth, they attack and ingest *Tripos spp*. prey readily. The dinoflagellate ingested 0-0.8 cells grazer^{-1} d^{-1} for *T. tripos* and 2.1-5.8 cells grazer^{-1} d^{-1} for *T. lineatum* (Skovgaard, 1996b; Hansen & Nielson, 1997). The mechanisms of prey selectivity of *F. subglobosum* are not well known. Hansen & Nielson (1997) observed greater growth and grazing responses in *F. subglobosum* when fed with the larger species *T. tripos* than with the smaller species *T. fusus* and *T. furca*. However, they cannot conclude that such prey selectivity was solely based on cell size because another study showed that the growth rates of *F. subglobosum* feeding on *T. tripos* and *T. lineatum*, two prey species with very contrasting cell volumes, were similar (Skovgaard, 1996b). Other mechanisms for the prey selectivity have been proposed. For instance, Skovgaard *et al.* (2000) suggested that carbon content of the prey, which is in turn affected by light intensity, could contribute to the variation in ingestion rates of prey cells. Rodriguez *et al.* (2014) suggested that lectin and carbohydrate-binding proteins could be the prey recognition mechanism of *Fragilidium* spp. We identified our prey dinoflagellate *T. tripos* based on its morphology (Tomas *et al*., 1996). Even though it could be another *Tripos* species and misidentified as *T. tripos*, the mixotroph *F. subglobosum* was expected to have at least a baseline ingestion rate toward the prey species. Misidentification of the prey species could not explain the observation that the *F. subglobosum* populations died off and had negligible specific growth rates in mixed cultures of our experiment (Fig. 2.2 & 2.3), unless the *Tripos* species we used was phagotrophic or could cause adverse effects on the growth of *F. subglobosum*.

Triggering of phagotrophy in presumed photosynthetic phytoplankton under certain conditions has been demonstrated in various species. For instance, the marine mixotrophic dinoflagellate *Tripos furca* was shown to feed on microzooplankton only when the cultures were grown under nitrogen (N) or phosphorus (P) depleted condition for > 10 days or shown to have high feeding rate only at low irradiance levels (Smalley *et al*., 2003; Smalley *et al*., 2012). Similarly, only when under N or P limitation, the dinoflagellate *Heterocapsa triquetra* was shown to ingest small flagellates, cyanobacterium and diatom species (Legrand *et al*., 1998), and the dinoflagellate *Prorocentrum minimum* was shown to ingest cryptophyte species (Johnson, 2015). There has been no reported N- or P-starvation related triggering of phagotrophy in *F. subglobosum* so far. In previous studies (Skovgaard, 1996b; Hansen *et al*., 2000; Skovgaard *et al*, 2000), the mixotroph was maintained in B-medium (Hansen, 1989) that was not significantly different from the modified F/2-Si medium we used in terms of chemical composition, except that there were no H_3BO_3 and trace amount of $CuSO_4 \cdot 5H_2O$ in the F/2-Si medium. However, these two compounds are not commonly reported as major nutrients required for the growth of phytoplankton species (Anderson, 2005). The lack of these two compounds in our medium should not be affecting the phagotrophic capability of *F. subglobosum*. Furthermore, prey ingestion rates of *F. subglobosum* were shown to vary with light intensity, with the highest ingestion rate towards *T. lineatum* at ~60 µE m^{-2} s^{-1} and reduced rates at lower and higher light intensities (Skovgaard, 1996b). In our experiment, the light intensity was maintained at approximately 60 µE m^{-2} s^{-1} throughout the whole experiment. Therefore, light intensity should not be a limiting factor that caused negligible prey ingestion in our experiment.

Another possibility for causing the observed discrepancy in prey ingestion rates between our experiment and previous studies could be intraspecific strain variation, which is largely understudied in mixotrophic phytoplankton. One study by Calbet *et al*. (2011) revealed that the 11 strains of the mixotrophic dinoflagellate *Karlodinium veneficum* showed diverse ingestion rates on *Rhodomonas salina*, with a range from 0.22-1.3 cells $grazer^{-1}$ d^{-1}, which was 8-52% of their daily ration. The *F. subglobosum* strain

we used originated from the Gulf of Mexico, which was different from the strain isolated from northern Europe and used in previous studies (Skovgaard, 1996b; Hansen *et al*., 2000; Skovgaard *et al*, 2000). It is possible that strain variability in the phagotrophic capacity of *F. subglobosum* led to the lack of prey ingestion in our experiments.

Photosynthetic performance and other cell traits at different temperatures

F. subglobosum showed a significantly ($P < 0.05$) higher maximum photosynthetic efficiency (Fv/Fm) at 19°C than at 23°C for both mono-specific and mixed cultures while there was not a difference in photosynthetic efficiency between the cultures at the same temperature (Fig. 2.4). Using the ^{14}C-uptake method, Skovgaard *et al.* (2000) reported an increase in photosynthesis rate of *F. subglobosum* for both phototrophic and mixotrophic growth at irradiance levels from 7 to 75 µE m^{-2} s^{-1}. Compared to strictly phototrophic growth, they found reductions in photosynthetic rates and cellular Chl-*a* content of the mixotroph under food-replete conditions. Though not directly comparable, the maximum photosynthetic efficiency of phytoplankton measured by the ^{14}C-uptake method and by the fast repetition rate fluorescence (FRRF) method were correlated on some occasions (Cermeno *et al*., 2005). By comparison, our results did not agree with the results from Skovgaard *et al*. (2000). Given the above-mentioned argument that the *F. subglobosum* used in our experiment was not mixotrophic, it is reasonable that there was no difference in the photosynthetic efficiency between the mono-specific and mixed cultures at the same temperature since *F. subglobosum* in both cultures was in autotrophic growth.

Changes in Fv/Fm as a function of temperature were mixed in the phytoplankton community and in mono-specific cultures. For instance, Quigg *et al*. (2013) separately measured the Fv/Fm ratios of phytoplankton communities in 2 fjords in Alaska, USA, with different median water temperatures and revealed no significant difference in the photo-physiology between the communities. Similarly, Rose *et al*. (2009) revealed that an increase of 4°C did not significant increase the Fv/Fm of the Antarctic phytoplankton assemblages, while the addition of the nutrient iron sharply increased the ratio. In

laboratory cultures, the ratio of Fv/Fm was shown to increase with increasing temperature for some phytoplankton species, such as *Emiliania huxleyi* (Feng *et al*., 2008) and *Microcystis aeruginosa* (Dong *et al*., 2015). However, the opposite pattern showing decreases in Fv/Fm with temperature or without significant change was observed in laboratory cultures of *Phaeodactylum tricormutum* (Geel *et al*., 1997), *Fragilariopsis cylindrus* (Mock & Hoch, 2005), *Monoraphidium* sp., *Staurastrum* sp., and *Raphidiopsis raciborskii* (Willis *et al*., 2019). The study by Akimov & Solomonova (2019) may suggest some conclusive insight into the controversy: species subjected to above-optimal temperatures tends to have decreased Fv/Fm while species grown at lower temperature and subjected to a near optimal higher temperature tend to have greater maximum photosynthetic efficiency. In other words, the relationship of Fv/Fm as a function of temperature for a phytoplankton species could be a bell-shape curve with the highest Fv/Fm at the optimal temperature and lower ratios at both ends. In our study, *F. subglobosum* was tested to have a physiological temperature range of > 18°C and < 24°C, where 24°C is the optimal temperature in terms of growth rate. If the bell-shape curve assumption is valid, the Fv/Fm of *F. subglobosum* should be as 23°C > 19°C. However, for unknown reasons, this was not the case in our observations.

Nevertheless, the cellular Chl-*a* content of cultures in the 23Mixed treatment was significantly ($P < 0.05$) higher than those in the other 3 treatments (Fig. 2.4). Phagotrophy of prey cells was believed to reduce cellular Chl-*a* content in the mixotroph *F. subglobosum* (Skovgaard, 1996a). Skovgaard *et al.* (2000) reported a 13-67% decrease in Chl-*a* content of *F. subglobosum* cells in mixotrophic growth when compared to phototrophic growth at the same light intensity. The reduction in cellular Chl-*a* content was thought to be solely due to the dilution effect from increased cell division with feeding in mixotrophically grown cells, and the net production of Chl-*a* was not inhibited by phagotrophy (Hansen *et al.*, 2000). There was inconsistency in our observation between the *per capita* ingestion rate and cellular Chl-*a*. Given that *F. subglobosum* in our experiments did not ingest any prey and the reported observation by Hansen *et al*. (2000) that Chl-*a* content was affected by prey ingestion during mixotrophic growth, the

difference in cellular Chl-*a* content of both the mono-specific and mixed cultures in our experiment cannot be explained.

F. subglobosum becomes more heterotrophic at increased temperature?

Previous studies have demonstrated increased prey grazing by other mixotrophic protists at elevated temperatures. Wilken *et al.* (2013) and Zhang *et al.* (2017) found increased grazing rates of the mixotrophic chrysophyte *Ochromonas* sp. towards the bacterium *Pseudomonas fluorescens* and the cyanobacterium *Microcystis* sp., respectively, at higher temperatures. Cabrerizo *et al.* (2019) showed an increased degree of bacterivory by the haptophyte *Isochrysis galbana* towards an unidentified bacterial species at higher temperature in cultures. Jeong *et al.* (2018) found that the mixotrophic dinoflagellate *Paragymnodinium shiwhaense* feeding on *Amphidinium carterae* demonstrated an increase in ingestion rate at temperatures from 5-20°C.

The feeding of *F. subglobosum* is thought to be characterized by the Holling type I functional response (Hansen & Nielson, 1997) which suggests that its ingestion rate increases linearly with prey concentration until the maximum rate is reached. To demonstrate that *F. subglobosum* shifts the balance towards phagotrophy at elevated temperature and becomes more heterotrophic, one must provide evidence that the increase in prey ingestion rate is greater than the increase in photosynthetic rate during mixotrophic growth. This study is the first attempt to investigate the changes in grazing of *Fragilidium* spp. in reaction to temperature variation. However, the results that the *F. subglobosum* populations died off in the mixed cultures at both temperature and there was no obvious prey ingestion suggest that the dinoflagellate we used was not mixotrophic. The lack of feeding in the mixotroph cultures used could be due to strain variation, triggering mechanisms, prey selectivity or other unknown reasons. Given that, the hypothesis that this mixotrophic species becomes more heterotrophic at elevated temperatures was therefore not tested by this study.

To put this result into a broader perspective, the global temperature is expected to rise by 1.5℃ or more near the end of this century, depending on the effort to reduce

greenhouse gas emission (IPCC, 2018). Regionally, the average sea surface temperature is projected to rise, with the strongest warming in the Bering Sea, the Norwegian and Barents seas, and the western North Atlantic (Alexander *et al*., 2018). The reaction of planktonic mixotrophs to the increase in seawater temperature is therefore related to their biogeographical distribution over the globe. Recent efforts to map the distribution of mixotrophs have revealed markedly different geographic distributions. For instance, non-constitutive mixotrophs (NCMs) with acquired phototrophy that rely on "stolen" plastids were found to dominate productive areas while those that rely on endosymbionts were found to be abundant in oligotrophic areas (Leles *et al*., 2017). Mixotrophic nanoflagellates were predicted to increase in abundance at lower latitudes and in productive coastal areas as driven by increases in light availability and in nitrogen input, respectively (Edwards, 2019). *F. subglobosum*, being a constitutive mixotroph (CM), was regarded as an outlier of the > 20 μm dinophytes group that were over-represented in a biogeographic survey of mixotrophs (Leles *et al*., 2018). Although we did not prove or disapprove that *F. subglobosum* becomes more heterotrophic at elevated temperature, how the routine sampling methods select against other under-represented mixotrophs and undermine our true understandings to their contributions to the biogeochemical cycling of carbon and other substances at a warmer environment is worthwhile of further investigations.

CONCLUSION

Contrary to expectations, the strain of *F. subglobosum* isolated near Florida did not grow well in cultures with added *T. tripos* as prey and obtained negligible or negative specific growth rate in the mixed cultures. This discrepancy could be related to prey selectivity, triggering of phagotrophy or intraspecific strain variation of the *F. subglobosum* culture used in our experiment. The dinoflagellate species also showed reduced maximal photosynthetic efficiency but no difference in the *per capita* ingestion rate at higher temperature. We suspect that the Florida strain of *F. subglobosum* cultures

used are not mixotrophic and therefore this study does not prove or disapprove that this mixotrophic species became more heterotrophic at elevated water temperature.

ACKNOWLEDGEMENTS

The authors greatly thank Dr. Diane Stoecker for her opinions that inspired us to improve our experimental design. We are grateful to Dr. Deana Erdner for letting us use the FASTact system for the FRRF measurements.

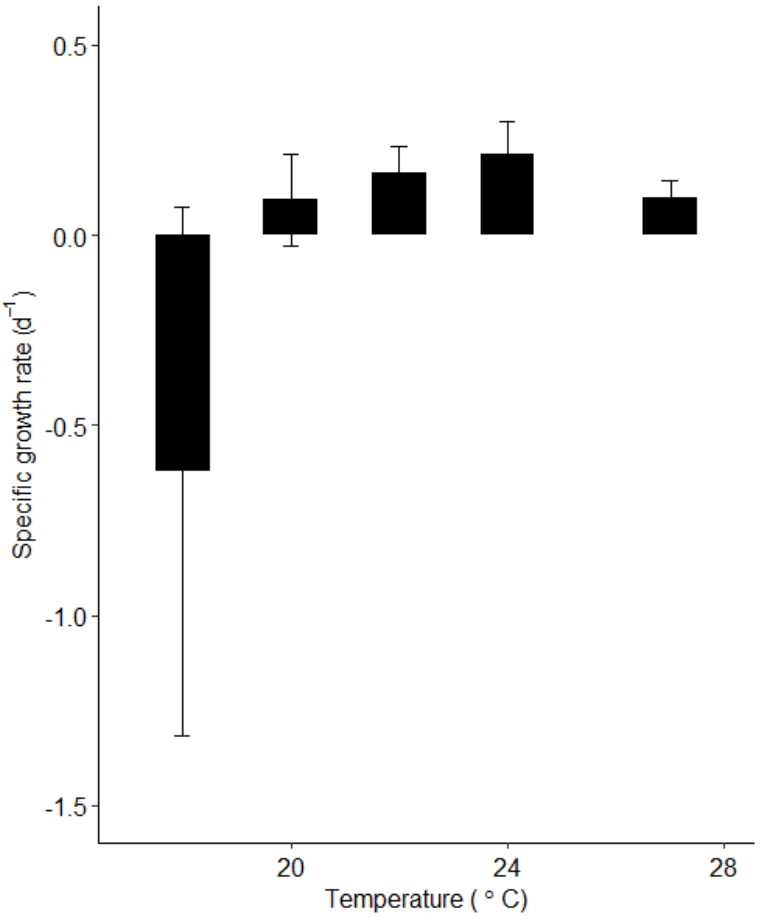

Figure 2.1 Mean specific growth rates (±1 S.D.) of *F. subglobosum* in mono-specific culture at various temperatures at the same light intensity.

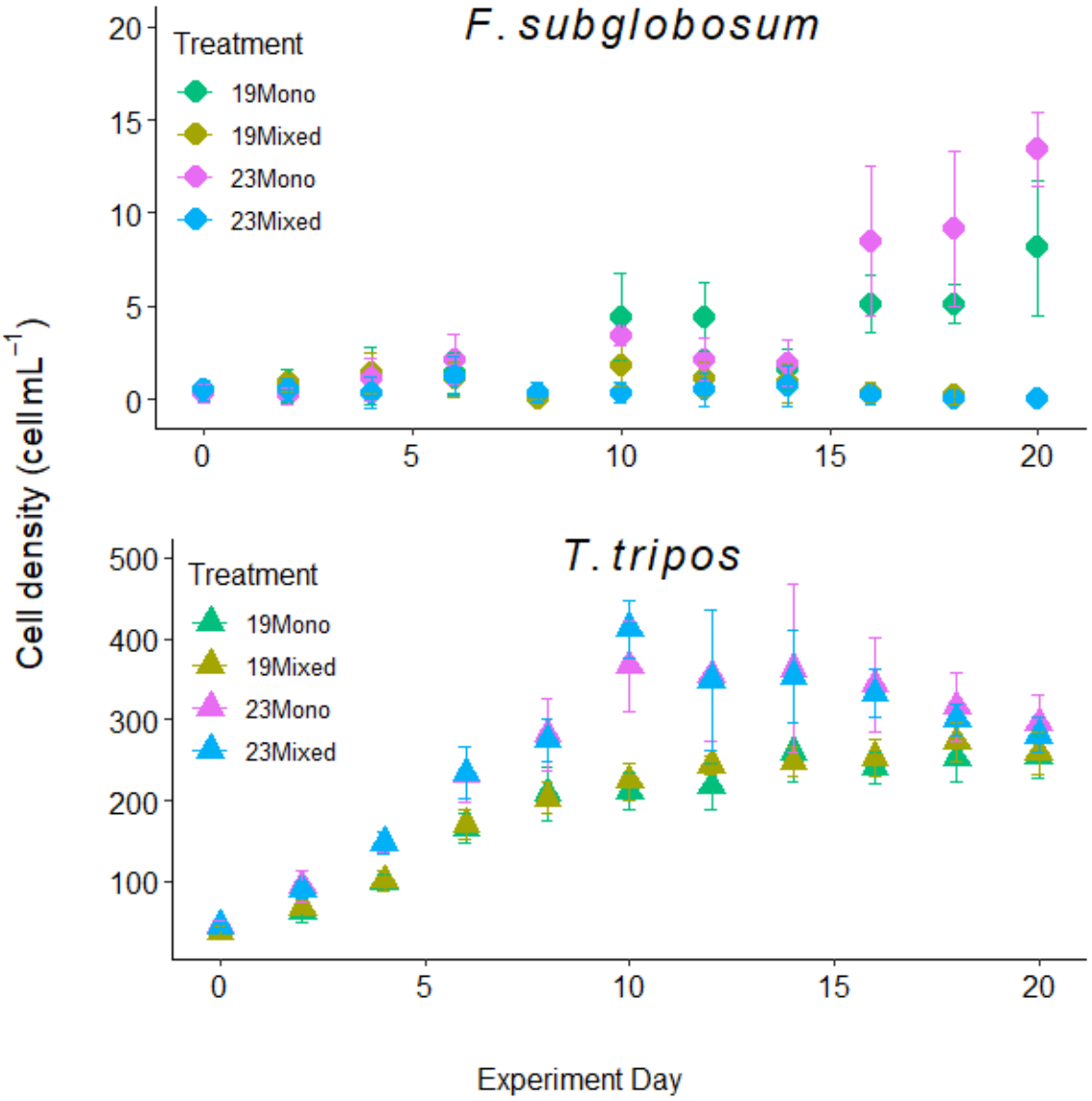

Figure 2.2 Mean cell densities (±1 S.D.) of *F. subglobosum* and *T. tripos* in the 4 treatments throughout the experiment.

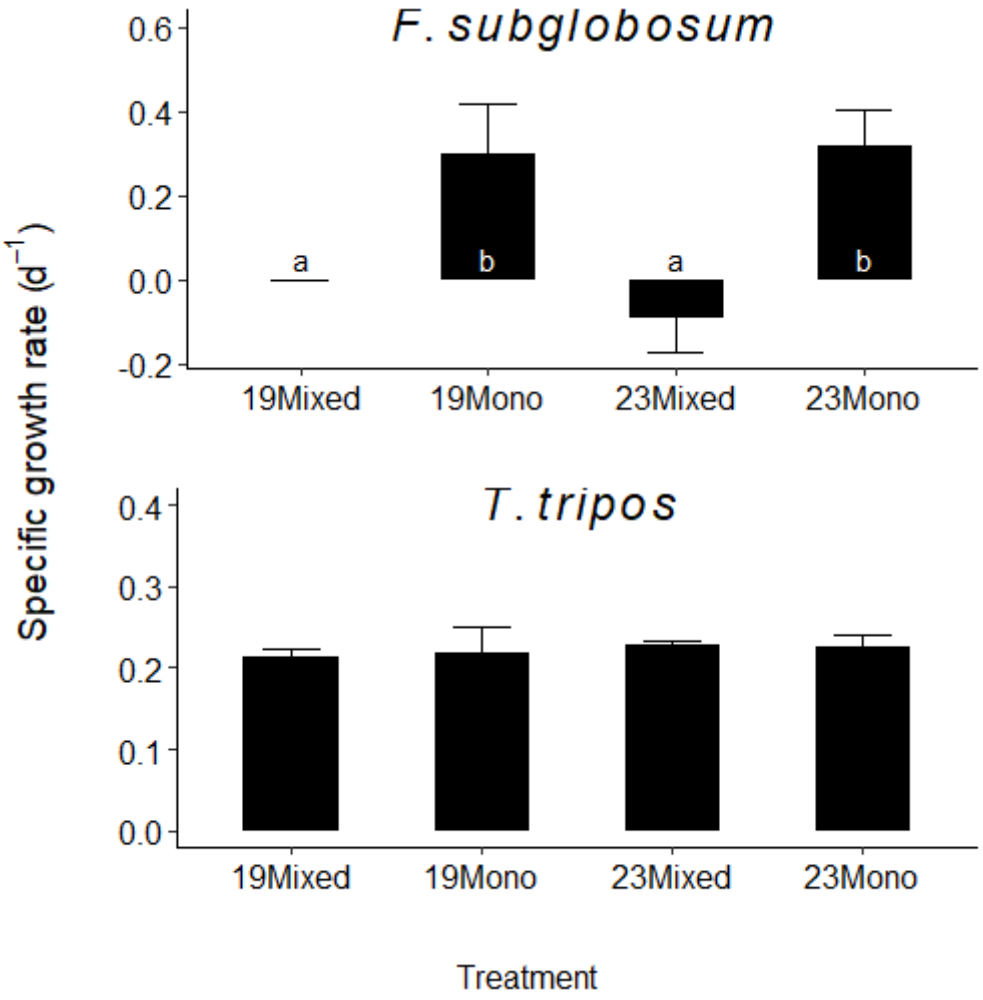

Figure 2.3 Mean specific growth rates (±1 S.D.) of *F. subglobosum* and *T. tripos* in the 4 treatments. Lower case letters denote statistical significance ($\alpha = 0.05$) of pairwise comparison in Tukey's test.

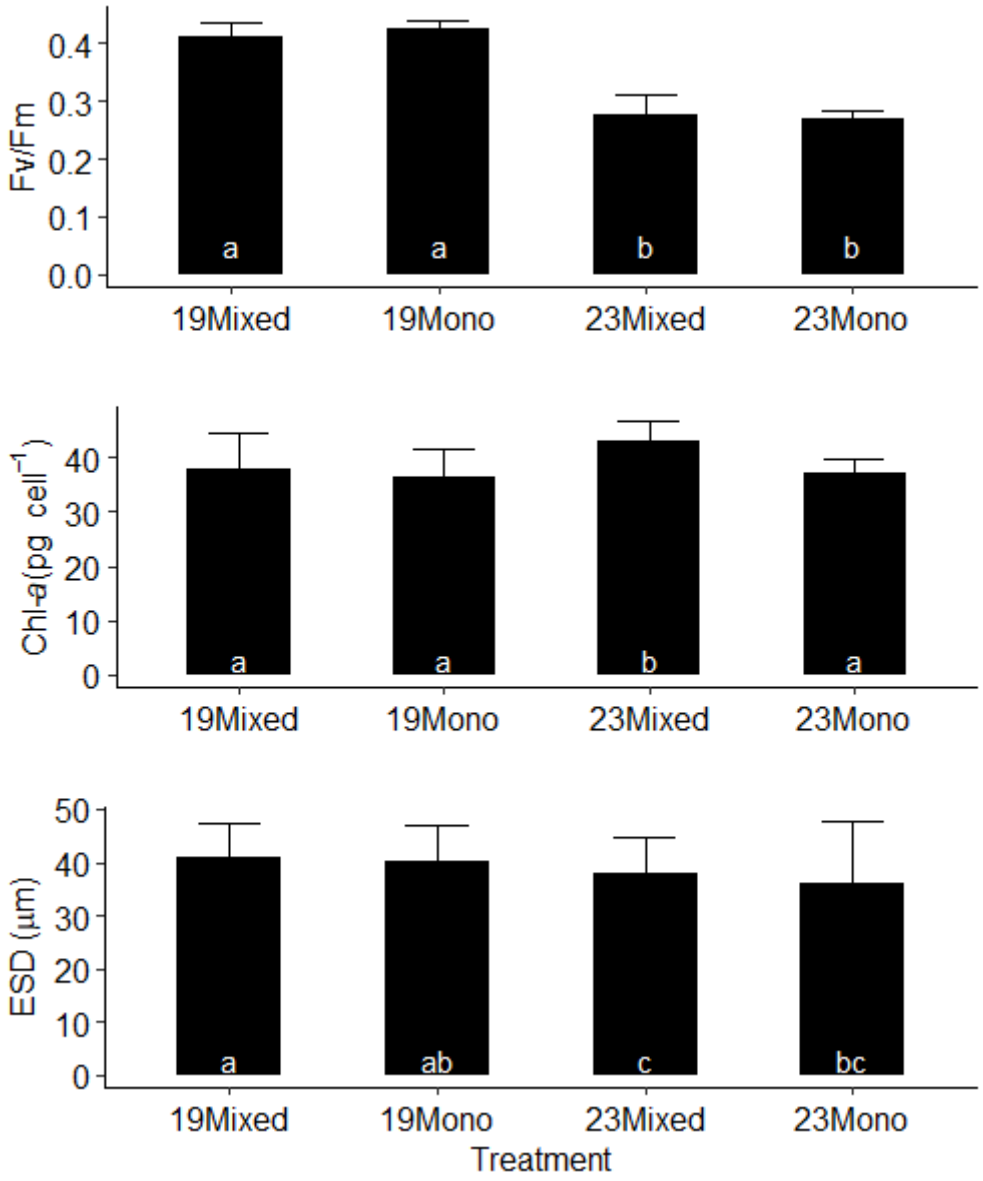

Figure 2.4 Mean maximum photosynthetic efficiencies (Fv/Fm) (±1 S.D.), cellular Chl-*a* contents (Chl-*a*) (±1 S.D.) and the estimated equivalent spherical diameters (ESD) (±1 S.D.) of *F. subglobosum* in the 4 treatments. Lower case letters denote statistical significance ($\alpha = 0.05$) of pairwise comparison in Tukey's test.

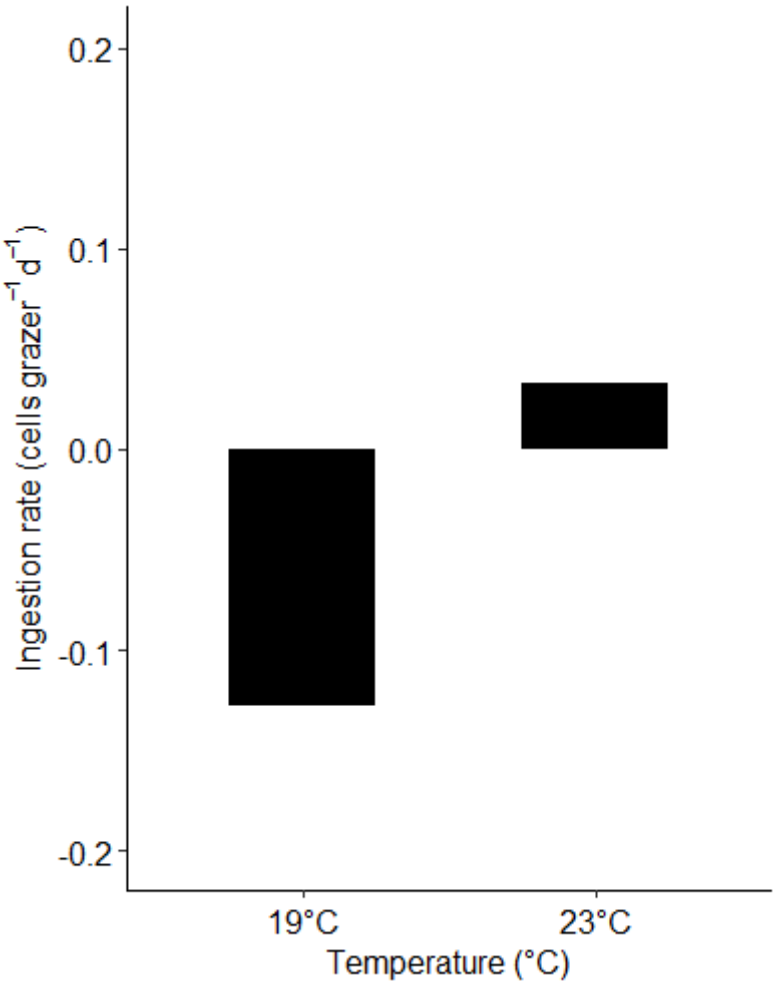

Figure 2.5 *Per capita* ingestion rates of *T tripos* by *F. subglobosum* at 19°C and 23°C.

Chapter 3: Effects of Water Accommodated Fraction of Crude Oil and Dispersant on the Growth and Grazing of Heterotrophic Dinoflagellates and Ciliates

ABSTRACT

The water accommodated fraction (WAF) of crude oil containing soluble aromatic hydrocarbons is thought to be highly toxic to aquatic organisms. The application of chemical dispersants to crude oil increases the bioavailability and the toxicity of these compounds. Exposure to such toxicants causes lethal and sub-lethal effects to marine protists, depending on the concentration. Heterotrophic dinoflagellates and ciliates are the most important components of microzooplankton, which are the major consumers of phytoplankton in the oceans. Exposure experiments were conducted to investigate the sub-lethal effects of WAF on the grazing and growth of these protozoa and their algal prey species in cultures. In exposure to 0-30 μL L^{-1} of chemically enhanced WAF (CEWAF), protozoan *Protoperidinium* sp. and *Metacylis* sp., fed with algal prey, were highly sensitive and showed drastically reduced specific growth rates even at low concentrations while their prey exhibited widely varying sensitivities in mono-specific cultures. Additionally, in exposure to the treatments of WAF, dispersant alone (Disp), and CEWAF of the same concentration, protozoa *Oxyrrhis marina* showed reduced grazing impact towards its algal prey population in all three treatments when compared to the control. Similarly, *Protoperidinium* sp. and *Metacylis* sp. had reduced *per capita* prey ingestion rates in exposure to WAF or CEWAF. However, the gross growth efficiencies of these two grazer species apparently were not affected by the hydrocarbon toxicity. With suppressed growth and impaired grazing of the protozoan species at high CEWAF concentrations, accumulation of their algal prey in the culture containers was observed. This suggested the potential link between impaired grazers and the formation of algal blooms when exposed to soluble oil pollutants.

INTRODUCTION

There are estimated > 1.2 million tons of oil released into the marine waters per year globally (NRC, 2003). Water accommodated fraction (WAF) of crude oil contains soluble aromatic components, such as benzene, toluene, ethylbenzene and xylenes (BTEX), and polycyclic aromatic hydrocarbons (PAHs), that are regarded as the most important substances for the toxicity of petroleum hydrocarbons (NRC, 2003; Boehm & Page 2007; Forth *et al.*, 2017a). While the application of chemical dispersant in remediation of oil spill events is still controversial (Fiocco & Lewis, 1999; George-Ares & Clark, 2000; Wise & Wise, 2011), dispersants are thought to increase the area of the water-oil interface and the release of soluble compounds into seawater, and therefore enhance their bioavailability to aquatic organisms (Hansen *et al.*, 2012; Jung *et al.*, 2012).

Marine protozoa, mainly heterotrophic dinoflagellates and ciliates, play an important role in the recycling of carbon and nutrients in the ecosystem by being both the main consumers of primary production and an important constituent of copepod's diet (Sherr & Sherr, 2002; Calbet & Saiz, 2005). Exposure to the toxic substances of petroleum hydrocarbons causes lethal or sub-lethal effects on marine protists (Connell *et al.*, 1981). Their sensitivities to pollutants are taxon-specific. For instance, Almeda *et al*. (2014b) exposed ciliates and heterotrophic dinoflagellates to a mixture of crude oil and Corexit dispersant for ≤ 48 hours and showed that the ciliates *Strombidium* sp., *Spirostrombidium* sp., and *Eutintinnus pectinis* were more sensitive to the toxicity than the ciliate *Favella ehrenbergii*, and heterotrophic dinoflagellates *Gyrodinium spirale* and *Protoperidinium divergens*.

Although protozoan species could be exposed to the adverse effects of petroleum hydrocarbons by ingestion of tiny oil droplets (Bonnet *et al*., 2005; Almeda *et al*., 2014a), direct uptake of dissolved components of crude oil through the cell membrane (Lindmark, 1981; Bamdad *et al*., 1997; Kim *et al*., 2017) and ingestion of toxicant-loaded prey items (Tso & Taghon, 1998; Moore *et al*., 2006; Gomiero *et al*, 2012) are of greater concern. We conducted exposure experiments on the soluble components of various combinations of crude oil and dispersant on 4 different protozoan species in cultures,

including *Oxyrrhis marina* and one species from each of the following genera: *Protoperidinium, Euplotes* and *Metacylis*. *O. marina* is a heterotrophic dinoflagellate of widespread distribution and is frequently used as a model organism for ecological experiments (Montagnes *et al*. 2011; reviewed in Guo *et al*., 2013). The hypotrich ciliates *Euplotes* spp. are frequently used in ecotoxicity tests and pre-chemical screenings for anthropogenic stresses at estuarine and coastal sites (Tso & Taghon, 1998; Trielli *et al*., 2007; Kim *et al*., 2014). The heterotrophic dinoflagellate *Protoperidinium* spp. and the tintinnid ciliate *Metacylis* spp. are commonly found in the Gulf of Mexico and are often used in growth and feeding studies (Jeong & Latz, 1994; Buskey, 1997; Clough & Strom, 2005; Menden-Deuer *et al*., 2005; Graham & Strom, 2010; Lee & Choi, 2016). This project's objective is to investigate the sub-lethal effects of the soluble components of petroleum hydrocarbons and dispersant on the grazing and growth responses of these protozoan species.

METHODOLOGY

Preparation and maintenance of plankton cultures

Algal prey cultures of *Isochrysis galbana, Rhodomonas salina, Peridinium sociale, Zooxanthella microadriatica* and the heterotrophic dinoflagellate *Oxyrrhis marina* were obtained from the UTEX Culture Collection of Algae (Texas, USA). The diatom *Ditylum brightwellii*, dinoflagellate *Protoperidinium* sp. and ciliates *Euplotes* sp. and *Metacylis* sp. were isolated from water samples collected from the Ship Channel of Port Aransas (Texas, USA). Clonal cultures of protozoan species were maintained in autoclaved 0.2 µm filtered seawater (AFSW, 28-32 PSU) and fed regularly with mono-specific cultures of the corresponding algal prey (Table 3.1) which were maintained in F/2-Si (Guillard, 1975) enriched AFSW. All protistan cultures were non-axenic and grown in clean containers (72 or 250 mL) with regular inoculation with fresh enriched AFSW. They were maintained at 20±1°C, except *Protoperidinium* sp., with illumination at light:dark cycle of 12:12 at light intensity of ~30-70 µmol photon m^{-2} s^{-1}. Cultures of

Protoperidinium sp. were maintained in 72 mL containers held in a transparent plastic tube on a bench roller (~0.5 rotations per minute) and placed inside an incubator that was maintained at 24±1°C with the same illumination as the other cultures.

The cell volume of each protistan species was estimated by imaging preserved cells in acidic Lugol's (~2%) and glutaraldehyde (~2%), separately, under microscope and by measuring the cell dimensions using ImageJ software (version 1.52h, N.I.H.). The calculation of cell volume (without cell shrinkage or swelling corrections since Menden-Deuer *et al*. (2001) showed that the fixatives Lugol's and glutaraldehyde could lead to mixed effects on the changes of cell volume of dinoflagellates and diatoms) was based on the geometric models proposed by Sun & Liu (2003, Table II): shape code 1-H for *I. galbana*, *P. sociale* and *Z. microadriatica*; shape code 2-H for *R. salina* and *O. marina*; shape code 3-H for *Euplotes* sp.; shape code 9-H for *Metacylis* sp.; shape-code 30-H for *D. brightwellii*; and modified shape code 25-SL for *Protoperidinium* sp.

Crude oil and dispersant treatments

Light Louisiana Sweet crude oil and Corexit 9500A dispersant were used and the ratio of nominal concentrations of crude oil to dispersant was 20:1. The crude oil was provided by BP Exploration & Production Inc. as a surrogate for the oil released during the Deepwater Horizon oil spill, and the dispersant was provided by Nalco/Exxon Energy Chemicals, I.P. The non-weathered crude oil and dispersant were stored in capped glass bottles in darkness at ~4°C and warmed at room temperature for ≥ 1 hour before use. Overall, four types of test media were used: 1) control (Ctrl): 0.2 μm filtered seawater (FSW) without the addition of crude oil or dispersant; 2) dispersant alone (Disp): dispersant in FSW; 3) water accommodated fraction (WAF): crude oil in FSW; and 4) chemically enhanced WAF (CEWAF): crude oil in FSW with the addition of dispersant. The preparation of Disp, WAF and CEWAF media followed the standardized protocol (Singer *et al.*, 2000) with modifications. Briefly, crude oil and (or) dispersant were added to 1 L of FSW in a capped glass aspirator bottle pre-cleaned by soaking in 2% Micro-90 solution (Cole-Parmer, USA), followed by rinsing with deionized water. The mixture in

the aspirator bottle was physically mixed with a magnetic stir bar for 18 hours in darkness at room temperature while maintaining a vortex of ~20% of the depth of the water column inside the bottle. After mixing, the solution was settled for > 3 hours. To minimize the amount of tiny oil droplets in the test media, only the subsurface part of the settled solution in the aspirator bottle was collected and used in experiments.

To determine the effects of petroleum hydrocarbons on the growth responses of marine protists, CEWAF media at a range of nominal concentrations (0 to 30 μL L^{-1}) were prepared. To determine the effects of petroleum hydrocarbons on the grazing responses of marine protozoa, four different treatments (i.e. Ctrl, Disp, WAF, and CEWAF) at certain nominal concentrations were prepared.

Assuming that light Louisiana crude oil has a density of 0.839 g cm^{-3} at 15°C and 0% volume of evaporation (FISG, 2010), the concentrations of total PAHs (TPAH50, consist of 23 parent PAHs and 27 alkylated homologs) and some of the individual PAHs were estimated based on the published data by Forth *et al*. (2017b) and were presented in Table 3.2. In their assessment, Coexit 9500 dispersant and MC252 crude oil were used, where MC252 is of similar chemical composition and toxicity to the surrogate light Louisiana crude oil we used. We chose their reported average TPAH50s of source CEWAF (1981 μg L^{-1}) and LEWAF (196 μg L^{-1}) and the percentage composition of individual PAHs to estimate the concentrations of PAHs in our CEWAF and WAF treatments, respectively, since similar methods of preparation of the test media were used, except that the preparation of LEWAF in Forth *et al*., (2017b) did not mix the seawater-oil mixture with a visible vortex as we did for the WAF test medium and the volume ratio of crude oil to dispersant used was 10:1 rather than 20:1 in our experiment. In Table 3.2, abbreviation Chr represents the combined concentration of alkylated C1-C4 chrysenes; C/T represents the combined concentration of chrysene and triphenylene; Flo represents the combined concentration of fluorene plus C1-C3 fluorenes; F/P represents the combined concentration of alkylated C1-C4 fluoranthenes or pyrenes; Nap represents the combined concentration of naphthalene plus the alkylated C1-C4 naphthalenes; Phe

represents the combined concentration of phenanthrene plus alkylated C1-C4 phenanthrene or anthracenes.

Growth responses of grazers and algal prey in CEWAF

Specific growth rate

Mono-cultures of algal prey and grazers were separately exposed to nominal concentrations from 0 to 30 µL L^{-1} of CEWAF by adding the protistan stock culture to the prepared CEWAF solutions in capped polystyrene containers (72 mL for algal cultures and 250 mL for grazers with added algal prey) in triplicate. For the grazers *Protoperidinium* sp. and *Metacylis* sp., 5 and 50, respectively, actively swimming cells were picked with a glass pipette and added to the containers. Additionally, algal prey was added to all the grazer cultures at the beginning of the experiment. To minimize the dilution effect to the CEWAF, the addition of stock cultures to the CEWAF medium was limited to ≤ 10% of the total volume of the mixture. Enrichments of major and trace elements (Guillard, 1975) were added to make the final concentrations in the incubation containers exceeded 0.88 mM nitrate (NO_3^-) and 0.036 mM phosphate (PO_4^{3-}). All containers were incubated at the same temperature and illumination conditions as those in culture maintenance except for *Protoperidinium* sp. for which the cultures were incubated on a bench roller at room temperature (~21-27°C) near the window with natural sun light (~38-142 µE m^{-2} s^{-1}). Except for *Protoperidinium* sp., subsamples of mono-specific algal prey (2 mL) and grazers (30-50 mL for each sampling) were collected regularly from each container without medium replacement (eventually 100-180 mL removed in total after all samplings), preserved with acidic Lugol's solution (~2-5% final concentration) and enumerated under microscope to estimate the cell densities. For *Protoperidinium* sp., different sets of triplicate cultures were sacrificed for sample collection at time intervals. Specific growth rates (SGR, d^{-1}) of the algal prey and grazers were calculated based on the changes in cell densities during the exponential growth phase as:

$$SGR = \ln\left(\frac{N_t}{N_0}\right)/t \qquad \text{Eqn 3.1}$$

where N_t is the cell density at time t, N_0 is the cell density at the previous time point, and t is the time duration of incubation in days.

The relationship between the natural-log of cell volume and SGR of protistan species in normal growth condition (i.e. without the addition of CEWAF) was explored to reveal the possible linkage between cell size and growth rates using model II linear regression (standard major axis).

Toxicant sensitivity

The median growth inhibition concentration (IC_{50}) of CEWAF of each protistan species was estimated by fitting the SGR data into the 4-parameter log-logistic model (Ritz *et al.*, 2015) as:

$$SGR = c + \frac{d-c}{1+\exp(b(\log(Con)-\log(e)))} \qquad \text{Eqn 3.2}$$

where Con is the nominal concentration of CEWAF, d and c are the upper and lower asymptotes or limits of SGR, respectively, b is the slope of the sigmoidal curve, and e is the IC_{50}. Only the protistan species with a good fit of the SGR data to the model were included for further analysis and discussion. The relationships between the estimated IC_{50} and the cell volume of the protistan species were then investigated using natural-log bivariate model II linear regressions (standard major axis).

Grazing by protozoan grazers in different combinations of crude oil and dispersant

Grazing impact on algal prey population

The grazing rates of *O. marina* and *Euplotes* sp. were determined using the dilution method (Landry & Hassett, 1982). Pre-diluted stock mixtures of grazers and prey were prepared to obtain a gradient of dilution fractions (e.g. 0.2, 0.5, 1.0 of undiluted stock mixtures) by mixing stock cultures with FSW. The pre-diluted stock mixtures were then added to the test media, namely Ctrl, Disp, WAF, and CEWAF, with the same

concentrations for crude oil and dispersant when applicable. For the grazer-prey pair of *O. marina* and *I. galbana*, the nominal concentrations of 10 µL L^{-1} of crude oil and 0.5 µL L^{-1} of dispersant were used. For that of *Euplotes* sp. and *Rhodomonas salina*, the nominal concentrations were 3 µL L^{-1} and 0.15 µL L^{-1} for crude oil and dispersant, respectively. These concentrations were chosen based on the results from the growth experiment in CEWAF exposure, where at the concentration a substantial drop in the SGR was observed. Again, to minimize the dilution effect to the test media, the addition of protistan stock mixtures to the media was limited to ≤ 13% of the total volume of the mixture. Enrichments of major and trace elements (Guillard, 1975) were added (≥ 0.88 mM NO_3^- and ≥ 0.036 mM PO_4^{3-} final concentrations) to eliminate the possibility that phytoplankton growth is limited by nutrient availability. The mixture was then filled into a 72 mL polystyrene tissue-culture flask in duplicate or triplicate and incubated for 24 hours in conditions identical to those used in culture maintenance. Subsamples of 2 mL were taken from the common medium mixture in duplicate before incubation and from each incubation flask after incubation. All subsamples were preserved with acidic Lugol's solution (~2-5% final concentration) for estimation of cell densities.

The coefficients of instantaneous population growth (µ, d^{-1}) and grazing mortality (g, d^{-1}) of algal prey were obtained from the linear regression analysis according to Landry & Hassett (1982):

$$\ln\left(\frac{N_t}{N_0}\right) = (\mu - Dg)t \qquad \text{Eqn 3.3}$$

where N_t is the algal density after incubation and N_0 is the initial algal density before incubation. Symbol D represents the dilution fractions and t is the time duration of incubation in days. The slope and the y-intercept of the linear regression, which respectively represent the grazing mortality (in negative value) and population growth rates of algal prey, of each treatment were tested against all treatments for statistical difference.

Per capita grazing rate

The *per capita* grazing rates of *Protoperidinium* sp. and *Metacylis* sp. in various treatment media, namely Ctrl, Disp, WAF, and CEWAF with the same concentrations for crude oil and dispersant when applicable, were determined. For the grazer-prey pair of *Protoperidinium* sp. and *D. brightwellii*, the nominal concentrations of 1 µL L^{-1} of crude oil and 0.05 µL L^{-1} of dispersant were used. For *Metacylis* sp. and *P. sociale and Z. microadriatica*, the nominal concentrations were 5 µL L^{-1} and 0.25 µL L^{-1} for crude oil and dispersant, respectively. These concentrations were chosen based on the results from the growth experiment in CEWAF exposure, where at the concentration a substantial drop in the SGR was observed.

One set of the mono-specific cultures of *D. brightwellii* was prepared by adding the stock culture to the test media without the addition of a grazer. It was then enriched with major and trace nutrients (Guillard, 1975) ($\geq$ 0.88 mM NO_3^- and $\geq$ 0.036 mM PO_4^{3-} final concentrations) and incubated in a capped 72 mL polystyrene flask in triplicate at conditions identical to those used in culture maintenance of *Protoperidinium* sp. Meanwhile, 10 actively swimming *Protoperidinium* sp. cells were picked from the stock culture with a glass pipette, added to another set of 72 mL flasks of algal prey cultures in test media with nutrient enrichment, and incubated in triplicate for 4 days at conditions identical to those used in culture maintenance. Again, to minimize the dilution effect to the test media, the addition of stock cultures to the media was limited to $\leq$ 10% of the total volume of the mixture. The same experimental procedures were repeated for the ciliate *Metacylis* sp. and the prey mixture of *P. sociale* and *Z. microadriatica,* except that 30 actively swimming *Metacylis* sp. cells were added to each tissue-culture flask with grazer addition and all containers were incubated for 2 days. The initial prey:predator density ratios were approximately 130:1 and 3400:1 for *Protoperidinium* sp. and *Metacylis* sp., respectively. Subsamples of algal prey (2 mL) were collected before and after incubation, and those of grazers (50 mL) were collected only after incubation. The samples were preserved with acidic Lugol's solution (~2-5% final concentration) for estimation of cell densities under the microscope. The ingestion rate (IR, cells $grazer^{-1}$ d^{-}

[1]) of protozoan grazers in each test medium was determined based on the methods of Frost (1972) and Heinbokel (1978) as

$$IR = \frac{(\mu_c - \mu_g) \cdot N_P}{N_G} \qquad \text{Eqn 3.4}$$

where μ_c is the specific growth rate of the algal prey without grazer addition and μ_g is the specific growth rate of the algal prey with grazer addition. N_P represents the geometric mean density of algal prey during incubation in cultures with the grazer addition while N_G represents the geometric mean density of the grazer (Gallegos *et al.*, 1996) during incubation in cultures.

Gross growth efficiency

The gross growth efficiencies (GGEs) of *Protoperidinium* sp. and *Metacylis* sp. in the four different treatments were calculated (Montagnes & Lessard, 1999) based on the data of SGR and IR as:

$$GGE = \frac{SGR \times V_G \times pgC}{V_P \times pgC \times IR} \qquad \text{Eqn 3.5}$$

where V_G and V_P represent the cell volumes of grazers and prey, respectively. The conversions from cell volume to carbon content (pgC) for the diatom and the dinoflagellates were pgC cell^{-1} = 0.288 x volume$^{0.811}$ (µm^3) and pgC cell^{-1} = 0.760 x volume$^{0.819}$ (µm^3) (Menden-Deuer & Lessard, 2000), respectively, and for the tintinnid was pgC cell^{-1} = 0.19 x volume (µm^3) (Putt & Stoecker, 1989).

Statistical analysis

All statistical analyses and graphical presentations were conducted using R version 3.6.1 (R Core Team, 2019) and packages *lmodel2* version 1.7-3 (Legendre, 2018), *drc* version 3.0-1(Ritz *et al.*, 2015), *emmeans* version 1.5.0 (Lenth, 2020), and *ggplot2* version 3.2.1 (Wickham, 2016).

Model II linear regressions tests (with 50,000 permutations) were applied to test for the presence of a significant relationship between SGR and the natural-log of cell volume, and between the natural-log of IC_{50} and the natural-log of cell volume using the

package *lmodel2* in R. Considering that the independent variables (i.e. the natural-log of cell volume for both cases) were subject to natural variation and measurement error, and the fact that both independent and dependent variables were not in comparable units of measurement, results from the standard major axis regression analysis were chosen for further result presentations and discussion (Sokal & Rohlf, 2012).

To fit the SGR data into the log-logistic model (Eqn 3.2) using the *drc* package in R, the model was simplified by setting coefficient c (i.e. the lower limit of SGR) at 0 for most of the cases, except *Metacylis* sp. and *P. sociale*. The model for *Metacylis* sp. was not simplified (i.e. 4-parameter model) while that of *P. sociale* was further simplified by setting coefficient d, the upper asymptote of SGR, at 0.35 as well. The lack-of-fit test is a built-in test (against one-way ANOVA model) of the package that was used as one of the criteria for choosing the current model among the candidates. The larger the *P* value, the better the model fit in general. The no-effect test is another built-in function that was applied by using the Chi-square test to test for the presence of a significant dose-response relationship ($\alpha = 0.05$).

RESULTS

Specific growth rate of grazers and algal prey in CEWAF

The mean specific growth rates (SGRs) of *O. marina* ranged from 0.43-0.52 d^{-1} when exposed to CEWAF at nominal concentrations from 0 µL L^{-1} to 30 µL L^{-1}, with the highest growth rate at 20 µL L^{-1} (Fig. 3.1). On the other hand, the mean SGRs of its prey, *I. galbana*, in mono-specific cultures, decreased from 0.61 d^{-1} at 0 µL L^{-1} to 0.42 d^{-1} at 30 µL L^{-1}. Unexpectedly, the lowest rate was found at 1 µL L^{-1} CEWAF, with a mean SGR of 0.01 d^{-1} (Fig 3.1). This lowest SGR of *I. galbana* was due to the averaging of both positive and negative values of SGRs of replicates. If only positive value is reported, the SGR at 1 µL L^{-1} CEWAF would be 0.39 d^{-1}.

The SGRs of *Euplotes* sp. averaged 0.84 d^{-1} at 0 µL L^{-1} CEWAF and decreased to the lowest at 0.44 d^{-1} at 20 µL L^{-1} CEWAF (Fig. 3.1). The mean SGRs of *R. salina* in

mono-specific cultures was 0.61 d^{-1} at 0 µL L^{-1}. It dropped to below zero at 10 µL L^{-1} CEWAF and increased to 0.25 d^{-1} at 20 µL L^{-1} CEWAF (Fig. 3.1).

The mean SGRs of *Protoperidinium* sp. were 0.77 d^{-1} and 0.52 d^{-1} at 0 µL L^{-1} and 1 µL L^{-1} CEWAF, respectively. The rates dropped drastically to near zero or became negative when the concentrations of CEWAF were > 1 µL L^{-1} (Fig. 3.1). In contrast, the mono-specific cultures of *D. brightwellii* showed relatively high SGRs, with a mean rate of 0.96 d^{-1} at 0 µL L^{-1} and decreasing gradually to 0.69 d^{-1} at 30 µL L^{-1} CEWAF (Fig. 3.1). Additionally, the cell densities of *D. brightwellii* at the beginning and the end of the experiment (on the 6^{th} day) in the grazer-prey cultures were determined. The ratios of final:initial prey densities were 31.1 at 0 µL L^{-1} and ranged from 36.6-41.5 at higher CEWAF concentrations (Table 3.2).

The mean SGRs of *Metacylis* sp. were 0.52 d^{-1} and 0.57 d^{-1} at 0 µL L^{-1} and 1 µL L^{-1} CEWAF, respectively. The rates were below zero when exposure concentrations were ≥ 15 µL L^{-1} CEWAF (Fig. 3.1). The mean SGRs of one of its prey species, *P. sociale*, ranged from 0.27 d^{-1} to 0.36 d^{-1} except that the SGR was 0.47 d^{-1} at 1 µL L^{-1} CEWAF. The other prey species, *Z. microadriatica*, obtained mean SGRs ranging from 0.32 d^{-1} to 0.37 d^{-1} across the exposure concentrations in mono-specific cultures (Fig. 3.1). The ratios of final:initial prey density of *Z. microadriatica* in the grazer-prey cultures after a 5-day CEWAF exposure ranged from 0.0-0.1 at 0-5 µL L^{-1} CEWAF and were ≥ 1.7 at higher concentrations (Table 3.2).

Model II linear regression (standard major axis) revealed no significant relationship (R^2 = 0.04, P = 0.64) between the natural-log of cell volume and the mean SGR of the tested species grown at 20±1°C in the control treatment (i.e. 0 µL L^{-1} CEWAF) (Fig. 3.2).

Toxicant sensitivities of protistan plankton to CEWAF

The fitted dose-response curve of each protistan species in exposure to CEWAF is presented in Fig 3.3. Data of *R. salina, D. brightwellii, Euplotes* sp., *Protoperidinium* sp. and *Metacylis* sp. showed a good fit of the SGRs to the model (Table 3.4). Estimated

median growth inhibition concentration (IC_{50}) of CEWAF to the SGR revealed relatively high toxicity tolerance of *D. brightwellii* among the algal prey species, with an estimated IC_{50} at ~169 µL L^{-1} while *R. salina* was very sensitive, with an estimated IC_{50} at 0.9 µL L^{-1} CEWAF. The dinoflagellate grazer *O. marina* was apparently highly tolerant to CEWAF toxicity (an estimated IC_{50} at ~297 µL L^{-1}), even though there was a large standard error of the estimation and a poor model fit. Grazers *Protoperidinium* sp. and *Metacylis* sp. were highly sensitive, with estimated IC_{50} at 1.1 µL L^{-1} and 5.9 µL L^{-1}, respectively. The sensitivity of *Euplotes* sp. was between those of the protistan grazers, with an estimated IC_{50} at 26.1 µL L^{-1} CEAWAF (Table 3.4).

When considering only the good-fit estimations of IC_{50}, model II linear regressions (standard major axis) between the natural-log of cell volume and the natural-log of IC_{50} revealed a weak positive relationship for the algal prey species (R^2 = 1.00, *P* = not available) and a weak negative relationship for the grazer species (R^2 = 0.77, *P* =0.31). When all species were considered, there was a weak positive relationship between the variables (R^2 = 0.01, *P* = 0.89) (Fig. 3.4).

Grazing rate of *O. marina* and *Euplotes* sp. in different combinations of crude oil and dispersant

At 10 µL L^{-1} of crude oil and 0.5 µL L^{-1} of dispersant, dilution experiments with the predator-prey pair of *O. marina* and *I. galbana* revealed varying rates of population growth (µ) and grazing mortality (g) of the algal prey among treatments. The values of µ and g were 1.17 d^{-1} and 1.05 d^{-1}, respectively, in the Ctrl treatment while they respectively ranged from -0.03-0.32 d^{-1} and from -0.13-0.02 d^{-1} in the treatments of Disp, WAF, and CEWAF. Comparison of the coefficients of linear regressions among the treatments revealed that g and µ in the Ctrl treatment were significantly different (*P* < 0.05) from those in the other treatments. In other words, at these exposure concentrations, *O. marina* showed negligible grazing rate on algal prey populations in all crude oil or dispersant loaded treatments when compared to the Ctrl treatment (Fig. 3.5). Compared to the SGRs results (Fig. 3.1) in CEWAF exposure at 10 µL L^{-1}, there was apparent

discrepancy in the growth rates of *I. galbana* between the growth experiment and dilution experiment. Explanation for the possible reasons is discussed below.

For the predator-prey pair of *Euplotes* sp. and *R. salina* exposed to 3 µL L^{-1} of crude oil and 0.15 µL L^{-1} of dispersant, the population growth rates of algal prey were exceptionally high in all treatments, with the highest population growth rate of 4.54 d^{-1} in the Ctrl treatment and a range of 3.3-3.4 d^{-1} in the treatments of Disp, WAF, and CEWAF (Fig. 3.5). Comparison of the coefficients of linear regressions among the treatments revealed that µ in the Ctrl treatment was significantly different ($P < 0.05$) from those in the other treatments (Fig. 3.5). Grazing mortality rates of *R. salina* were unusually high as well. They ranged from 2.19 d^{-1} to 2.74 d^{-1} among treatments, with the highest rate in the Ctrl treatment. The abnormally high population growth and grazing mortality rates of *R. salina* were due to its low cell density in the samples before incubation that could have introduced measurement errors in the haemocytometer counting and exaggerated the change in cell densities between before and after incubations. Caution should be used when interpreting these exceptionally high values of both the population growth and the grazing mortality rates.

Ingestion rates and gross growth efficiencies of *Protoperidinium* sp. and *Metacylis* sp. in different combinations of crude oil and dispersant

At the nominal concentrations of 1 µL L^{-1} of crude oil and 0.05 µL L^{-1} of dispersant, *Protoperidinium* sp. feeding on *D. brightwellii* showed ~60 cells $grazer^{-1}$ d^{-1} ingestion rates in the Ctrl, Disp and WAF treatments while that in the CEWAF treatment dropped to ~34 cells $grazer^{-1}$ d^{-1} (Fig. 3.6). The growth rates of *Protoperidinium* sp. in Ctrl and WAF were 0.28 d^{-1} and 0.31 d^{-1}, respectively, while that in CEWAF was 0.18 d^{-1}. Interestingly, the growth rate in Disp was much lower than the other treatments (Fig. 3.6). The estimated gross growth efficiencies (GGEs) of *Protoperidinium* sp. ranged from 0.17 to 0.20 in the treatments of Ctrl, WAF, and CEWAF. The GGE was abnormally low at 0.03 in the Disp treatment (Table 3.5). The seemingly contrasting ingestion rate and growth rates of *Protoperidinium* sp. in the Disp treatment (Fig. 3.6) were due to

averaging all the positive and negative values of growth rates from replicates. If only the positive value is used, the growth rate in the Disp treatment would be at 0.29 d^{-1} and the corresponding GGE would be 0.20 in Table 3.5.

At the nominal concentrations of 5 µL L^{-1} of crude oil and 0.25 µL L^{-1} of dispersant, the combined ingestion rates of *Metacylis* sp. feeding on a prey mixtures of *P. sociale* and *Z. microadriatica* were ~400 cells $grazer^{-1}$ d^{-1} in the Ctrl and Disp treatments. The rates changed drastically to below zero in the WAF and CEWAF treatments (Fig. 3.6). The growth rates of *Metacylis* sp. in the Ctrl and Disp treatments were ~0.5 d^{-1} while that in WAF was the highest among treatment, reaching 0.70 d^{-1}. The growth rate of *Metacylis* sp. in CEWAF was slightly below zero (Fig. 3.6). The seemingly contrasting ingestion rates and growth rates of *Metacylis* sp. in the WAF treatment were due to the fact that the estimation of ingestion rate relied on the changes in the combined cell density of both *P. sociale* and *Z. microadriatica*, where the latter species predominated the prey population in term of cell abundance. When only considering the cell density of *P. sociale*, *Metacylis* sp. ingested 2.7 and 2.0 cells $grazer^{-1}$ d^{-1} for *P. sociale* in the WAF and CEWAF treatments, respectively, while those in the Ctrl and Disp treatments were 4.7 and 4.3 cells $grazer^{-1}$ d^{-1}, respectively. *P. sociale* has a cell volume ~100 times of that of *Z. microadriatica* (Table 3.1). Although *Metacylis* sp. showed a negative ingestion rates on the combined population of *P. sociale* and *Z. microadriatica*, the 2.7 cells $grazer^{-1}$ d^{-1} on *P. sociale* could have contributed to the growth of the grazer in the WAF treatment (Fig. 3.6). The estimated GGEs of *Metacylis* sp. in the Ctrl and Disp treatments were 0.44 and 0.40, respectively. The GGEs in the WAF and CEWAF treatments were not estimated due to the negative IRs of the grazer (Table 3.5).

DISCUSSION

Protists' growth in normal condition

It has been commonly reported that different species of phytoplankton have different growth rates at a given temperature (Eppley, 1972, Montagnes & Franklin,

2001) and that smaller protistan species tend to have faster growth rates than larger ones (Chisholm, 1992; Hansen *et al.*, 1997). Testing the relationship between cell size and growth rates under normal conditions without the addition of crude oil or dispersant was not the primary objective of this study. However, the results can complement the discussion about the relationship between the cell traits and the growth responses in oil-polluted waters. In the Ctrl treatment (i.e. 0 µL L^{-1} CEWAF), results showed taxon-dependent growth rates in the photosynthetic phytoplankton species tested. At the same temperature (i.e. 20°C), the SGR of the diatom *D. brightwellii* was higher than those of the phytoflagellates *I. galbana* and *R. salina* and the dinoflagellates *Z. microadriatica* and *P. sociale* (Fig. 3.1). In agreement with Banse (1982), there was a weak dependence of maximal growth rates of phytoplankton with cell volume or mass. We found the eight tested species grown at 20°C in the control treatment did not show an inverse relationship between cell volume and SGR. In contrast, a weak positive relationship between these two variables was observed (P = 0.64, Fig. 3.2). Although all the phytoplankton species were grown in nutrient enriched media at 20°C, the light intensity they were provided in this study varied in the range of 30-70 µE m^{-2} s^{-1}, which may not be the optimal irradiance for them to achieve maximal growth. Limited irradiance could have also caused some phytoplankton species to experience reduced sensitivity to temperature. Edwards *et al.* (2016) complied data from 57 species of freshwater and marine phytoplankton and found that the chlorophyll-specific carbon uptake rates showed no trend with increasing temperatures (median 17°C) when the irradiance was < 20 µE m^{-2} s^{-1} but increased with temperatures when the irradiance was between 100-200 µE m^{-2} s^{-1}. In our study, the lack of significant relationship between the growth rate and cell volume of the tested protistan species in the control treatment could be due to limited irradiance or other factors that hindered them from achieving maximal growth rate at the given temperature.

Growth responses in exposure to CEWAF

Cell size and sensitivity to CEWAF

It has been reported that smaller cells tend to be more sensitive to the toxicity of petroleum hydrocarbons in culture (Echeveste *et al.*, 2010a; Othman *et al.*, 2012, Ozhan *et al.*, 2014). Nevertheless, a different pattern has also been reported in a natural phytoplankton community in which the persistence of picophytoplankton in the population and the lack of correlation between phytoplankton cell size and PAHs sensitivity were observed (Othman *et al.*, 2018). In our study, the estimated IC_{50} was used to reflect the protists' sensitivity to hydrocarbon toxicity (Table 3.4). Unfortunately, the lack of fit to the log-logistic model for some species hindered the estimation of their sensitivity. When considering only the good-fit IC_{50} estimations, the linear relationship between cell volume and the IC_{50} for all plankton species was not statistically significant (P = 0.89, Fig. 3.4), indicating that cell volume was not the sole contributor to the species' sensitivity to the toxicity. As mentioned above, limited irradiance or other factors could have affected the growth of the tested species and influenced the estimation of IC_{50} which was based on the SGR data. Interestingly, when considering only the grazer species, a negative relationship was revealed, though not statistically significant (P = 0.31, Fig. 3.4). This could suggest that the larger the grazer cell, the more sensitive it is to the toxicity of petroleum hydrocarbons. This sounds counterintuitive and, obviously, more data on the response of various protozoan species to increasing CEWAF concentrations are needed to draw a solid conclusion. A few possible scenarios that could support the observation are provided.

First, the intake of soluble petroleum hydrocarbons through ingestion of hydrocarbon-loaded prey items could have accumulated inside the cell body of grazers and hence strengthened the toxic effect on larger grazers. For instance, in a feeding experiment where female copepods of *Calanus helgolandicus* were exposed to ^{14}C-1-naphthalene, the uptake of the PAH through the ingestion of food particles (barnacle nauplii or diatoms) was much higher than the direct uptake from the culturing medium.

One third of the hydrocarbons remained inside the animals after 10 days, suggesting bioaccumulation and low elimination rates of the PAH for the copepods (Corner *et al.*, 1976). Liu *et al.* (2007) found approximately a 10-fold increase in the concentration of hexachlorobenzene in a majority heterotrophic plankton community than that in the ambient water of a river. This suggests a significant intake of hydrocarbons occurs through the dietary route rather than by passive diffusion or active transport through cell membrane. In fact, though the intake amount of hydrocarbons through ingestion of algal particles depends on the species-dependent bioconcentration (passive uptake) by the algal cells, the total intake amount by the grazers tend to be large for larger grazers since the *per capita* intake of prey biovolume increases with the predator's body size (DeLong & Vasseur, 2012). Therefore, larger grazers could be subject to a stronger bioaccumulation effect of toxicant through consuming more toxicant-loaded food items than smaller grazers, leading to their higher sensitivity to the toxic medium.

Second, some protistan species are known to have detoxification mechanisms. For example, Bamdad *et al.* (1997) showed that the ciliate *Tetrahymena pyriformis* was resistant to as high as 37 µM of individual PAHs (benzo[a]pyrene, 3-methylcholanthrene, benzanthracene, and 7,12-dimethylbenzanthracene) through rapid elimination. The organisms lost half of the accumulated hydrocarbons mostly within 60 min through an efflux mechanism. The elimination of accumulated hydrocarbons in other ciliates and dinoflagellate grazers is largely understudied, not to mention that the relationship between cell size and elimination efficiency is not well understood. Hence, it was possible that the inter-species variations in the ability to eliminate the accumulated toxicants contributed to the observed inverse relationship between CEWAF sensitivity and cell volume of protistan grazers in this study.

Taxonomy and sensitivity to CEWAF

Despite the reported taxon-dependent growth rates of protistan species under normal condition (Banse, 1982), the group-dependent vulnerability and changes in growth rates in response to the toxicity of CEWAF was not obvious. In this study, the

diatom *D. brightwellii* showed relatively high tolerance (IC_{50} ~170 µL L^{-1}, Table 3.4; equivalent to ~283 µg L^{-1} of TPAH50, Table 3.2) to hydrocarbon toxicity. Ozhan *et al.* (2014) reported higher tolerances of the diatoms species *D. brightwellii* and *Chaetoceros socialis* than the dinoflagellates *Heterocapsa triquetra*, *Pyrocystis lunala*, and *Scrippsiella trochoidea* to > 1200 ppb total petroleum hydrocarbons (TPH) (i.e. > ~1200 µg L^{-1}) from a mixture of South Louisiana sweet crude oil and Corexit EC9500A. However, in another study the same researcher reported the opposite pattern that *D. brightwellii* was more vulnerable than *H. triquetra* to the individual PAH components naphthalene and benzo[a]pyrene (Ozhan & Bargu, 2014c). The reported 50% growth inhibition concentrations of benzo[a]pyrene were 1.13 µg L^{-1} for *D. brightwellii* and 7.02 µg L^{-1} for *H. triquetra*, and those of naphthalene were 1011 µg L^{-1} for *D. brightwellii* and 1653 µg L^{-1} for *H. triquetra*. These studies demonstrated the mixed responses of phytoplankton to hydrocarbon toxicity in terms of taxon-dependency.

For protistan grazers, Almeda *et al.* (2014b) found higher vulnerability of ciliates species (*Strombidium* sp., *Spirostrombidium* sp., *Eutintinnus pectinis* and *Favella ehrenbergii*) than heterotrophic dinoflagellates species (*Gyrodinium spirale* and *Protoperidinium divergens*) in a 48-hour exposure to dispersant-treated crude oil. The same pattern, however, was not observed in this study. Among the protistan grazers tested, dinoflagellate species *O. marina* had the highest tolerance to CEWAF, despite the larger standard error in the IC_{50} estimation, while *Protoperidinium* sp. had the lowest IC_{50} of specific growth rate. The estimated IC_{50} values of ciliate species *Euplotes* sp. and *Metacylis* sp. fell between those of the two dinoflagellate grazers (Table 3.4).

Toxicity tolerance and associated bacteria

Species-specific growth responses to CEWAF exposure were observed on the tested protistan species. The diatom *D. brightwellii*, the cryptophyte *R. salina*, and the dinoflagellate *Protoperidinium* sp. showed decreasing specific growth rates (SGRs) with increasing CEWAF concentrations of up to 30 µL L^{-1}, while the decreasing trend of change in SGR was not observed on the haptophyte *I. galbana*, the dinoflagellates *P.*

sociale and *Z. microadriatica,* in the tested concentration range of CEWAF and led to poor model fit to the dose-response curve (Fig. 3.3). As mentioned above, some phytoplankton species are highly tolerant to petroleum hydrocarbons. *C. socialis, H. triquetra, P. lunala,* and *S. trochoidea* had an estimated 50% growth inhibition at concentrations of TPH at 1000-1800 ppb (i.e. ~1000-1800 μg L^{-1}) and of PAHs at 7-25 ppb (i.e. ~7-25 μg L^{-1}) (Ozhan *et al.*, 2014). One possible reason for the lack of decrease in SGRs for some species in our study was that these species could be highly tolerant to petroleum hydrocarbons toxicity and even the highest tested CEWAF concentration in this experiment (i.e. 30 μL L^{-1}, estimated to be ~50 μg L^{-1} of TPAH50, Table 3.2) was not high enough to cause a significant reduction in their growth. High tolerance of the algal cells could be mediated by antioxidant enzymes and non-enzymatic substances that counteract the damages by the reactive oxygen species produced in exposure to petroleum pollutants. Antioxidant enzymes include the superoxide dismutase, catalase, and glutathione peroxidase involved in the biochemistry of the photosystems (reviewed in Lesser, 2006) and non-enzymatic antioxidants include β-carotene pigment and vitamin E (Ozhan *et al*., 2015).

Apart from cell tolerance of the protist itself, the associated microbes of the algal cells could be responsible for the tolerance of the host cells by degrading the toxic hydrocarbons (Mishamandani *et al.*, 2016; Thompson *et al.*, 2017). Since all protistan species in this study were grown in non-axenic cultures, , their associated bacteria might comprise hydrocarbonoclastic species that were capable of breaking down the toxic compounds in the test media and potentially contributed to the tolerance to hydrocarbon toxicity of the host species. For example, Abed *et al.* (2010) reported that the addition of an aerobic heterotrophic bacteria strain that was phylogenetically related to known oil-degrading species to the cultures of the cyanobacterium *Synechocystis* sp. caused a 8-fold increase in the biomass of the cyanobacteria in hydrocarbon-loaded media. They further argued that the exudates of the cyanobacteria, in turn, facilitated the degradation activities of the heterotrophic bacteria. However, the causation relationship was not always evident for some algal species. Severin & Erdner (2019) found the presence of oil-degrading

bacteria associated with the dinoflagellates *Amphidinium carterae* and *P. sociale.* but the associated bacteria did not cause significant changes in the growth or photosynthetic performance of their host cells. Overall, more research could be done to investigate the contribution of the associated microbes of phytoplankton cells to the tolerance of their host cells.

Grazing responses when exposed to the combination of petroleum hydrocarbons and dispersant

Sub-lethal effects of petroleum hydrocarbons on protozoan grazing

Exposure to the soluble components of petroleum hydrocarbons caused the reduction in grazing activities of the grazers *O. marina*, *Protoperidinium* sp., and *Metacylis* sp. (Figs. 3.5 & 3.6). Among the soluble compounds, polycyclic aromatic hydrocarbons (PAHs) are considered Class 1 narcotic (non-ionic organic) chemicals (Hermens, 1989; Verhaar *et al.*, 1992), and those with relatively lower molecular weight are thought to be the most toxic to aquatic organisms (NRC, 2003; Boehm & Page 2007; Forth *et al.*, 2017a). The reduced grazing and ingestion rates of protozoan grazers in cultures could be a result of the toxic effects of petroleum hydrocarbons and (or) dispersant exposure that may alter the physiological and behavioral biology of the organisms (Connell *et al.*, 1981).

The Louisiana sweet crude oil used in this study contains high relative abundance of the PAHs naphthalene and phenanthrene (Table 3.2; Fig. 4.1 in Dissertation Chapter 4; Almeda *et al.*, 2013). These two PAHs are highly water soluble (31.0 g m^{-3} and 4.57 g m^{-3} for naphthalene and phenanthrene, respectively, Dabestani & Ivanov, 1999) and therefore were at high concentrations in the WAF and CEWAF media. Though the concentrations of PAHs were not directly determined, the concentrations of them in the CEWAF and WAF treatments were estimated based on published data (Forth *et al.*, 2017b). At the initial nominal concentration of 10 μL L^{-1} of CEWAF and WAF, there could be 11.2 μg L^{-1} of naphthalene and its alkylated homologs and 1.9 μg L^{-1} of

phenanthrene and its alkylated homologs in CEWAF and 1.2 μg L^{-1} of naphthalene and its homologs in WAF (Table 3.2). Naphthalene was shown to cause declines in motility, egg and fecal pellet production, clearance rate, and daily ration in the marine copepods *Paracartia grani* in a 4-day exposure at 130 μg L^{-1} (Calbet *et al.*, 2007) and *Oithona davisae* in a 24-hour exposure at ≥ 1000 μg L^{-1} (Saiz *et al.*, 2009). Phenanthrene was reported to cause impairment of embryogenesis and larval development of the oyster *Crassostrea gigas* in a 24-hour exposure at 2.0 μg L^{-1} (Nogueira *et al.*, 2017). A detergent component, the linear alkylbenzene sulphonate, was shown to reduce the swimming speed and the grazing rate of blue mussel larvae (Hansen *et al.*, 1997). The authors suspected that exposure to the chemical may have damaged the larval ciliary apparatus that is crucial for the animal's swimming behavior. Although scientific literature on the effects of soluble PAHs on the behavioral physiology of unicellular plankton is less available, presumably, the mechanistic steps in prey capture by protozoa, including searching, capture, processing, and ingestion (Montagnes *et al.*, 2008), could be interfered with by petroleum hydrocarbons exposure through the chemosensory and mechanosensory system pathways, and hence led to reduced grazing activity in the tested protozoa.

CEWAF is the most toxic among treatments

Exposure to either Corexit 9500A dispersant alone (Disp), Louisiana sweet crude oil alone (WAF), or a combination of crude oil and dispersant (CEWAF) at concentrations below 10 μL L^{-1} caused decline in grazing rates of the protistan grazers tested, except for *Euplotes* sp. (Figs. 3.5 & 3.6). In agreement with previous studies (Rogerson & Berger, 1981; Hemmer *et al.*, 2011; Jung *et al.*, 2012; Almeda *et al.*, 2014b; Ozhan *et al.*, 2014), a combination of crude oil and dispersant caused the most adverse effects to the protistan grazers *Protoperidinium* sp. and *Metacylis* sp. in general in this study. *Protoperidinium* sp. showed a greater drop in *per capita* ingestion rate in CEWAF (~45% drop) than in Disp (~10% drop) or WAF (~5% increase) media at 1 μL L^{-1} when compared to the Ctrl treatment. Similarly, *Metacylis* sp. showed zero *per capita* ingestion

rate (i.e. 100% drop) in both WAF and CEWAF media at 5 μL L^{-1} compared to the Ctrl treatment. While the Corexit 9500A dispersant itself can be toxic to aquatic species (George-Ares & Clark, 2000; Rico-Martinez *et al.*, 2013), the application of this dispersant to Louisiana sweet crude oil likely increased the water solubility and thus the bioavailability of petroleum hydrocarbons to the tested aquatic species (Fiocco & Lewis, 1999). Ozhan *et al.* (2014) reported a 50-fold increase in the concentration of TPH in South Louisiana sweet crude oil in the water column when Corexit EC9500A dispersant was added. In our study, at the initial nominal concentration of 5 μL L^{-1}, the estimated concentration of TPAH50 in the CEWAF treatment was 8.3 μg L^{-1}, which is approximately 10 times of that in the WAF treatment (Table 3.2) It is therefore reasonable that at the same nominal concentration, the CEWAF treatment containing higher concentration of water-soluble toxic components caused greater decline in grazing rate of the tested protozoan species than the WAF treatment.

However, the same pattern was not observed for *O. marina* and *Euplotes* sp., where the grazing rates did not differ significantly ($P > 0.05$) among the Disp, WAF and CEWAF treatments at the exposed nominal concentrations (Fig. 3.5). For the dilution experiment at 10 μL L^{-1} of crude oil and 0.5 μL L^{-1} of dispersant, the exposure to the CEWAF test medium caused near zero population growth and grazing mortality rates of *I. galbana* (Fig. 3.5), which was contradicting the results of SGRs at the same exposure concentration where mono-specific culture of *I. galbana* obtained a mean SGR of 0.39 d^{-1} (Fig. 3.1). As discussed above, the associated bacteria or the pelagic bacteria in the cultures could have contributed to the degradation of the toxic compounds of petroleum hydrocarbons and thus the increased toxicity tolerance of the algal host cells. It could therefore have contributed to the tolerance of *I. galbana* to 10 μL L^{-1} CEWAF in the mono-specific culture in the SGR experiment. On the other hand, in the dilution experiment, though the grazing mortality of *I. galbana* by *O. marina* was near zero at 10 μL L^{-1} CEWAF, *O. marina* is reported to graze on bacteria as well (reviewed in Guo *et al.*, 2013), which could include the oil-degrading bacteria related to the tolerance of *I. galbana* to CEWAF. With the helpful bacteria being grazed down by *O. marina*, *I.*

galbana in the dilution experiment could therefore showed susceptibility to CEWAF toxicity and obtained a near zero growth rate. Meanwhile, in the dilution experiment, *O. marina* could be mainly consuming the bacterial prey and therefore its grazing rate towards the algal prey were negligible in exposure to crude oil pollutants.

Gross growth efficiency apparently not affected by hydrocarbon pollutants

The gross growth efficiency (GGE) represents the conversion fraction of prey carbon consumed to the predator carbon. The GGEs of *Metacylis* sp. in the Ctrl and Disp treatments were 0.44 and 0.40 (Table 3.5), respectively, which were within the reported range of 0.26-0.49 of the tintinnid ciliate *Favella taraikaensis* feeding on the dinoflagellate *Alexandrium tamarense* (Kamiyama *et al*., 2005). For *Protoperidinium* sp., the GGEs in the Ctrl, WAF, and CEWAF treatments were at similar levels of 0.17-0.20 (Table 3.4). These GGEs were within the range reported by Buskey *et al*. (1994) that the dinoflagellate *Protoperidinium huberi* feeding on *D. brightwellii* had GGEs ranged from 0.17 to 0.59, with a decreasing trend at higher food concentrations. The abnormality of GGE in the Disp treatment was caused by the unexpectedly low growth rate of the grazers (Fig. 3.6). As explained above, the low growth rate was resulted from averaging all the positive and negative values. If only the positive value is used, the growth rate in the Dips treatment would be 0.29 d^{-1} and the corresponding GGE would be 0.20.

The similar GGEs of the grazers *Protoperidinium* sp. and *Metacylis* sp. among the various treatments suggested that the conversion of prey carbon to predator carbon by the grazers was not affected by crude oil and dispersant at the tested concentrations (Table 3.5). It implies that the difference in the growth of grazers among treatments was due to the different degrees of hindrance to the grazing of grazers, that is, the total carbon intake from prey items, but not the toxic effect of hydrocarbons on the growth mechanisms *per se*. However, as also acknowledged by other studies (Ohman & Snyder, 1991; Buskey *et al*., 1994), our results should be interpreted with caution. We did not directly determine the carbon:volume ratio of the prey and grazers but relied on the conversion factors in the literature. Although we kept the prey densities at the start of the incubation experiment at

similar levels for the 4 treatments and used the geometric mean densities of prey and grazers for calculation of IRs, the prey densities at the end of experiment varied greatly among treatments (data not shown) due to the differential vulnerability to potential toxicants in different treatments. This might lead to incomparability of GGEs among treatments since GGE tends to change with food concentrations (Straile, 1997).

Implications of impaired protozoan grazing by petroleum hydrocarbons exposure

Overall, this study provided evidence of the differential sensitivities of protistan species in cultures (both algal prey and grazers) towards petroleum hydrocarbons. In the > 5-day exposure to CEWAF in the growth responses experiments, the varying toxicity tolerance between the grazer and the prey and the impairment of grazing activities by the grazers led to the increased abundance and accumulation of algal prey in the incubation containers of grazers. For instance, the grazer cultures of *Protoperidinium* sp. and *Metacylis* sp. had higher ratios of final:initial prey density at high CEWAF concentrations (≥ 1 and ≥ 15 $\mu L\ L^{-1}$, respectively) than those in the Ctrl treatment (Table 3.3). In other words, algal prey species were released from grazing of the protozoan grazers and given opportunities to proliferate in exposure to petroleum hydrocarbons due to the differences in vulnerability between the grazer and the prey. The more important question is, could such differences potentially lead to phytoplankton blooms in the field? To answer the question, one should consider: 1) the differentiation in toxicity vulnerability is dependent on the grazer-prey pairs; 2) cultures in controlled incubation conditions in the laboratory had high initial prey cell densities and nutrients enrichment; 3) laboratory cultures excluded the dilution and mixing effects to the plankton assembly which may affect the prey cell patches in the field; 4) laboratory cultures neglect the grazing impact from predators other than protozoan grazers on the algal prey population; 5) the concentrations of petroleum hydrocarbons in the field after an oil spill could be much higher that both the grazers and algal prey are severely affected; and so on. Without a solid answer to each of the questions, we can only argue that the differential

vulnerability between grazers and prey led to the accumulation of prey cells in laboratory cultures.

Nevertheless, there are studies showing the possible linkage between a disrupted top-down control by protozoa and the potential for the formation of algal blooms in mesocosm studies or in the field (Johansson *et al.*, 1980; Riaux-Gobin, 1985; Sheng *et al.*, 2011; Tang *et al.*, 2019). In another study, we found a mismatch between phytoplankton growth and microzooplankton grazing in a mesocosm study when a natural plankton community was exposed to chemically dispersed crude oil (Dissertation Chapter 4). Although an accumulation of phytoplankton cells (as reflected by Chl-*a* concentration) was not observed, phytoplankton growth recovered on the 6th day of pollutants exposure while microzooplankton grazing remained negligible. Almeda *et al.* (2018) monitored the abundance of bloom forming protistan species in exposure to petroleum hydrocarbons in the northern Gulf of Mexico and suggested that disrupted predator-prey interaction resulted from oil spills and dispersant application could indirectly induce potential harmful algal blooms. However, there are occasions when the linkage between algal proliferation and oil pollution is not obvious. For examples, Hu *et al.* (2011) used satellite data and numerical modelling to investigate the relationship between the Deepwater Horizon oil spill in 2010 and the anomalies of the fluorescence-based detection of phytoplankton biomass after the spill event. Unfortunately, there was not enough direct evidence to support their hypothesis.

CONCLUSIONS

In exposure to 0-30 μL L^{-1} of CEWAF, protistan species showed varying growth responses when exposed to the soluble components of petroleum hydrocarbons. Algal prey *R. salina* and grazers *Protoperidinium* sp. and *Metacylis* sp. showed high sensitivity while diatom prey *D. brightwellii* were highly tolerant. The relationship between toxicant sensitivity and cell size or taxonomic grouping of the protistan species was not strong. In terms of the sub-lethal effect on reducing the grazing activity of protozoan species, a combination of crude oil and dispersant (i.e. CEWAF) caused more negative effect to the

grazers *Protoperidinium* sp. and *Metacylis* sp. than that by dispersant alone or crude oil alone. Proliferation and accumulation of prey cells in predator-prey mixture upon CEWAF exposure was observed when protozoan grazing was impaired. It suggested that algal prey could be alleviated from the toxicant-impaired grazing by predators due to the vulnerability difference between the grazer and the prey.

ACKNOWLEDGEMENTS

We are thankful to Cammie Hyatt for providing some of the protist cultures. Our gratitude to Dr. Paul Zimba for the usage of the microscope in the laboratory as well. This research was made possible by a grant from The Gulf of Mexico Research Initiative. Data are publicly available through the Gulf of Mexico Research Initiative Information & Data Cooperative (GRIIDC) at https://data.gulfresearchinitiative.org.

Plankton species	Class	*Estimated cell volume ±1 S.D. (μm^3)	Algal prey added
Isochrysis galbana	Prymnesiophyceae	4±2 x10	NA
Rhodomonas salina	Cryptophceae	21±7 x10	NA
Zooxanthella microadriatica	Dinophyceae	40±14 x10	NA
Peridinium sociale	Dinophyceae	49±20 $x10^2$	NA
Ditylum brightwellii	Bacillariophyceae	94±39 $x10^2$	NA
Oxyrrhis marina	Dinophyceae	26±13 $x10^2$	*I. galbana*
Euplotes sp.	Spirotrichea	21±8 $x10^3$	*R. salina*
Metacylis sp.	Oligotrichea	19±5 $x10^4$	*P. sociale & Z. microadriatica*
Protoperidinium sp.	Dinophyceae	23±4 $x10^4$	*D. brightwellii*

Table 3.1 Protozoan grazers and their corresponding algal prey in culture. * Estimation based on the geometric models in Sun & Liu (2003) (see Methodology for details). NA represents data not applicable.

	CEWAF									WAF				
Nominal concentration (μL L^{-1})	1	3	5	10	15	20	30	100	200	1	3	5	10	30
Nominal loading (mg L^{-1})	0.8	2.5	4.2	8.4	12.6	16.8	25.2	83.9	168	0.8	2.5	4.2	8.4	25.2
Estimated concentration (μg L^{-1})														
TPAH50	1.7	5.0	8.3	16.6	24.9	33.2	49.9	166	332	0.2	0.5	0.8	1.6	4.9
Chr	0.0	0.1	0.1	0.3	0.4	0.6	0.9	3.0	6.0	0.0	0.0	0.0	0.0	0.0
C/T	0.0	0.0	0.0	0.0	0.0	0.1	0.1	0.3	0.6	0.0	0.0	0.0	0.0	0.0
Flo	0.1	0.3	0.5	1.1	1.6	2.1	3.2	10.6	21.3	0.0	0.0	0.0	0.0	0.1
F/P	0.0	0.1	0.2	0.3	0.5	0.6	0.9	3.2	6.3	0.0	0.0	0.0	0.0	0.0
Nap	1.1	3.4	5.6	11.2	16.8	22.4	33.6	112	224	0.1	0.4	0.6	1.2	3.7
Phe	0.2	0.6	1.0	1.9	2.9	3.9	5.8	19.5	38.9	0.0	0.0	0.0	0.0	0.1

Table 3.2 Estimated initial concentrations of total PAHs (TPAH50) and the components of PAHs in the CEWAF and WAF treatments. Chr: C1-C4 chrysenes; C/T: chrysene + triphenylene; Flo: fluorenes + C1-C3 fluorenes ; F/P: C1-C4 fluoranthenes/pyrenes; Nap: naphthalene + C1-C4 naphthalenes; Phe: phenanthrene + C1-C4 phenanthrene/anthracenes.

CEWAF (µL L^{-1})	*Protoperidinium* sp. feeding on *D. brightwellii*		*Metacylis* sp. feeding on *Z. microadriatica*	
	Initial prey density (cells mL^{-1})	Ratio of final:initial prey density	Initial prey density (cells mL^{-1})	Ratio of final:initial prey density
0		31.1		0.0
1		40.8		0.0
5	49.9±4.5	40.5	270.0±224.1	0.1
15		41.5		2.0
30		36.6		1.7

Table 3.3 Mean initial prey cell densities (±1 S.D.) and the final:initial prey density ratios of *Protoperidinium* sp. and *Metacylis* sp. with > 5 days exposure to CEWAF.

Species	Estimated IC_{50} ($\mu L\ L^{-1}$)	Lack-of-fit test (*P* value)	No-effect test (*P* value)
I. galbana	0.7 (32.1)	0.002	0.979
R. salina	**0.9** (3.3)	0.714	0.028
D. brightwellii	**168.7** (67.0)	0.528	0.000
P. sociale	2.5 (4045.8)	0.001	0.241
Z. microadriatica	0.0 (0.2)	0.805	0.991
O. marina	297.1 (147160)	0.700	0.807
Euplotes sp.	**26.1** (17.4)	0.949	0.056
Protoperidinium sp.	**1.1** (0.8)	0.746	0.000
Metacylis sp.	**5.9** (4.1)	0.116	0.000

Table 3.4 Estimated IC_{50} (S.E.) of the SGRs of experimental organisms with exposure to CEWAF. The lack-of-fit *F* test with $P < 0.05$ indicates there is a lack of fit in the logistic model. No-effect chi-square test with $P > 0.05$ indicates there is no dose effect on the response (i.e. SGR) within the tested concentration range of CEWAF. Bold IC_{50} value denotes a good fit to the log-logistic model of the protistan species.

	Protoperidinium sp.	*Metacylis* sp.
Ctrl	0.17	0.44
Disp	0.03	0.40
WAF	0.19	NA
CEWAF	0.20	NA

Table 3.5 Estimated GGEs of *Protoperidinium* sp. and *Metacylis* sp. in various treatments. NA represents data not available due to the negative IR rates of the grazers.

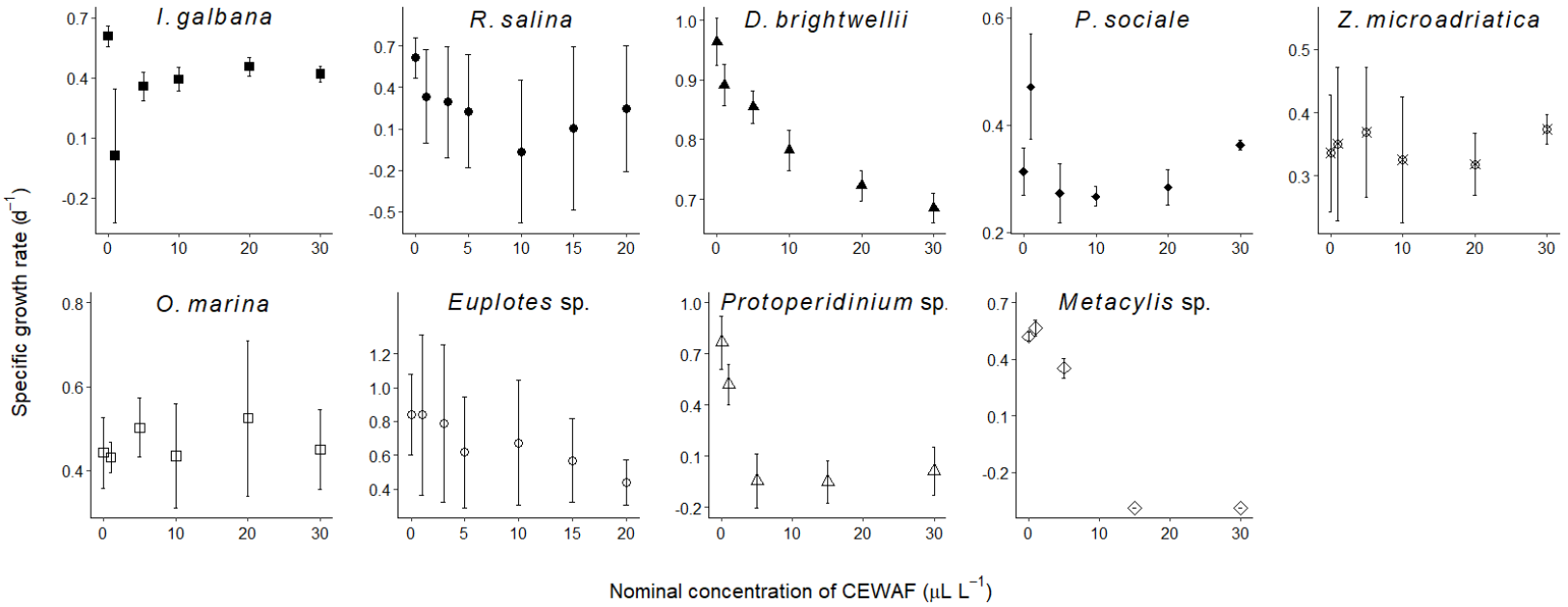

Figure 3.1 Mean specific growth rates (±1 S.D.) of algal prey and protozoan grazers in exposure to the nominal concentrations of CEWAF.

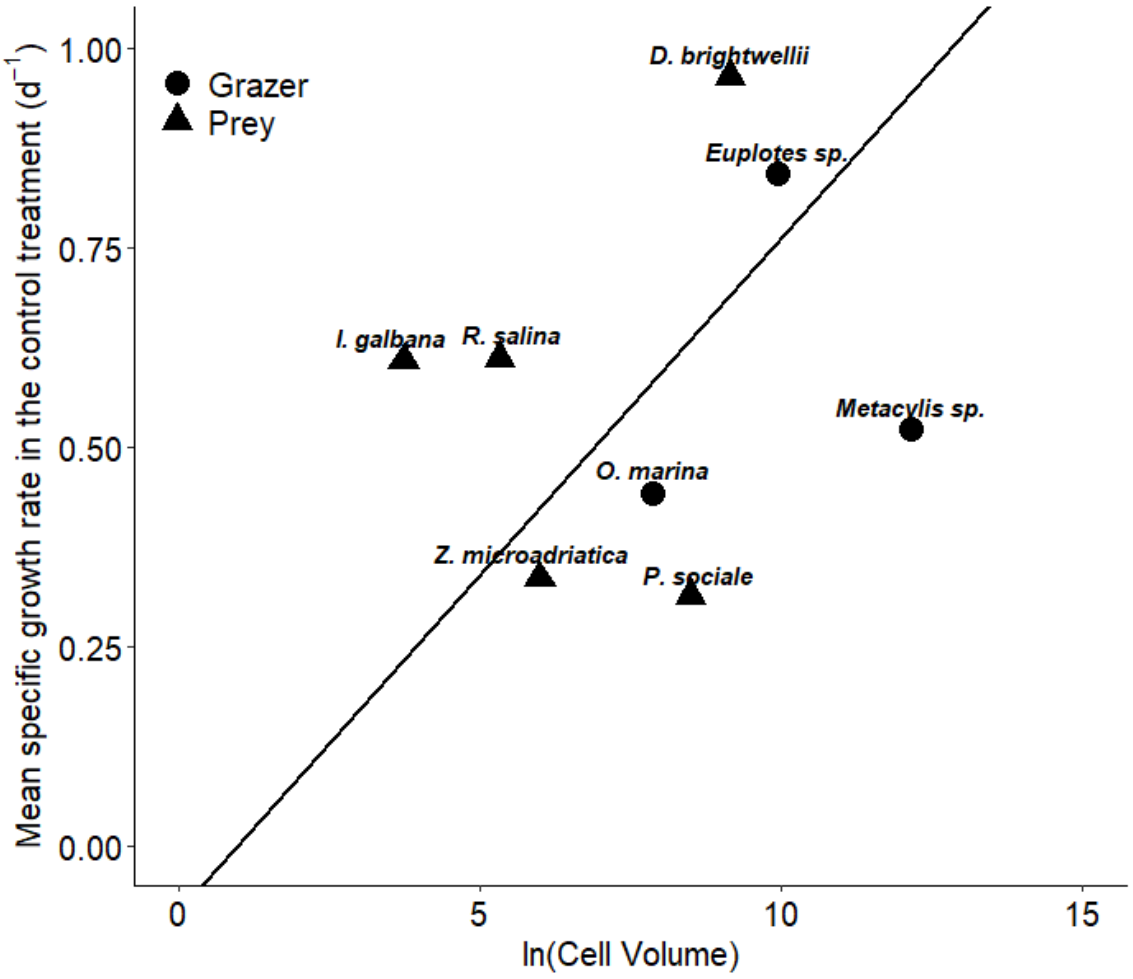

Figure 3.2 Model II standard major axis regression between the natural-log of cell volumes and mean specific growth rate in the control treatment (0 µL L^{-1} of CEWAF) of planktonic species grown at 20°C (solid line: R^2 = 0.04, P = 0.64).

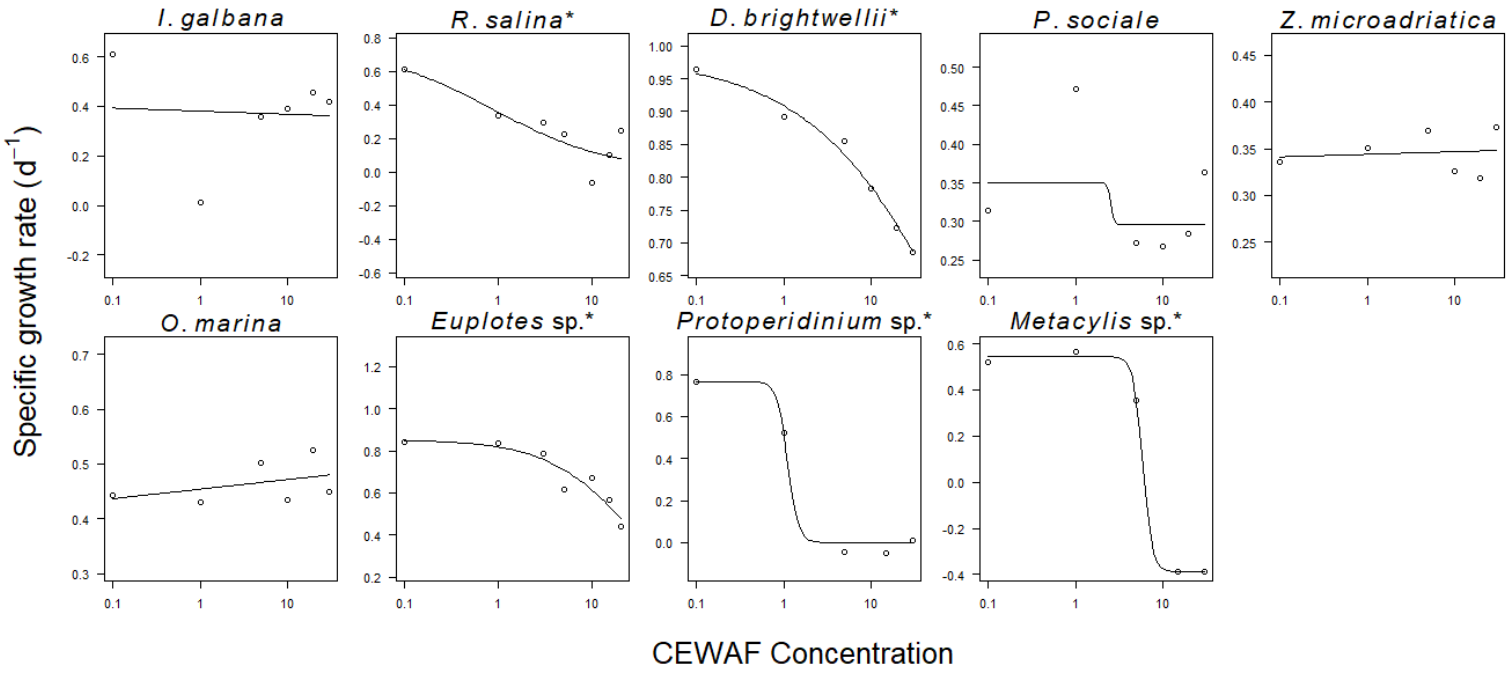

Figure 3.3 Fitted log-logistic model of the mean SGRs of algal prey and protistan grazer species in exposure to CEWAF. * denotes good model fit of the SGR data (see Table 3.4 for details).

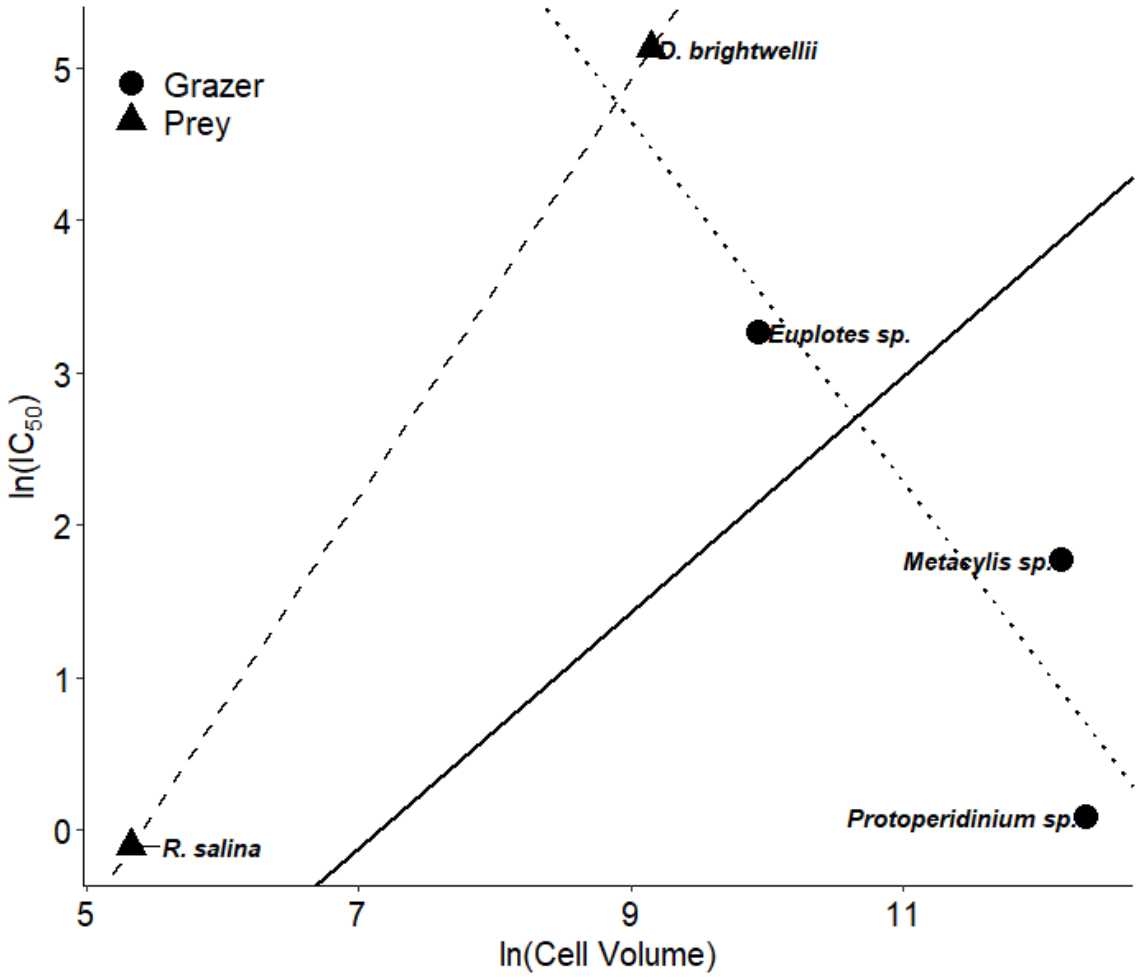

Figure 3.4 Model II standard major axis regression between the natural-log of cell volume and the natural-log of IC_{50} of prey species (dashed line: $R^2 = 1.00$, P = not available), grazer species (dotted line: $R^2 = 0.77$, $P = 0.31$), and all protistan species (solid line: $R^2 = 0.01$, $P = 0.89$) in CEWAF exposure.

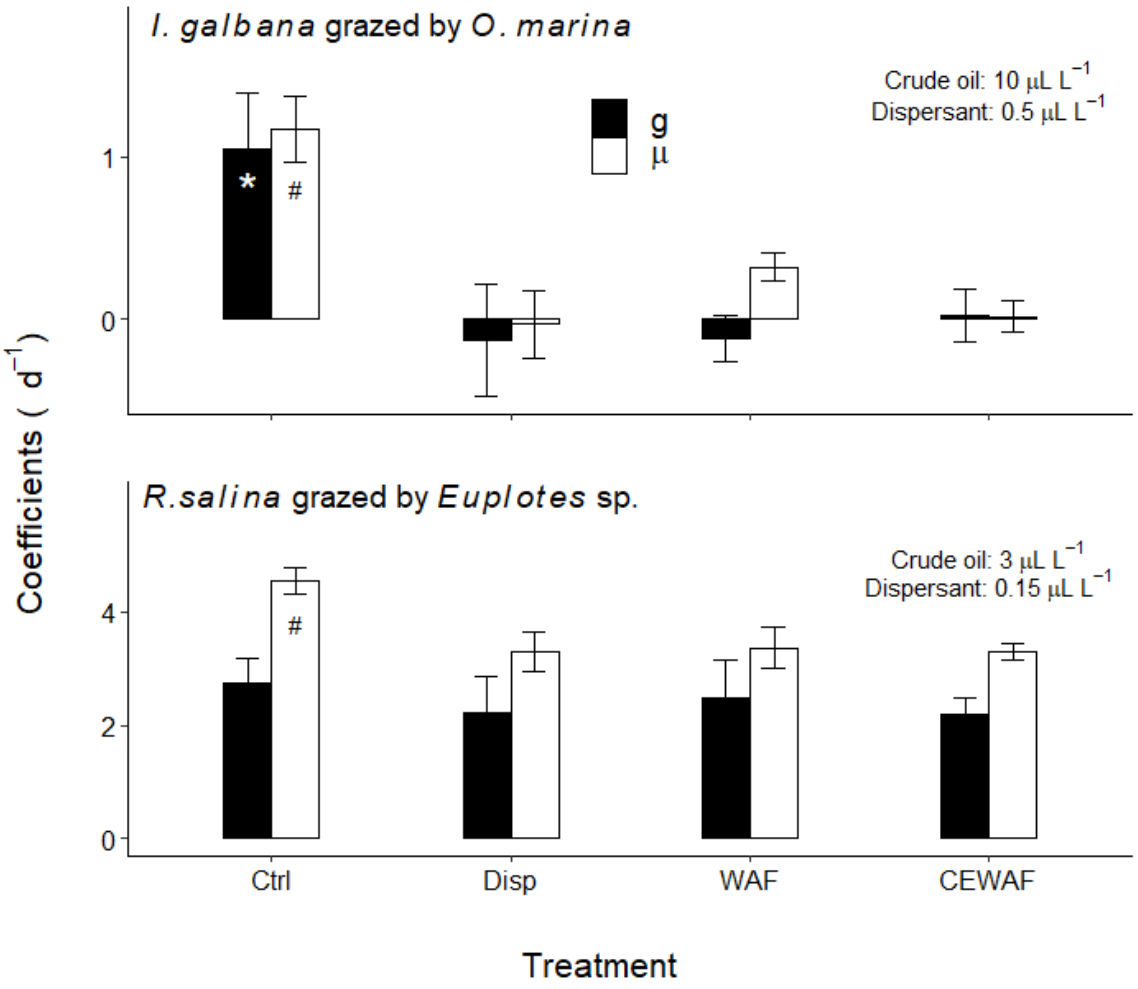

Figure 3.5 Coefficients (S.E.) of grazing mortality (g, filled bar) and population growth (µ, empty bar) of *I. galbana* by grazer *O. marina*, and *R. salina* by grazer *Euplotes* sp. in exposure to different treatments. Symbols "*" and "#" represent significant ($P < 0.05$) statistical difference among treatments for the coefficients g and µ, respectively.

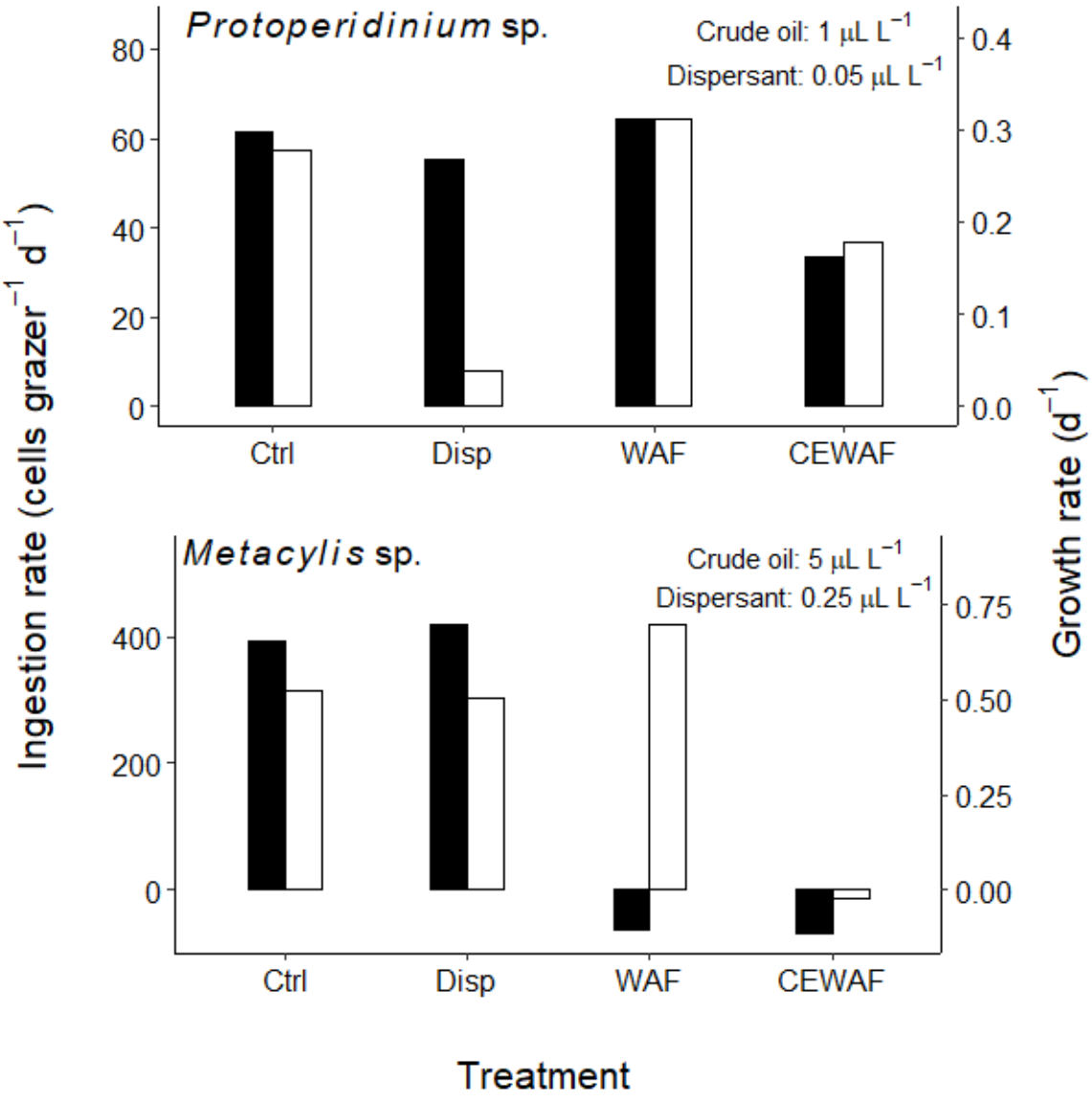

Figure 3.6 Ingestion (filled bar, left y-axis) and growth rates (empty bar, right y-axis) of *Protoperidinium* sp. fed on *D. brightwellii* and of *Metacylis* sp. fed on *Z. microadriatica* and *P. sociale* in exposure to different treatments.

Chapter 4. Microzooplankton Herbivory Reduced by Petroleum Pollutants in a Mesocosm Study

ABSTRACT

Microzooplankton are major consumers of phytoplankton and essential components in the biogeochemical cycling of carbon and nutrients in the oceans. However, their ecological functions in marine ecosystems could be substantially affected by crude oil pollution originating from anthropogenic activities, such as disastrous oil spills, or chronic natural seeps that occur in various regions of the ocean. Since on-site measurement of its effects on microzooplankton immediately after crude oil exposure is not always possible, a mesocosm study simulating an oil spill incident was conducted to investigate its effects on the grazing impact of microzooplankton on phytoplankton. A natural plankton community was exposed to 10 µL L^{-1} of chemically dispersed crude oil (DOil) in outdoor mesocosms for 7 days, with control (Ctrl) mesocosms set up for comparison. Dilution experiments were conducted to estimate the grazing rates of microzooplankton on the 2nd and 6th days of pollutants exposure. Results based on chlorophyll-*a* concentrations revealed that microzooplankton grazing rates in the Ctrl mesocosms ranged from 0.4-2.3 d^{-1} on the 2nd and 6th days. There was a lack of obvious microzooplankton grazing in the DOil mesocosms on both days, as reflected by negative grazing rates. While the coefficients of *in situ* phytoplankton growth rates in the Ctrl mesocosms average -0.32 d^{-1} and 1.68 d^{-1} on Days 2 and 6, respectively, , those in the DOil mesocosms were negative on the 2nd Day but averaged 2.16 d^{-1} on the 6th day. A significantly positive relationship between *in situ* phytoplankton growth and microzooplankton grazing rates was found in the Ctrl treatment but not in the DOil treatment. This suggests a de-coupling between phytoplankton growth and microzooplankton in oil-polluted seawater.

INTRODUCTION

Microzooplankton (20-200 μm) are important consumers of primary production (Strom *et al.*, 2001) that are capable of consuming > 60% of primary production daily in areas including open oceans, coastal region and estuaries (Calbet & Landry, 2004; Calbet, 2008). They are an essential food source of mesozooplankton as well (Stoecker & Capuzzo,1990; Calbet & Saiz, 2005). Toxic hydrocarbon components of crude oil cause lethal and sub-lethal effects on marine planktonic organisms that eventually change the abundance and composition of the plankton community (Dahl *et al.*, 1983; Sargian *et al.*, 2005; Gonzalez *et al.*, 2009; Gilde & Pinckney, 2012). For example, the water-soluble fraction of diesel fuel oil increased the abundance of bacterivorous nanoflagellates but decreased the abundance of micro- and mesozooplankton (Koshikawa *et al.*, 2007). In a mesocosm study, exposure to dispersed crude oil drastically increased abundance of bacteria and heterotrophic flagellates and sharply reduced that of phytoplankton and zooplankton within the first 2 days (Jung *et al.*, 2012).

Crude oil released into aquatic ecosystems originates from sources such as natural seeps and incidents of leaks, oil spills, and discharges related to anthropogenic activities. The combined amount of pipeline and oil tank spills from 1990 to 1999 averaged 112 kilotons annually, accounting for 9% of total crude oil entering the marine environment (Burgherr, 2007). During real-world oil spill events, however, the immediate effects of petroleum pollutants on microzooplankton are not well understood due to the delay in detection of spill incidents or difficulties in getting to the spill site promptly. While previous studies focused only on the changes in abundance and composition of planktonic organisms in reaction to crude oil pollutants, the effect of crude oil and dispersants on the trophic interactions of natural assemblages of microzooplankton is rarely investigated.

In this study, we simulated an oil spill in outdoor mesocosms containing natural whole seawater to test the hypothesis that oil pollutants adversely interfere with the trophic interaction of microzooplankton. This study is one of the few that focused directly

on the effect of oil pollution on the grazing impact of microzooplankton on phytoplankton in semi-controlled conditions.

METHODOLOGY

Mesocosm set-up and sampling

Six 500 L mesocosms (3 for the control treatment and 3 for the oil-spill treatment) containing whole seawater (WSW) from Ship Channel (Port Aransas, Texas) were set-up at the Fisheries and Maricultural Laboratory of the Marine Science Institute in May 2017. To maintain steady water temperature, all mesocosms were partially submerged into a rectangular trough with circulating water connected to a water cooler set at 25°C. To avoid damaging delicate planktonic organisms, artificial mixing by aeration was not employed in the mesocosms. Instead, seawater in mesocosms was manually mixed using paddles twice daily. Water temperature and salinity of the control treatment mesocosms were measured occasionally throughout the experimental period.

To simulate an oil spill incident in the sea, three of the mesocosms were dosed with chemically dispersed crude oil (DOil) one hour after filling-in with WSW. Light Louisiana Sweet crude oil mixed with Corexit 9500A dispersant at a volume ratio of 20:1 was used. The non-weathered crude oil and dispersant were stored in capped glass bottle in darkness at ~4°C and warmed at room temperature for ≥ 1 hour before use. The DOil mixture was pre-mixed using a magnetic stir-bar (at ~20-25% vortex) for one hour in a 1 L glass capped aspirator bottle with 0.2 µm filtered seawater in darkness at room temperature. The mixture was then added into the mesocosm to make the final nominal concentrations of crude oil and dispersant to be 10 µL L^{-1} and 0.5 µL L^{-1}, respectively. Control (Ctrl) mesocosms containing WSW without the addition of DOil were set-up in triplicate for comparison.

Concentrations of petroleum hydrocarbons

Triplicate 40 mL water samples were collected below the surface from each DOil mesocosm for identification and quantification of polycyclic aromatic hydrocarbons (PAHs) and total petroleum hydrocarbon (TPH) at several time points: immediately after addition of pre-mixed DOil (as Day 0), on Day 1, Day 3, and Day 7. Hydrocarbon analyses using gas chromatography mass spectrometry were conducted by ALS Environmental (Houston, Texas).

The petroleum hydrocarbon concentrations were further processed to obtain the degradation rates of PAHs. By assuming the degradation follows a first order reaction kinetics, the rate constant of degradation of each PAH component was computed as

$$C_t = C_0 e^{-kt} \qquad \text{Eqn 4.1}$$

where C_t is the instantaneous concentration at different time points and C_0 is the initial concentration. The character k represents the rate constant and t represents time in days. The coefficient of k was estimated as the negative value of the slope of the linear regression of ln(Ct) against t. The half-life in days of the PAH component was calculated as ln(2)/k.

Chlorophyll-*a* concentrations and microzooplankton herbivory

To investigate the grazing impact of microzooplankton on phytoplankton under the influence of petroleum pollutants, dilution experiments (Landry & Hassett, 1982) were conducted on Days 2 and 6 to estimate the coefficients of population growth (μ) and grazing mortality (g) of phytoplankton in the mesocosms. WSW from each mesocosm was collected in the sub-surface (~0.5 m depth) using a Van Dorn water sampler, transported to the laboratory and processed within one hour. A portion of the WSW was filtered through GF/F filters (0.7 μm porosity, Whatman) to obtain filtered seawater (FSW). The remaining WSW was filtered through 200 μm mesh to remove large plankton and detritus. Dilutions fractions of 10%, 37%, 100% of WSW in duplicate were prepared by mixing 200 μm filtered WSW and FSW accordingly. Nutrient amendments

of nitrate (NO_3^-), phosphate (PO_4^{3-}), and silicate (SiO_3^{2-}) were added to each dilution fraction to make the final concentrations in the 125 mL glass incubation bottles exceed 0.88 mM, 0.036 mM, and 0.1 mM, respectively. Dilution fraction of 100% (i.e. undiluted) without nutrient amendment was prepared in duplicate to estimate *in situ* growth rate of phytoplankton (μ_0) in mesocosms. All incubation bottles were incubated in the outdoor rectangular trough in the sub-surface (~0.5 m depth) for 24 hours. The bottles were manually inverted upside-down a few times for mixing during the incubation period.

Chlorophyll-*a* (Chl-*a*) concentrations of each dilution fraction before and after incubation were determined by filtering 10 mL of water sample onto GF/F glass fiber filters. The filters were then extracted for photosynthetic pigments with 90% acetone in darkness at 4°C for 24 hours. Concentrations of Chl-*a* were measured using a Trilogy Spectrometer (Turner Designs) with a Chl-NA Module. Coefficients of population growth (μ) and grazing mortality (g) of phytoplankton of the enriched bottles were estimated according to method of Landry & Hassett (1982) based on the Chl-*a* concentrations. Coefficients of *in situ* phytoplankton growth were calculated using the growth rate of the 100% unamended bottles with correction for microzooplankton grazing when a statistically significant positive grazing was found in the dilution experiment. A subsample of 40-50 mL from each incubation bottle was preserved with acidic Lugol's solution (~5% final concentration) for identification and enumeration of phytoplankton and microzooplankton.

Statistical analysis

All statistical analyses and graphical presentations were conducted using R version 3.6.1 (R Core Team, 2019) and packages *lmodel2* version 1.7-3 (Legendre, 2018), *ggplot2* version 3.2.1 (Wickham, 2016), and *ggforce* version 0.3.2 (Pedersen, 2020).

Model II linear regressions tests (with 50,000 permutations) were applied to test for the presence of a significant relationship between the *in situ* population growth and

grazing mortality rates of phytoplankton in the Ctrl and DOil treatments using the package *lmodel2* in R. Considering that the independent variables (i.e. the *in situ* population growth rate) were subject to natural variation and measurement error and both variables were in comparable units of measurement, results from the major axis regression analysis was chosen for further presentation and discussion of results (Sokal & Rohlf, 2012).

RESULTS

Temperature, salinity of seawater and concentration of PAHs in mesocosms

The temperature of seawater inside the Ctrl mesocosms ranged from 20.6-25.9 °C on average during the experiment period. Salinities of the Ctrl mesocosms increased from 30.6 PSU on Day 0 to 32.1 PSU on Day 6 on average (Table 4.1).

The concentrations of TPH averaged 16.6 mg L^{-1} on Day 0 and dropped to 6.1 mg L^{-1} on Day 1. The concentrations were below the detection limit of 0.19 mg L^{-1} on Days 3 and 7 (Fig. 4.1). The concentration of naphthalene on Day 0 was 4.2 µg L^{-1} (Table 4.2). It dropped to 3.6 µg L^{-1} on Day 1 and to < 0.1 µg L^{-1} on Day 7 (Fig. 4.1). Phenanthrene was the most abundant component of PAHs of the crude-oil-dispersant mixture used in the experiment. Immediately after addition of pre-mixed DOil into the mesocosms, the average concentration of phenanthrene, fluorene, and chrysene were 13.3 µg L^{-1}, 3.3 µg L^{-1}, and 1.6 µg L^{-1}, respectively, on Day 0 (Table 4.2). The concentrations of phenanthrene and fluorene dropped drastically to approximately 9% and 17%, respectively, within one day. On Day 7, the average concentrations of these 2 components were 0.3 µg L^{-1} and 0.1 µg L^{-1}, respectively, while concentrations of other PAH components were mostly below the detection limit of 0.1 µg L^{-1} (Fig. 4.1). Except for Benzo[a]pyrene, the rate constants of degradation of other PAH components ranged from 0.30 d^{-1} to 0.70 d^{-1}, and the half-lives of all components ranged from 0.7 to 2.3 days (Table 4.2).

Chlorophyll-*a* concentration and abundance of plankton

Chlorophyll-*a* (Chl-*a*) concentration was used as a proxy to reflect the abundance of phytoplankton. Unexpectedly, Chl-*a* concentrations were highly variable among mesocosms of the same treatment on both days, particularly in the DOil mesocosms. On Day 2, the Chl-*a* levels ranged from 0.15-3.50 µg L^{-1} in the DOil mesocosms and from 1.41-3.59 µg L^{-1} in the Ctrl mesocosms (Fig. 4.2). Such great variation in the Chl-*a* levels could be due to the natural variation that was introduced during the set-up of mesocosms when natural seawater was collected directly from the Ship Channel and filled into the mesocosms. On Day 6, the average Chl-*a* concentration in the Ctrl mesocosms was higher than that in the DOil mesocosms, reflecting relatively higher abundance of pigmented plankton in the Ctrl mesocosms (Fig. 4.2).

Unfortunately, some of the preserved plankton samples were lost in storage due to Hurricane Harvey in 2017. Enumeration of available samples revealed that the mean cell densities of microplankton grazers including aloricate ciliates (1 cells mL^{-1} in the Ctrl mesocosms and 0-0.8 cells mL^{-1} in the DOil mesocosms), loricate ciliates (0-2 cells mL^{-1} in the Ctrl mesocosms and 0 cells mL^{-1} in the DOil mesocosms), and dinoflagellates (3-8 cells mL^{-1} in the Ctrl mesocosms; 0-3.5 cells mL^{-1} in the DOil mesocosms) were relatively low in the DOil treatment (Table 4.3). There was a predominance of unidentified cells (< 5 µm) in both treatments on Day 6, with mean cell densities as high as up to 3 orders of magnitude greater than those of diatoms and dinoflagellates (Table 4.3).

Microzooplankton herbivory and phytoplankton growth

Coefficients of population growth (µ) and grazing mortality (g) of phytoplankton were estimated based on Chl-*a* concentrations. Even though some of the estimated grazing coefficients were not statistically significant or only marginally significant (P > 0.05, Table 4.4), coefficient g in the Ctrl mesocosms ranged from 0.36-1.38 d^{-1} on Day 2 and from 1.00-2.28 d^{-1} on Day 6 while coefficients µ ranged from1.61-1.89 d^{-1} on Day 2

and from 2.25-3.12 d^{-1} on Day 6. When both days are considered, *in situ* phytoplankton growth coefficients (μ_0) in the Ctrl mesocosms ranged from -0.44 d^{-1} to 2.86 d^{-1} and were always lower than the corresponding μ (Table 4.4). On the other hand, coefficient μ was negative on Day 2 in the DOil mesocosms while they varied widely from -0.28 d^{-1} to 2.15 d^{-1} on Day 6. Unexpectedly, coefficient μ_0 was mostly higher than the corresponding μ in the DOil mesocosms. In the DOil mesocosms, the coefficient μ_0 averaged 0.40 d^{-1} on Day 2 and 2.16 d^{-1} on Day 6. Coefficient g in the DOil mesocosms on Days 2 and 6 were all negative (Table 4.4), indicating negligible grazing impact of microzooplankton. Model II linear regression (major axis) between coefficients g and μ_0 revealed a statistically significant relationship in the Ctrl mesocosms ($g = 0.47\mu_0 + 0.91$; $R^2 = 0.63$; $P < 0.05$) but not in the DOil mesocosms ($g = -0.20\mu_0 - 1.23$; $R^2 = 0.15$; $P = 0.22$) (Fig. 4.3).

DISCUSSION

Simulation concentration and the rapid loss of petroleum hydrocarbons

In real oil spill incidents in the oceans, the concentration of spilled oil in the water column depends on the total amount of the oil released into the environment and the various factors that affect the transport, distribution, and fate of the oil (NRC, 2003). For example, the reported range of the dissolved/dispersed crude oil in the surface water found at sites near the *Prestige* oil spill in Spain days after the incident was from 0.19-28.8 μg L^{-1} (Gonzales *et al.*, 2006). Other researchers reported higher concentrations of total soluble hydrocarbons in the same spill, with the highest concentration of 140 μg L^{-1} shortly after the spill and a peak concentration of 75 μg L^{-1} months later (Bode *et al.*, 2006). A more disastrous oil spill occurred in the Gulf of Mexico in 2010. It was estimated that a total of 4.9 million barrels (~779,000 metric tons) of oil were released during the *Deepwater Horizon* spill event (Kerr, 2010), which was much higher than the total amount of spilled oil in the *Prestige* disaster (> 60,000 metric tons, Garcia-Soto, 2004). Conceivably, the concentrations of soluble hydrocarbons at sites near the *Deepwater Horizon* spill right after the disaster would be higher than those detected in

the *Prestige* oil spill. The point is, the concentrations of oil in the water column after an oil spill could vary greatly, depending on the scale of the oil release and the fates of the spilled oil.

In our experiment, we used a nominal concentration of 10 µL L^{-1} of chemically dispersed Louisiana sweet crude oil to simulate an oil spill event in the mesocosms. Assuming the crude oil has similar physical properties to those of Macondo (MC252) crude oil and an evaporation of ~45% volume at 15°C, its density would be ~0.9 g cm^{-3} (FISG, 2010), and the concentration of 10 µL L^{-1} could therefore be equivalent to ~9 mg L^{-1}. Although this concentration was higher than some detected concentrations in oil spill events (e.g. 140 µg L^{-1} in the *Prestige* oil spill, Bode *et al.* (2006)), similar or even higher concentrations were used in other ecotoxicity studies on aquatic organisms. For example, Ozhan *et al.* (2015) exposed marine phytoplankton *Ditylum brightwellii* and *Heterocapsa triquetra* to as high as 8 mg L^{-1} of total petroleum hydrocarbons and found that the antioxidant enzymes of the organisms were able to protect the phytoplankton species for concentrations < 4 mg L^{-1}. Gertler *et al.* (2010) exposed marine protozoan grazers and heterotrophic bacteria in 500 L mesocosms spiked with 2.5 L heavy fuel oil (~4.5 g L^{-1} of oil, assuming a density of 0.9 g cm^{-3}) and found changes in the community composition of protozoan grazers and increases in abundance of flagellates and ciliates associated with biofilms of oil-degrading microbes. Cohen *et al.* (2014) incubated a coastal copepod species, *Labidocera aestiva*, in the water accommodated fraction with a nominal loading of 50 mg L^{-1} of Macondo crude oil and observed impaired swimming and reduced swimming speed of the animals shortly after exposure. Given the wide variety of the physiological responses and the toxicity tolerance of the planktonic organisms, the simulation concentration of 10 µL L^{-1} of chemically dispersed crude oil was chosen for our study. It was expected to observe affected microzooplankton grazing activity at this concentration when compared to the control treatment.

In the DOil mesocosms of the current study, the concentrations of total petroleum hydrocarbons (TPH) dropped drastically from 16.6 mg L^{-1} on Day 0 to 6.1 mg L^{-1} on Day 1, and below 0.19 mg L^{-1} on Day 3. This indicated the rapid disappearance of petroleum

hydrocarbons in general. The concentrations of most components of the polycyclic aromatic hydrocarbons (PAHs) dropped to a half in approximately 1-2 days (Table 4.2). Similarly, Yamada *et al.* (2003) found in a mesocosm study that PAHs with less than three benzene rings (e.g. naphthalene and phenanthrene) disappeared mostly within 2 days while those with more than 4 rings (e.g. pyrene and chrysene) remained in the water column for up to 9 days. Our results indicated that the concentration of the most abundant component, phenanthrene, dropped to ~9% within 1 day while that of the second most abundant component, naphthalene, dropped to ~42% on Day 3 (Fig. 4.1). The disappearance of pyrene and chrysene was more rapid than reported by Yamada *et al.* (2003), with a concentration percentage of < 2% on Day 3 for both components (Fig. 4.1). Petroleum hydrocarbons in the outdoor mesocosms could be lost through various mechanisms in this study. For example, surface evaporation, photooxidation, emulsification, sedimentation, adsorption to inner surfaces of containers, intake by organisms, and biodegradation (NRC, 2005) are all possible sources of loss. Prince *et al.* (2017) reported that, though concentration dependent, the half-life of detectable oil hydrocarbons through biodegradation was from 7-14 days in the sea. Given the rapid loss of PAHs components to below the detection limit within the first 3 days in this study, it suggested that mechanisms other than biodegradation contributed substantially to the loss of petroleum hydrocarbons.

Crude oil toxicity and phytoplankton growth

Concentration of Chl-*a* was used as a proxy for phytoplankton abundance in this study. Ozhan *et al.* (2015) showed that an increase in crude oil concentration did not affect the cellular Chl-*a* content but did alter the cell abundance of the diatom *D. brightwellii* and the dinoflagellate *H. triquetra*. In our study, the drop in Chl-*a* concentration from Day 2 to Day 6 in DOil mesocosms might reflect a similar negative effect that cell abundance of photosynthetic cells was lowered by hydrocarbons toxicity, despite that phytoplankton growth rates were higher on Day 6 in general (Table 4.4).

Given that grazing mortality of phytoplankton was negligible in the DOil mesocosm (Table 4.4), the reduced growth of phytoplankton on Day 2, compared to the Ctrl mesocosms, could have resulted from the toxicity of petroleum hydrocarbons. Louisiana sweet crude oil contains a high proportion of low molecular weight polycyclic aromatic hydrocarbons (PAHs) such as naphthalene and phenanthrene (Almeda *et al.*, 2013; this study). It is commonly believed that PAHs of crude oil are the major substances causing adverse effects to aquatic organisms due to their high solubility in water and thus high bioavailability (NRC, 2005). For example, Hjorth *et al.* (2008) showed a drastic decline in Chl-*a* concentration (to as low as 20% of control) in mesocosms after one day exposure to a nominal concentration of 50 nM of the PAH pyrene. In another study, pyrene and phenanthrene caused a decrease in the cell abundance in cultures of *Synechococcus* sp., *Chlorella* sp., *Micromonas* sp., and *Phaeodactylum* sp. (Echeveste *et al.*, 2010a). Other components of PAHs, such as chrysene, could also affect the phytoplankton community. Using the oil source from the *Prestige* oil spill and the reported concentrations of hydrocarbons right after the spill (23 μg L^{-1} of chrysene equivalents L^{-1}), Gonzalez *et al.* (2009) observed decreases in both the Chl-*a* concentration and the photosynthetic activity of the exposed natural phytoplankton assemblages from both the oceanic and coastal regions. However, in a 120-hour exposure, they also observed a size-dependent sensitivity of autotrophic plankton to the hydrocarbons that increased the biomass of nanoflagellates and diatom < 20 μm but decreased the biomass of picophytoplankton and diatom > 20 μm. The use of dispersant facilitates dissolution of PAHs by breaking down crude oil into smaller droplets, which further increases the dissolution of soluble toxins, increasing their toxicity (Wolfe *et al.*., 1998; Yamada *et al.*, 2003). Dispersant alone can also be harmful to aquatic species (George-Ares & Clark, 2000; Ozhan & Bargu, 2014a).

In the Ctrl treatments, *in situ* phytoplankton growth rates (μ_0) were generally lower than those in the enriched incubation bottles (μ) (Table 4.4), suggesting nutrient limitation of phytoplankton growth inside the mesocosms. In contrast, coefficients μ_0 were generally greater than the corresponding μ in the DOil mesocosms. One plausible

explanation could be the result of under-estimation of μ in dilution experiment when the regression slope is positive and statistically significant (i.e. lowered value of y-intercept of the linear regression between dilution fractions and apparent growth rates of phytoplankton when the slope is positive).

Phytoplankton on Day 6 in the Ctrl treatment obtained population growth rates μ of 2.25-3.12 d^{-1} in the enriched incubation and those in the DOil treatment obtained *in situ* growth rates μ_0 ranged from 0.46-3.37 d^{-1} in unamended incubations (Table 4.4). Phytoplankton in the DOil mesocosms obtained an *in situ* growth rate (μ_0) of 2.16 d^{-1} on Day 6 on average (Table 4.4), it indicated that the phytoplankton community recovered from the toxicity of pollutants on Day 6. It co-occurred with the drastic drops in the concentrations of most PAH components near the end of the experiment (Fig 4.1). Admittedly, these growth rates were relatively high compared to the reported range, however, they were not impossible. In a compilation of data that included 788 paired observations from 66 studies (Calbet & Landry, 2004), there were occasions that the phytoplankton growth rates exceeded 2.5 d^{-1} and reached as high as ~3.5 d^{-1} while the microzooplankton grazing rates ranged from approximately 0.5-2.0 d^{-1}. With nutrient enrichment and outdoor incubation (i.e. light intensities averaged ~505 μE m^{-2} s^{-1} when all the 15-minute-interval measured data points during May 1st-31st, 2017, where considered. Data retrieved from http://cdmo.baruch.sc.edu/get/landing.cfm; the Ship Channel station), the phytoplankton in the Ctrl mesocosms could therefore reach very high population growth. Similarly, the high *in situ* population growth of phytoplankton in the DOil mesocosms on Day 6 could be related to outdoor incubation, though not nutrient-enriched, and the lack of microzooplankton grazing (Table 4.4). Additionally, the presence of oil-degrading bacteria in the mesocosm could have increased the remineralization of nutrients and thus promoted the growth of phytoplankton (e.g. Abed, 2010; Discussion in Dissertation Chapter 3).

Despite the high population growth rates of phytoplankton on Day 6 in both treatments, there was no increase in Chl-*a* concentration of the mesocosms when compared to Day 2 (Fig. 4.2). In the Ctrl treatment, microzooplankton grazing accounted

for only 47% of the phytoplankton growth while that in the DOil treatment was negligible (Fig 4.3). This suggested that mechanisms other than microzooplankton grazing could have also contributed to the loss of phytoplankton cells in the mesocosms. These mechanisms could include mesozooplankton grazing, viral lysis or sedimentation of phytoplankton cells to the bottom of the mesocosms. Future research efforts are needed to investigate the effects of these mechanisms on the loss of phytoplankton cells in oil-polluted seawater.

Microzooplankton herbivory in oil-polluted seawater

Grazing coefficients in the Ctrl mesocosms ranged from 0.36-2.28 d^{-1} (Table 4.4), which were within the reported range of other studies (Nejstgaard *et al.*, 1997; Suzuki *et al.*, 2002; Calbet & Landry 2004; Sommer *et al.*, 2005; Suffrian *et al.*, 2008; Chen *et al.*, 2009; Liu *et al.*, 2014), while those in the DOil mesocosms were negligible on both Days 2 and 6. The relatively low abundance of microplankton grazers (heterotrophic dinoflagellates and ciliates) in the DOil mesocosms (Table 4.3) could be the reason for low microzooplankton herbivory, which is also evident in other mesocosm studies (Jung *et al.*, 2012; Ortmann *et al.*, 2012).

Components of PAHs such as phenanthrene, fluoranthene, fluorene, pyrene, and benzo[a]pyrene have been shown to cause adverse effects on microzooplankton species at cellular and sub-cellular levels in laboratory studies (Pillai *et al.*, 2003; Gomiero *et al.*, 2012; Nogueira *et al.*, 2017; Han *et al.*, 2019). Specifically, petroleum toxicity affects the grazing behavior of marine protozoa. The heterotrophic dinoflagellate *Oxyrrhis marina*, *Protoperidinium sp.*, and the ciliate *Metacylis* sp. exhibited lower grazing impact towards algal prey in exposure to the water accommodated fraction of petroleum hydrocarbons (Dissertation Chapter 3). Apart from direct adverse effects on the grazers, petroleum hydrocarbons could have been taken up by protistan grazers through direct ingestion of oil droplets (Almeda *et al*., 2014a) or through the dietary route (Corner *et al*., 1976; Liu *et al*., 2007) and bioaccumulated inside their bodies. Even though the concentrations of PAHs in the DOil mesocosms dropped drastically within one day, the intermediate

products generated by photodegradation of petroleum hydrocarbons could persist or enhance their toxicity (reviewed in Pelletier *et al.*, 2006) to negatively affect the microzooplankton community. For instance, the bioaccumulated hydrocarbons inside the cell body of protistan grazers could produce reactive oxygen species under the ultra-violet exposure from sun light through the process of photosensitization and cause damage to the tissue of the grazers (Barron *et al.*, 2017).

The mesocosms were filled with whole seawater without pre-screening to remove mesozooplankton during the experiment initiation. Top-down control on microzooplankton by mesozooplankton could have occurred in both the Ctrl and DOil treatments. For example, Buskey *et al.*, (2003) showed a significantly higher ciliates population in mesocosms with approximately half of the copepod *Acartia tonsa* removed from the zooplankton community. When the abundance of phytoplankton in the ambient water is low, ciliates can provide approximately 50% of copepods' diet in terms of carbon (Calbet & Saiz, 2005). In exposure to petroleum hydrocarbons, copepods generally have higher tolerance to petroleum hydrocarbons than microzooplankton (Avila *et al.*, 2010; Jiang *et al.*, 2012; Cohen *et al.*, 2014). Therefore, apart from hydrocarbon toxicity, we cannot rule out the possibility that the microzooplankton communities in the DOil mesocosms were further subject to the grazing from the less susceptible mesozooplankton. Though the density of mesozooplankton in the mesocosms and their grazing impact on the microzooplankton community were not determined in this study, our samples from Day 6 indicated that the DOil mesocosms had comparatively lower abundance of microzooplankton grazers (e.g. aloricate and loricate ciliates) than the Ctrl mesocosms (Table 4.3). At the current exposure concentration of dispersed crude oil (10 $\mu L\ L^{-1}$), less susceptible copepods could therefore have preyed on the oil-affected microzooplankton community, further reducing the micro-size grazers abundance in the DOil mesocosms when compared to the Ctrl treatment.

Contrary to some studies indicating that plankton species of smaller cell size or biovolume are more sensitive to the toxicity of PAHs (Echeveste *et al.*, 2010a; Echeveste *et al.*, 2011; Othman *et al.*, 2012), Lugol's preserved samples of Day 6 revealed the

predominance of unidentified cells < 5 μm (Table 4.3) in both the Ctrl and DOil treatments, indicating that these small cells were relatively unaffected by hydrocarbons toxicity. Dalby *et al.* (2008) examined the communities of microeukaryotes in oil-polluted systems of 100 ppm of crude oil and 10 ppm dispersant using genetic markers and revealed high abundance of the bacterivores *Paraphysomonas* spp. and *Monosiga* sp. phylotypes, which usually have cell size ≤ 6 μm in cultures. It is possible that the predominant small cells in our samples were heterotrophic flagellates that feed on small non-pigmented eukaryotic or prokaryotic microbes. Their grazing activities in the Ctrl and DOil mesocosms were therefore not effectively detected by experimental estimations based on the concentrations of Chl-*a*. Future research is needed to determine the population dynamics and degree of grazing impact of nano-size heterotrophic flagellates on small eukaryotes and bacteria in oil-polluted seawater.

The coupling between phytoplankton growth and microzooplankton grazing

Coupled phytoplankton growth and microzooplankton grazing was found in the Ctrl mesocosms but not in the DOil mesocosms (Fig. 4.3). Microzooplankton are commonly thought to be more important than mesozooplankton as consumers of primary producers due to their relatively higher growth rate, great feeding capability on diverse phytoplankton types, and rapid response to changes in food availability at both individual and population levels (Banse, 1982; Hansen *et al.*, 1997; Strom & Morello, 1998; Hansen & Calado, 1999). Microzooplankton grazing is therefore thought to be an effective control of phytoplankton biomass, even during episodes of phytoplankton blooms (Sherr & Sherr, 1994; Strom *et al.*, 2001; Calbet & Landry, 2004), though the suggestion that herbivorous protists are capable of controlling the initiation and development of algal blooms is questioned (Sherr & Sherr, 2009). In the present study, the relationship between *in situ* phytoplankton growth and grazing mortality in the Ctrl treatment showed that microzooplankton grazing accounted for 47% of phytoplankton growth based on the slope of Model II linear regression (Fig. 4.3). This means that nearly half of the phytoplankton cells produced daily in the Ctrl mesocosms were consumed by

microzooplankton. Other mechanisms like grazing by mesozooplankton, viral lysis, natural mortality or sinking to the container's bottom could have contributed to the removal of phytoplankton cells from the water column in addition to microzooplankton grazing.

In contrast to the Ctrl treatment, the lack of a significant relationship between *in situ* phytoplankton growth and grazing mortality in the DOil treatment (Fig. 4.3) suggested a de-coupled interaction between phytoplankton growth and microzooplankton grazing. Previous studies showed that differential sensitivity of planktonic species to crude oil and dispersant could contribute to the disruption of trophic interaction in oil-polluted seawater (Echeveste *et al.*, 2010b; Perez *et al.*, 2010; Ozhan *et al.*, 2014). In our study, the differential sensitivity of plankton was evident: compared to Day 2, *in situ* phytoplankton growth in the DOil mesocosms increased to the average of 2.16 d^{-1} on Day 6 while microzooplankton grazing remained negligible (Table 4.4). Additionally, in other exposure experiments, it was reported that low concentration of petroleum hydrocarbons could stimulate phytoplankton growth or toxin production by harmful algal species (Dunstan *et al.*, 1975; Huang *et al.*, 2011; Ozhan & Bargu, 2014b). Strom (2002) argued that grazing-deterring toxins and other exudates produced by algal prey, and poor nutritional status or food quality of prey for micro-grazers could depress microzooplankton grazing, and thus contribute to the decoupling between phytoplankton growth and microzooplankton grazing.

The consequences of de-coupled phytoplankton growth and microzooplankton grazing related to crude oil pollution is not well-known. Phytoplankton could proliferate rapidly *in situ* during the window of opportunity when microzooplankton grazing is disrupted by various mechanisms (Buskey *et al.*, 1997; Irigoien *et al.*, 2005; Stoecker *et al.*, 2008). Reduced herbivory of microzooplankton by the toxicity of petroleum hydrocarbons could release phytoplankton from grazing pressure and allow them the opportunity to thrive. In a laboratory study, microzooplankton grazers were shown to be more likely influenced by petroleum toxicity than their algal prey in cultures and had a reduced grazing impact towards their prey (Dissertation Chapter 3). In the field,

combined with environmental factors, phytoplankton blooms were shown to be potentially related to oil spill events as well (Johansson *et al.*, 1980; Riaux-Gobin, 1985; Sheng *et al.*, 2011; Tang *et al.*, 2019). All these findings suggest that de-coupled phytoplankton growth and microzooplankton grazing in oil-polluted seawater could potentially contribute to the occurrence of algal blooms, though more direct evidence is needed.

CONCLUSION

This study is one of the few that investigate the trophic response of the microzooplankton community in oil-polluted seawater. Compared to the control treatment, exposure to chemically dispersed crude oil of 10 µL L^{-1} led to reduced phytoplankton growth and negligible microzooplankton herbivory on the 2^{nd} day of exposure. Phytoplankton growth recovered on the 6^{th} day while microzooplankton grazing remained negligible under the influence of toxicity of petroleum hydrocarbons. Results suggested a decoupling between phytoplankton growth and microzooplankton grazing in oil-polluted seawater, which could potentially lead to phytoplankton blooms in the field under certain conditions.

ACKNOWLEDGEMENTS

The authors are thankful for the help provided by Sarah Cosgrove, Maud Moison, and Tracy Weatherall for setting up the mesocosms. This research was made possible by a grant from The Gulf of Mexico Research Initiative. Data are publicly available through the Gulf of Mexico Research Initiative Information & Data Cooperative (GRIIDC) at https://data.gulfresearchinitiative.org.

	Temperature (°C)	Salinity (PSU)
Day 0	25.9±0.1	30.6±0.2
Day 2	20.6±0.2	30.8±0.1
Day 6	23.3±0.0	32.1±0.1

Table 4.1. Mean temperatures and salinities (±1 S.D.) in the Ctrl mesocosms.

PAHs	Day 0 concentration ±1 S.D. (μg L^{-1})	k (SE) (day^{-1})	Half-life (day)	R^2
Acenaphthene	0.97 ±1.08	**0.41** (0.16)	1.7	0.422
Acenaphthylene	0.45 ±0.22	**0.47** (0.10)	1.5	0.710
Anthracene	0.30 ±0.16	**0.31** (0.12)	2.2	0.447
Benz[a]anthracene	0.34 ±0.20	0.30 (0.14)	2.3	0.369
Benzo[a]pyrene	0.24 ±0.13	**1.03** (0.12)	0.7	0.918
Benzo[b]fluoranthene	0.11 ±0.13	**0.66** (0.27)	1.1	0.459
Benzo[g,h,i]perylene	0.08 ±0.03	**0.70** (0.07)	1.0	0.934
Chrysene	1.56 ±0.96	**0.58** (0.15)	1.2	0.606
Dibenz[a,h]anthracene	0.07 ±0.03	**0.62** (0.08)	1.1	0.887
Fluoranthene	0.48 ±0.28	**0.62** (0.15)	1.1	0.690
Fluorene	3.26 ±1.87	**0.36** (0.07)	1.9	0.705
Indeno[1,2,3-cd]pyrene	0.07 ±0.02	**0.62** (0.05)	1.1	0.951
Naphthalene	4.20 ±1.39	**0.65** (0.09)	1.1	0.850
Phenanthrene	13.26 ±8.44	**0.43** (0.10)	1.6	0.660
Pyrene	0.39 ±0.22	**0.59** (0.14)	1.2	0.680

Table 4.2 Mean concentrations (±1 S.D.) on Day 0, the rate constants (k, with S.E. in parenthesis) of degradation, and the half-lives of individual PAH components in DOil mesocosms. R^2 value represents the determination coefficient of the linear regression. Bold k value denotes $P < 0.05$ of the linear regression.

Taxonomic group	Cell density (cells mL^{-1})					
	Ctrl1	Ctrl2	Ctrl3	DOil1	DOil2	DOil3
Diatoms	4.5±3.4	0	0	0	0	0
Dinoflagellates	8.0±4.5	5.3±6.7	3.0±3.5	3.5±4.7	1.5±1.7	0
Aloricate ciliates	1.0±2.0	1.0±2.0	1.0±2.0	0	0.8±1.5	0
Loricate ciliates	0	0	2.0±2.3	0	0	0
Unidentified cells (< 5 μm)	8939±2127	1610±682	1070±446	4269±1838	980±262	715±442

Table 4.3. Mean cell densities (±1 S.D.) of major taxonomic groups of < 200 μm plankton in the Ctrl and DOil mesocosms of Day 6 samples.

	Mesocosms	μ (d^{-1})	μ_0 (d^{-1})	g (d^{-1})	*P* value
Day 2	DOil1	-0.18 (0.15)	-0.54	-0.63 (0.25)	0.06
	DOil2	-0.63 (0.18)	-0.25	**-2.16** (0.30)	0.00
	Ctrl1	1.61 (0.37)	-0.44	1.38 (0.60)	0.08
	Ctrl2	1.89 (0.73)	-0.20	0.36 (1.18)	0.78
Day 6	DOil1	-0.28 (0.13)	0.46	**-0.76** (0.17)	0.05
	DOil2	0.22 (0.22)	2.64	**-2.31** (0.36)	0.00
	DOil3	2.15 (0.20)	3.37	**-1.42** (0.32)	0.01
	Ctrl1	3.08 (0.36)	2.86	**2.28** (0.58)	0.02
	Ctrl2	2.25 (0.55)	0.82	1.00 (0.89)	0.33
	Ctrl3	3.12 (0.38)	1.37	1.62 (0.62)	0.06

Table 4.4. Coefficients (S.E.) of population growth in enriched seawater (μ) and unamended seawater (μ_0), and grazing mortality (g) of phytoplankton < 200 μm in the DOil and Ctrl mesocosms. *P* values represent the statistical significance of the slope of linear regression and coefficient of g in bold indicates $P \leq 0.05$.

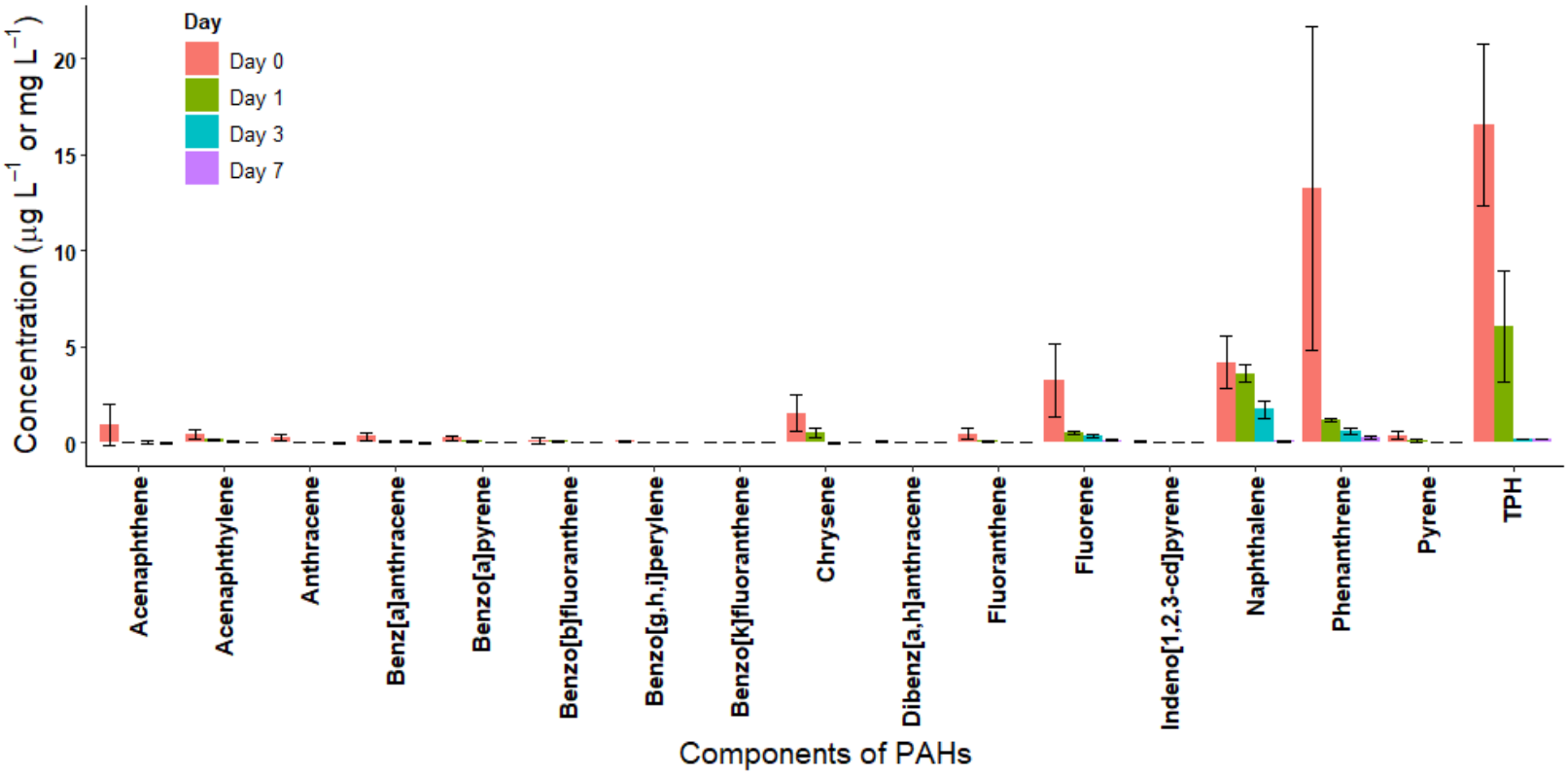

Figure 4.1. Mean concentrations (±1 S.D.) of the components of polycyclic aromatic hydrocarbons (PAH, µg L^{-1}) and total petroleum hydrocarbons (TPH, mg L^{-1}) in the DOil mesocosms on Days 0, 1, 3 and 7.

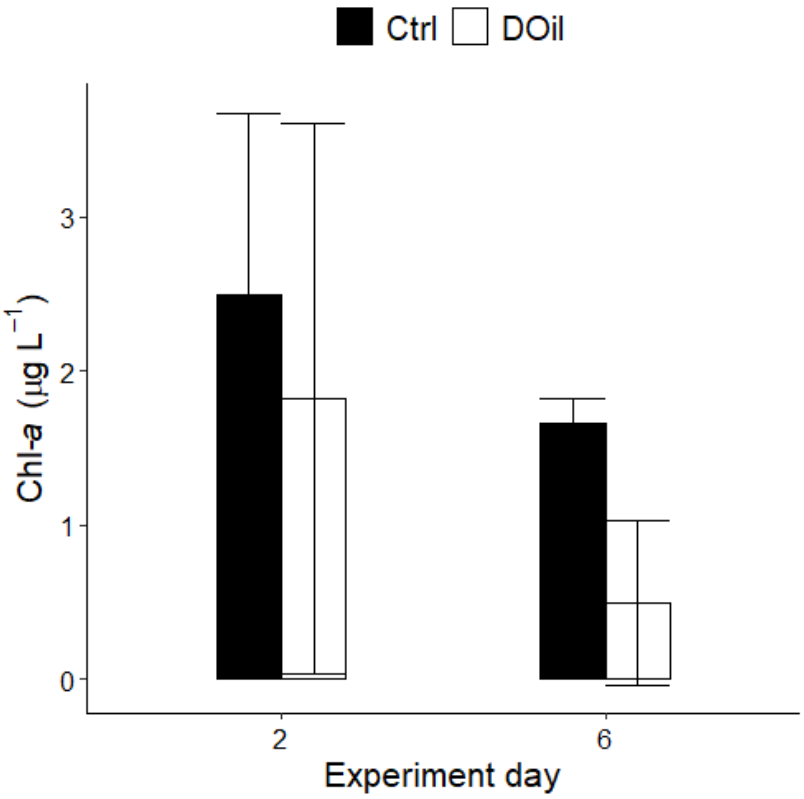

Figure 4.2 Mean chlorophyll-*a* concentrations (±1 S.D.) in the Ctrl and DOil mesocosms on Days 2 and 6.

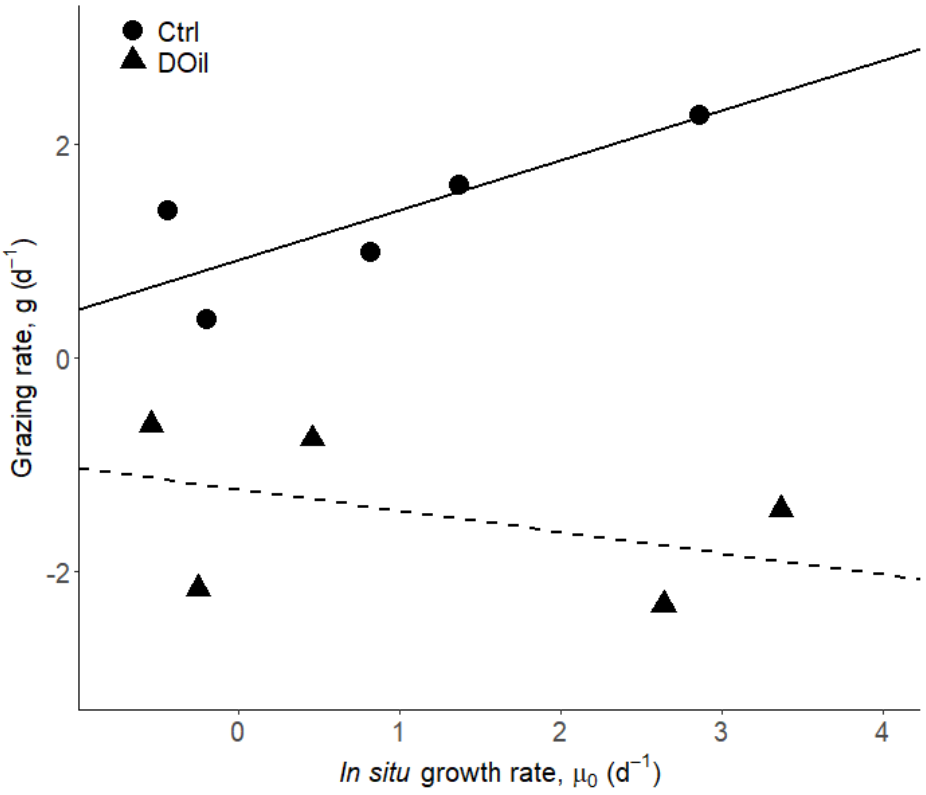

Figure 4.3. Model II linear regression (major axis) between *in situ* population growth (μ_0) and grazing mortality (g) in the Ctrl and DOil mesocosms. Solid line represents the relationship of the Ctrl treatment ($g = 0.47\mu_0 + 0.91$; $R^2 = 0.63$; $P < 0.05$) while dashed line represents that of the DOil treatment ($g = -0.20\mu_0 - 1.23$; $R^2 = 0.15$; $P = 0.22$).

Chapter 5: Bacterivory by Nanoplankton in Oil-Polluted Seawater and Its Effect on the Biodegradation of Petroleum Hydrocarbons

ABSTRACT

Petroleum hydrocarbons released into seawater are eventually biodegraded by bacteria and other microbes. While nanoplankton (2-20 μm) are the major consumers of marine bacteria, their effect on the process of biodegradation of oil hydrocarbons is still debated. A 14-day microcosm experiment was conducted to investigate the degree of bacterivory by nanoplankton in oil-polluted seawater and its effect on the biodegradation of petroleum hydrocarbons. The coefficients of population growth and grazing mortality of bacteria estimated with the dilution method did not differ among the treatments of control (Ctrl), low dose chemically dispersed oil (LDOil, 2 μL L^{-1}) and high dose chemically dispersed oil (HDOil, 8 μL L^{-1}). The estimated percentages of standing stock and net production grazed were 30-80% and 37-156%, respectively, when all treatments were considered. The lack of increase in the cell density of bacterial cells in the oil-loaded treatments is believed to be due to the tight coupling of nanoplankton grazing and bacterial growth. The shift in the community composition of prokaryotes and the relatively high abundance of oil-degrading bacteria, including *Cycloclasticus* and *Alcanivorax* on Days 3-14 of the experiment confirmed the presence of biodegradation of oil in the LDOil and HDOil treatments. Throughout the 14 days, the community composition of bacteria in the LDOil and HDOil treatment became more similar and they both differed from that in the Ctrl treatment. The changes in the bacterial community composition is believed to be related to the addition of chemically dispersed crude oil rather than the top-down control from nanoplankton grazing.

INTRODUCTION

Crude oil entering the natural aquatic environment undergoes various weathering processes. Apart from abiotic weathering, most of the crude oil components, including *n*-

alkane compounds, small aromatics such as benzene and toluene, and polar molecules, are eventually removed from the ecosystem by microbial degradation (Prince, 2010). A recent list reported more than 320 genera of prokaryotes that can utilize hydrocarbons as sole or major energy source (Prince *et al.*, 2018). Most aerobically biodegrading bacteria belong to Gamma-proteobacteria, with representative groups *Alcanivorax* spp. and *Cycloclasticus* spp. that degrade straight-chain and branched alkanes, and polycyclic aromatic hydrocarbons (PAHs), respectively (reviewed in Head *et al.*, 2006; McGenity *et al.*, 2012).

Small sized protozoan grazers, particularly heterotrophic flagellates, are pivotal consumers of heterotrophic bacterioplankton (Fenchel, 1982; Landry *et al.*, 1984; Sherr & Sherr, 1994). Mounting evidence has shown that nano-sized (2-20 μm) heterotrophic flagellates and ciliates preferentially graze on prokaryotes, instead of on phototrophic microeukaryotes, and they could potentially alter the bacterial community composition and abundance in various aquatic ecosystems (del Giorgio *et al.*, 1996; Lavrentyev *et al.*, 2004; Okamura *et al.*, 2012; Sanders & Gast, 2012). Alteration of bacterial populations by protozoan grazing could therefore affect the microbial biodegradation process of petroleum hydrocarbons, though the effects are controversial. On one hand, protozoan grazing is thought to increase the biodegradation of petroleum hydrocarbons. For instance, Tso & Taghon (2006) showed that active protozoan grazing led to a 4-fold increase in the mineralization rate of the PAH naphthalene in sediments. They argued that the selective grazing on non-degrading bacteria by protozoa provided niches for naphthalene-degrading bacteria to thrive. On the other hand, protozoan grazing is shown to hinder biodegradation of hydrocarbons. Kota *et al.* (1999) discovered that when protozoan bacterivory was inhibited, the aerobic biodegradation of benzene, toluene, ethylbenzene, and xylene (BTEX) in aquifer sediments was enhanced.

Given the controversy, there is a great need to understand the changes in protozoan grazing in response to the presence of crude oil and dispersant, and how such changes could consequently affect the biodegradation of hydrocarbons in seawater. In this microcosm study, we investigated the degree of grazing by nano-sized protozoa on

bacteria. We hypothesized that oil pollutants interfere with the bacterivory by nanoplankton and in turn affect the abundance and the community composition of bacteria, and eventually influences the rate of degradation of petroleum hydrocarbons in seawater.

METHODOLOGY

Microcosms set-up

In March 2020, whole seawater (25 PSU) from the Ship Channel, Port Aransas (Texas) was collected from the sub-surface with a Van Dorn water sampler, filtered through a 20 µm nylon mesh and gently filled into nine 20 L translucent carboy microcosms through a siphoned funnel. The carboys were pre-rinsed with 2% Micro solution and subsequently with deionized water several times before use. All carboys filled with seawater were then brought back to the laboratory and positioned indoors on a bench near the window. The low dose dispersed oil (LDOil) treatment was set up by adding a pre-mixed solution of Louisiana sweet crude oil and Corexit 9500A dispersant to make the final nominal concentrations at 2 µL L^{-1} and 0.1 µL L^{-1}, respectively. The high dose dispersed oil (HDOil) treatment was prepared at the final nominal concentrations of 8 µL L^{-1} crude oil and 0.4 µL L^{-1} dispersant. The pre-mixed oil-dispersant solution was prepared by mixing the crude oil and dispersant in 0.2 µm capsule-filtered (Parker Dominick Hunter Demicap) seawater with a magnetic stir bar in a 1 L capped glass aspirator bottle for at least 1 hour. A control (Ctrl) treatment without the addition of crude oil or dispersant was also set up for comparison. All the Ctrl, LDOil and HDOil treatments in triplicate contained ~18 L seawater in the microcosms. All the carboys were capped loosely to reduce the evaporations of water and volatile hydrocarbons. Additionally, abiotic controls of the oil treatments, namely abHDOil (initial nominal concentration of 8 µL L^{-1} crude oil and 0.4 µL L^{-1} dispersant) and abLDOil (initial nominal concentration of 2 µL L^{-1} crude oil and 0.1 µL L^{-1} dispersant), were prepared in duplicate by adding the pre-mixed oil-dispersant solution into

presumably bacteria-free seawater which was twice filtered through 0.2 µm capsule filter. The abiotic control solution (~4 L) was held in a translucent Teflon (Welch Fluorocarbon) plastic bags to minimize the adsorption of petroleum hydrocarbons to the inner wall of the container. The bags were put inside a large glass beaker and sealed loosely except during the subsequent samplings.

The whole experiment lasted for 14 days. Light intensity reaching the outer surface of the carboy microcosms and the air temperature were measured daily during the time periods of 8-9 a.m., 12 noon – 1 p.m., and 4-5 p.m. The seawater in carboys was manually mixed in each of the three time periods by brief shaking for ~10 seconds.

Bacterivory by nano-plankton on microbes

Throughout the 14-day experiment, seawater (i.e. 20 µm pre-filtered) from each microcosm was collected to determine the impact of bacterivory by nanoplankton at different time points. A portion of the collected seawater was used to prepare bacterium-free seawater (FSW) by filtration through 0.2 µm cellulose nitrate membrane (Whatman) with ≤ 7 mmHg vacuum pressure by handpump to minimize the damages to delicate cells and the release of cellular substances that could affect the growth of bacteria or grazers. The remaining portion of seawater was mixed with the FSW to establish a gradient of dilution fraction of seawater (i.e. 20% and 100% of < 20 µm seawater). The mixture was then placed in duplicate 72 mL capped tissue-culture flasks and incubated, unamended, indoors at room temperature on a bench roller (~ 0.5 rpm) for 24 hours.

Before the incubation, duplicate subsamples were obtained from the common mixture of each dilution fraction. After incubation, duplicate subsamples from each 72 mL flask were obtained to determine the abundance of bacteria and nanoplankton. The seawater was serially filtered through 1.0 µm and 0.2 µm polycarbonate membrane (Poretics) filters to obtain nanoplankton and bacteria cells, respectively. The samples were stained with DAPI nuclear stain (0.4 µg mL^{-1} final concentration), preserved with glutaraldehyde (2% final concentration) and filtered onto membrane filters with a

vacuum pressure ≤ 7 mmHg using a hand pump. The membrane filters were then slide-mounted and stored in darkness at -20°C until analysis.

The slide-mounted membrane filters were observed under an epifluorescence microscope (Olympus BX60) with UV excitation at total magnifications of 200X for nanoplankton and 1000X for bacteria. Fifteen to twenty fields of view per membrane filter were randomly selected and captured using a digital camera connected to the microscope. All the pictures were processed with ImageJ software (ver. 1.52h, N.I.H.) to estimate the cell densities of bacterial and nanoplankton cells. Calculation of the grazing mortality of bacteria for each treatment was based on the dilution method (Landry & Hassett, 1982; Landry *et al.*, 1984) as

$$\ln\left(\frac{N_t}{N_0}\right) = (\mu - Dg)t \qquad \text{Eqn 5.1}$$

where N_t is the bacterial density after incubation and N_0 is the initial bacterial density before incubation. The symbol D represents the dilution fraction and t is the time duration of incubation in days. The symbols μ and g represent the coefficients of population growth and grazing mortality of the bacterial cells, respectively.

Based on the results of the dilution experiments, the percentage of standing stock of bacterial cells grazed per day (%SS) was calculated according to Safi *et al*., (2007) as

$$\%SS = (1 - \exp(-g)) \times 100 \qquad \text{Eqn 5.2}$$

And the potential percentage of net production grazed per day (%PP) was calculated as

$$\%PP = (1 - \exp(-g) / (1 - \exp(-\mu)) \times 100 \qquad \text{Eqn 5.3}$$

where μ and g are the coefficients of population growth and grazing mortality of the bacterial cells, respectively.

Changes in concentration of petroleum hydrocarbons

Subsamples of seawater (~200 mL) from each microcosm were drawn from the sub-surface using siphon handpumps that were rinsed with 2% Micro solution and subsequently deionized water each day after use (for the Ctrl, HDOil and LDOil treatments) or one-use-only autoclaved pipette tips (for the abHDOil and abLDOil

treatments), acidified with 2 mL 6N hydrochloric acid, and briefly extracted with 20 mL dichloromethane by gentle shaking. The mixture was stored in pre-cleaned amber glass bottles (2% Micro solution soaked and rinsed with deionized water) at 4°C in darkness until analysis. The concentrations of saturated and aromatic hydrocarbons were quantified by Dr. Zhanfei Liu's laboratory. Briefly, the samples were extracted with dichloromethane 3 times, concentrated by a gentle stream of nitrogen gas, and cleaned and fractionated with a chromatographic column that was dry-packed with activated silica gel, topped with anhydrous granular sodium sulfate, and conditioned with hexane. The saturated and aromatic hydrocarbons were eluted with hexane and 50% (v/v) benzene in hexane, respectively, and analyzed using a gas chromatography mass spectrometry (GC/MS) system (Shimadzu GC/MS QP2020) with the SH-Rxi-5Sil MS column (Shimadzu) according to an established protocol (Liu *et al.*, 2012). Concentrations of total GC-detectable saturated hydrocarbons (C9-C36 *n*-alkanes in this study) and the 16 EPA priority PAHs were estimated using a three-point calibration curve. For the determination of the concentration of individual hydrocarbons, samples with a signal:noise ratio < 3 were manually assigned 0. Negatives values, which indicate concentrations below the detection limit (0.1 μg L^{-1} for the 16 PAHs and *n*-alkanes C9-C35, and 5 μg L^{-1} for *n*-alkane C36), were assigned 0 as well.

Assuming the degradation of hydrocarbons follows the first order reaction kinetics, the rate constant of degradation of individual hydrocarbons was computed as:

$$C_t = C_0 e^{-kt} \qquad \text{Eqn 5.4}$$

where C_t is the instantaneous concentration at different time points and C_0 is the initial concentration. The coefficient k represents the rate constant and t represents time in days. The coefficient of k was estimated as the negative value of the slope of the linear regression of ln(Ct) against t.

Changes in community composition of bacteria

To determine the community composition of bacteria, subsamples of 400 mL from each microcosm were filtered serially through an autoclaved GF/A glass fiber filter

(1.6 µm porosity, Whatman) and bacterial cells were retained onto an autoclaved 0.2 µm porosity cellulose nitrate membrane filter (Whatman). The 0.2 µm membrane filters were kept frozen at -80 °C until DNA extraction.

The samples were extracted for DNA with DNeasy PowerWater Kit (Qiagen) according to the manufacturer's instructions. Amplifications of the V3-V4 region of the 16S rRNA gene of the DNA extracts were conducted using primers (forward: 5'-TCGTCGGCAGCGTCAGATGTGTATAAGAGACAGCCTACGGGNGGCWGCAG-3'; reverse: 5'-GTCTCGTGGGCTCGGAGATGTGTATAAGAGACAGGACTACHVGGGTATCTAATCC-3'). The PCR reactions were performed in a total volume of 25 µL containing 12.5 µL of KAPA HiFi HotStart ReadyMix PCR Kit (KAPA Biosystems), 0.4 µM of each primer and 5 µL of genomic DNA extract. The thermocycler parameters were as follows: 3 min at 95°C, 25 cycles of denaturation (30 sec at 95°C), annealing (30 sec at 60°C) and extension (30 sec at 72°C), and finally followed by 5 min at 72°C. The PCR products were then stained with SYBR Safe DNA Gel Stain (Invitrogen), separated in standard agarose gel electrophoresis (1%) in 1X TAE solution, and visualized with GelPic LED Box (FastGene). Visualized DNA bands of ~500 bp with reference to a DNA marker (Lambda DNA/HindIII Marker 2, Thermo Scientific) were excised from the gel and purified using a MinElute Gel Extraction Kit according to the manufacturer's instruction. The purified PCR products were checked for their A260/A280 ratio using a NanoVue Plus Spectrophotometer (Biochrom) and quantified for concentration using a Qubit 2 Fluorometer (Invitrogen) and Qubit dsDNA HS Assay Kits (Life Technologies). The purified amplicons were normalized in concentration and then sequenced in paired-end (2 x 300 bp) on an Illumina MiSeq platform by RTL Genomics (Lubbock, Texas).

The demultiplexed forward and reverse sequence data were separately trimmed, denoised, removed chimeras, and finally merged using the dada2 pipeline (Callahan *et al.*, 2016) in QIIME 2 software (2020.2) (Bolyen *et al.*, 2019). The denoised dataset contained 361,345 sequences (i.e. amplicon sequence variants (ASVs) for 45 samples. Samples with > 2000 AVSs were used to construct the percentage abundance bar charts with assigned taxonomic information by classifying the ASVs against the SILVA 132

gene sequence database with a trained feature-classifier (Bokulich *et al*., 2018) targeting the V3-V4 region of the gene at 7 taxonomic levels and 99% similarity. Assuming each bacterial phylotype has the same number of gene copies of the 16S rRNA gene (c.f. Farrelly *et al*., 1995; Klappenbach *et al*., 2000; Louca *et al*., 2018), the cell densities of the major bacterial phylotypes in samples were estimated based on their mean percentage abundance and the corresponding mean total cell density. A rooted phylogenetic tree of the ASVs was constructed *de novo* using the align-to-tree-mafft-fasttree pipeline (Katoh *et al*., 2002; Price *et al*., 2010). The ASV dataset was further explored for community diversity using the core-metric-phylogenetic pipeline in QIIME 2 with rarefication at a sampling depth of 5,000. Alpha diversity metrics including the Shannon's diversity index (Shannon & Weaver, 1949) and the Pielou's evenness index (Pielou, 1966) were computed. Beta diversity metrics including the unweighted UniFrac distance (Lozupone & Knight, 2005; McDonald *et al*, 2018) was computed as well. Results of the unweighted UniFrac distance were further tested for significant difference among treatments on separate experiment days using the permutational multivariate analysis of variance (PERMANOVA; Anderson, 2001) method with 9,999 permutations.

Statistical analysis

Except for the graphical presentations and statistical analyses that were generated with QIIME 2, all other analyses and graphical presentations were conducted using R version 3.6.1 (R Core Team, 2019) and packages *lmodel2* version 1.7-3 (Legendre, 2018), *ggplot2* version 3.2.1 (Wickham, 2016), *ggforce* version 0.3.2 (Pedersen, 2020), *tidyverse* version 1.3.0 (Wickham *et al*., 2019) and *qiime2R* version 0.99.34 (Bisanz, 2018).

Model II linear regressions tests (with 50,000 permutations) were applied to test for the presence of a significant relationship between the coefficients of population growth and grazing mortality of bacterial cells for the Ctrl, LDOil, and HDOil treatments using the package *lmodel2* in R. Considering that both coefficients were subject to natural variation and measurement error and were in comparable units of measurement, results

from the major axis regression analysis were chosen for further result presentation and discussion (Sokal & Rohlf, 2012).

RESULTS

Physical parameters

The average indoor air temperatures measured during daytime ranged from 22.1-22.6°C throughout the whole experiment. The average light intensities on the surface of the microcosms during daytime were within the range of 3.2-6.0 µE m^{-2} s^{-1} (Fig. 5.1).

Bacterial and nanoplankton abundances

The bacterial abundance of all microcosms varied differently throughout the experiment. On Day 0, before the addition of the crude oil and dispersant mixture, the mean bacterial densities in the Ctrl, LDOil and HDOil treatments were approximately 0.77, 0.66 and 0.79 x10^6 cells mL^{-1}, correspondingly (Fig. 5.2). In the following days, the mean density in the Ctrl treatment dropped to the lowest at 0.21 x10^6 cells mL^{-1} on Day 3, increased to 0.52 x10^6 cells mL^{-1} on Day 7 and dropped slightly to 0.44 x10^6 cells mL^{-1} on Day 14. The mean density in the LDOil treatment peaked on Day 1 at 0.86 x10^6 cells mL^{-1} and dropped drastically to 0.39 x10^6 cells mL^{-1} on Day 3. It then increased back to 0.74 x10^6 cells mL^{-1} on Day 10 and decreased to 0.45 x10^6 cells mL^{-1} on Day 14. The mean bacterial density in the HDOil treatment ranged from 0.57-0.79 x10^6 cells mL^{-1} during the first 8 days. It then dropped to 0.53 x10^6 cells mL^{-1} on Day 14 (Fig. 5.2).

Similarly, the nanoplankton abundance varied differently throughout the experiment. In the Ctrl treatment, the cell densities of nanoplankton were the highest at 1038 cells mL^{-1} on Day 0. It then dropped to the lowest of 377 cells mL^{-1} on Day 3 and increased to 543 cells mL^{-1} on Day 14. The nanoplankton densities in the LDOil treatments were at 817 cells mL^{-1} on Day 0, peaked at 1259 cells mL^{-1} on Day 7 and dropped to 587 cells mL^{-1} at the end of the experiment. In the HDOil treatment, the

density was 616 cells mL^{-1} on Day 0. It remained in the range of 1002-1270 cells mL^{-1} on Day 1 through Day 7, then dropped to 911 cells mL^{-1} on Day 14 (Fig 5.2).

Bacterivory by nanoplankton

Throughout the experiment, no obvious temporal trend of changes in the coefficients of population growth (μ, d^{-1}) and grazing mortality (g, d^{-1}) of bacteria were observed in all the treatments (Fig. 5.3). On Day 0, the mean values of μ and g in the Ctrl treatments were 0.56 d^{-1} and 0.89 d^{-1}, respectively. In the following days, the growth coefficients ranged from 0.73-1.67 d^{-1} while the grazing coefficients ranged from 0.38-1.65 d^{-1} on average. Model II linear regression (major axis) revealed a positive relationship between μ and g, though only marginally significant ($g = 0.96\mu - 0.29$; $R^2 = 0.24$; $P = 0.06$; Fig. 5.5). The percentage of standing stock grazed (%SS) ranged from 30% to 80%, with the lowest on Day 3 and the highest on Day 1. The percentage of potential production grazed (%PP) ranged from 37% to 156%, with the lowest on Day 3 and the highest on Day 0 (Fig. 5.4).

In the LDOil treatment, the mean values of μ and g were 0.97 d^{-1} and 1.03 d^{-1}, respectively, on Day 1. The mean growth coefficients ranged from 0.71-1.44 d^{-1} during the following days (Fig. 5.3), which were always higher than the grazing coefficient of the same day. A positive relationship was found between μ and g in the LDOil treatment though not statistically significant (($g = 1.33\mu - 0.71$; $R^2 = 0.09$; $P = 0.34$; Fig. 5.5). The %SS were relatively low, with a range between the lowest at 31% on Day 7 and the highest at 58% on Day 1. The %PP ranged from 48% to 97%, with the lowest and the highest percentages on Days 1 and 0, respectively (Fig. 5.4).

The same pattern of higher population growth than grazing mortality on the same day was observed in the HDOil treatment. The mean values of μ and g ranged from 0.85-1.80 d^{-1} and 0.55-1.49 d^{-1}, respectively, in this treatment (Fig. 5.3). A significantly positive relationship was found between these two coefficients in the HDOil treatment ($g = 0.82\mu - 0.10$; $R^2 = 0.86$; $P < 0.001$; Fig. 5.5). The %SS was 75% on Day 3 and ranged

between 40-49% on the other days. The %PP was the highest on Day 1 at 96% and decreased gradually to 67% at the end of the experiment (Fig. 5.4).

Concentrations of *n*-alkanes and PAHs

For the concentrations of *n*-alkanes, unexpected results were observed. In terms of total *n*-alkane hydrocarbons (TNAH, C9-C36), the mean concentrations in the HDOil and LDOil treatments were 1.65 µg L^{-1} and 1.35 µg L^{-1}, respectively, on Day 0. The mean concentrations unexpectedly increased to peaks on Day 3 at 6.00 µg L^{-1} for HDOil and 8.16 µg L^{-1} for LDOil, which were 347% and 631% greater, respectively, compared to the concentrations on Day 0 (Fig. 5.6). The same unexpected pattern was observed for samples in the abHDOil and abLDOil treatments. The mean TNAH concentrations on Day 0 were 24.02 µg L^{-1} and 2.02 µg L^{-1} for abHDOil and abLDOil, respectively. The concentrations reached a maximum at 97.35 µg L^{-1} (355% of that on Day 0) on Day 1 for abHDOil and 5.99 µg L^{-1} (285% of that on Day 0) on Day 7 for abLDOil (Fig. 5.6).

The individual *n*-alkane C9 was consistently detected in the four treatments throughout the experiment but with the peak concentrations occurring on different days (at 2.96 µg L^{-1} for HDOil on Day 14; at 2.23 µg L^{-1} for LDOil on Day 14; at 3.59 µg L^{-1} for abHDOil on Day 7; and at 2.82 µg L^{-1} for abLDOil on Day 7). Concentrations of heavier *n*-alkanes (C15-C36) were low in general, except that sudden spikes in C16-C35 *n*-alkanes were detected in the abHDOil treatment on Day 1, with the concentrations ranging from 2.31 µg L^{-1} to 8.44 µg L^{-1} (Fig. 5.7). Less intense spikes in the mean concentrations of individual *n*-alkanes (C14-C22) were also observed on Day1 through Day 7 in the LDOil, HDOil and abLDOil treatments (Fig. 5.7). Individual *n*-alkanes with mean concentrations consistently above the detection limit throughout the experiment, particularly the early stage of the experiment, were selected for the estimation of rate constants of degradation. The degradation rate constants of C9 *n*-alkane were negative in the HDOil, LDOil, and abHDOil treatments, which was practically impossible. The rate constants of C12, C14 and C15 *n*-alkanes in the abHDOil treatments were 0.13 d^{-1}, 0.57 $d^{-1}$and 0.38 d^{-1}, correspondingly (Table 5.1).

Unexpected results were also observed for the concentrations of PAHs. In terms of total PAHs (TPAH), the mean concentrations for HDOil and LDOil on Day 0 were 0.77 μg L^{-1} and 0.59 μg L^{-1}, respectively. The concentrations peaked at 3.29 μg L^{-1} (442% of that on Day 0) on Day 7 and dropped to ~0.1 % on Day 14 for HDOil. Similarly, the peak concentration for LDOil was at 1.69 μg L^{-1} (309% of that on Day 0) on Day 3. The concentration dropped to 18% on the last day of experiment (Day 14) (Fig. 5.6). The abnormal pattern was also observed on samples in the abHDOil and abLDOil treatments. The mean TPAH concentrations for abHDOil on Day 0 was 2.14 μg L^{-1}. It peaked on Day 7 at 5.11 μg L^{-1} (238% of that on Day 0) and dropped drastically to 6% on Day 14. The mean TPAH concentration for abLDOil on Day 0 was 0.50 μg L^{-1}. It peaked on Day 7 at 3.53 μg L^{-1} (741% of that on Day 0) and dropped to 0% on Day 14 (Fig. 5.6).

The individual PAHs naphthalene, fluorene and phenanthrene were consistently detected throughout the whole experiment in the HDOil, LDOil, and abHDOil treatments while naphthalene and fluorene were consistently detected in the abLDOil treatment. The peak mean concentrations of naphthalene were 0.63 μg L^{-1} on Day 1 for HDOil, 0.34 μg L^{-1} on Day 0 for LDOil, 1.81 μg L^{-1} on Day 3 for abHDOil, and 0.45 μg L^{-1} on Day 1 for abLDOil. The peak mean concentrations of phenanthrene were 0.57 μg L^{-1} on Day 1 for HDOil, 0.48 μg L^{-1} on Day 3 for LDOil, 1.07 μg L^{-1} on Day 3 for abHDOil, and 0.91 μg L^{-1} on Day1 for abLDOil. Those of fluorene were 0.30 μg L^{-1} on Day 1 for HDOil, 0.20 μg L^{-1} on Day 7 for LDOil, 0.68 μg L^{-1} on Day 3 for abHDOil, and 0.40 μg L^{-1} on Day 1 for abLDOil (Fig. 5.8). The unexpected spikes in concentrations of benzo[a]anthracene, benzo[b]fluoranthene, benzo[k]fluoranthene, benzo[a]pyrene, benzo[g,h,i]perylene, diben[a,h]anthracene, and indeno[1,2,3-cd]fluoranthene on Day 7 were observed in the HDOil, abHDOil, abLDOil treatments (Fig. 5.8). Individual PAHs with mean concentrations consistently above the detection limit throughout the experiment, particularly in the early stage of the experiment, were selected for the estimation of rate constants of degradation. The rate constants of naphthalene in the HDOil, LDOil, and abHDOil treatments were 0.20 d^{-1}, 0.08 d^{-1} and 0.19 d^{-1}, correspondingly. The rate constant of fluorene in the abHDOil treatment was 0.09 d^{-1} (Table 5.2).

Composition of bacterial communities

In the Ctrl treatment, a shift in the dominant bacterial genera throughout the experiment was observed. The HIMB11 (Rhodobacteraceae) bacterial genus was abundant on Day 0 (30% mean abundance, ~232 x 10^3 cells mL^{-1}) and Day 1 (40% mean abundance, ~223 x 10^3 cells mL^{-1}). Its dominance was replaced by uncultured *Actinomarina*, with the mean percentage abundance of *Actinomarina* at 25% (~129 x 10^3 cells mL^{-1}) and 24% (~107 x 10^3 cells mL^{-1}) on Days 7 and 14, respectively (Fig. 5.9 & 5.12). The mean abundance of the bacterial genus *Marinobacterium*, bacteria capable of degrading crude oil (Pham *et al*., 2009), was 11% (~88 x 10^3 cells mL^{-1}) on Day 0 and 5% (~29 x 10^3 cells mL^{-1}) on Day 1, and at very low abundance on the other days. Interestingly, aliphatic-hydrocarbon-degrading bacteria *Alcanivorax* (Yakimov *et al*., 1998) was observed in the Ctrl treatment throughout the whole experiment, with the mean abundance percentages ≤ 2% and the estimated cell densities ≤ ~9 x 10^3 cells mL^{-1} (Fig. 5.9 & 5.12). The Shannon's diversity index and Pielou's evenness index indicated that the bacterial community increased the within-sample species richness and evenness from Day 0 through Day 14, with the Shannon's index at 5.05 on Day 0, peaking at 5.98 on Day 7 and dropping slightly to 5.82 on Day 14 and the Pielou's evenness index at 0.70 on Day 0, peaking at 0.78 on Day 7 and decreasing to 0.76 on Day 14 (Fig. 5.13).

Similar dominance of HIMB11 (Rhodobacteraceae) and uncultured *Actinomarina* were observed in the LDOil treatment, with the mean abundance of HIMB11 (Rhodobacteraceae) at 28 % (~182 x 10^3 cells mL^{-1}) on Day 0, 43% (~371 x 10^3 cells mL^{-1}) on Day 1 and 2% (~10 x 10^3 cells mL^{-1}) on Day 14. The mean abundance of the uncultured *Actinomarina* was 9% (~57 x 10^3 cells mL^{-1}), 7% (~60 x 10^3 cells mL^{-1}) and 26% (~116 x 10^3 cells mL^{-1}) on Days 0, 1 and 14, correspondingly. *Marinobacterium* was mainly observed on Day 0 (14%, ~91 x 10^3 cells mL^{-1}) and Day 1 (6%, ~55 x 10^3 cells mL^{-1}) and diminished towards the end of the experiment (Fig. 5.10 & 5.12). Meanwhile, hydrocarbon-degrading bacteria *Cycloclasticus* (Dyksterhouse *et al*, 1995) and *Alcanivorax* were observed. *Cycloclasticus* was abundant on Day 3 (11%, ~42 x 10^3 cells mL^{-1}) and Day 7 (4%, ~24 x 10^3 cells mL^{-1}) while *Alcanivorax* was observed

throughout the whole experiment, with relatively higher mean abundance on Day 7 (4%, ~21 x 10^3 cells mL^{-1}) and Day 14 (1%, ~6 x 10^3 cells mL^{-1}) (Fig. 5.10 & 5.12). The Shannon's diversity indices in the LDOil treatment were 5.10, 6.24 and 5.73 on Days 0, 7 and 14, correspondingly, while the Pielou's evenness indices were 0.72, 0.82 and 0.75 on Days 0, 7 and 14, correspondingly (Fig. 5.13).

In the HDOil treatment, the dominance of HIMB11 (Rhodobacteraceae) and uncultured *Actinomarina* was observed. The mean percentage abundance of HIMB11 (Rhodobacteraceae) were 34% (~267 x 10^3 cells mL^{-1}) on Day 0, 43% (~334 x 10^3 cells mL^{-1}) on Day 1 and decreased to 2% (~10 x 10^3 cells mL^{-1}) on Day 14 (Fig. 5.11 & 5.12). Those of uncultured *Actinomarina* were 11% (~88 x 10^3 cells mL^{-1}), 8% (~63 x 10^3 cells mL^{-1}), and 4% (~20 x 10^3 cells mL^{-1}) on Days 0, 1 and 14, correspondingly. Meanwhile, *Alcanivorax* was observed throughout the whole experiment, with relatively higher mean abundances on Day 7 (6%, ~43 x 10^3 cells mL^{-1}) and Day 14 (8%, ~40 x 10^3 cells mL^{-1}). *Cycloclasticus* was first observed on Day 3, with a mean abundance of 12% (~67 x 10^3 cells mL^{-1}). It then decreased to 5% (~38 x 10^3 cells mL^{-1}) on Day 7 and 1% (~6 x 10^3 cells mL^{-1}) on Day 14 (Fig. 5.11 & 5.12). Similarly, *Marinobacterium* was observed during the early stage of the experiment, with a mean abundance of 6% (~46 x 10^3 cells mL^{-1}) on Day 0 and 3% (~26 x 10^3 cells mL^{-1}) on Day 1 (Fig. 5.11 & 5.12). The Shannon's diversity indices were 5.10, 6.61 and 6.17 on Days 0, 7 and 14, correspondingly, while the Pielou's evenness indices were 0.72, 0.86 and 0.81 on Days 0, 7 and 14, correspondingly (Fig. 5.13).

The principal coordinate analysis (PCoA) of the unweighted UniFrac distance of all samples revealed a tight cluster of all samples on Day 0 except 1 sample in the LDOil treatment. Tight clusters of samples in the LDOil and HDOil treatments were also observed on Days 3, 7 and 14, indicating a high community similarity among the samples in these 2 treatments. Meanwhile, samples in the Ctrl treatment were generally differentiated from samples in the LDOil and HDOil treatments. The first 2 principal components of the PCoA combinedly explained 45.9% of the total co-variation of the samples (Fig. 5.14). Results of the PERMANOVA revealed no significant difference (P =

0.94, Table 5.3) in the unweighted UniFrac distance among the 3 treatments on Day 0 but significant difference in the distance on Day 7 (P = 0.04) and Day 14 (P = 0.02). However, pairwise comparisons between the treatments on these 2 days did not reveal significant difference (P > 0.05) in the unweighted UniFrac distance (Table 5.3). Caution should be used when interpreting the results due to the small sample size.

DISCUSSION

Abundance of marine protists and bacterivory in the treatments

Despite the high bacterial growth rates (Ctrl: 0.56-1.67 d^{-1}; LDOil: 0.71-1.44 d^{-1}; and HDOil: 0.85-1.80 d^{-1}; Fig. 5.3), there were no obvious increases in the abundance of bacterial cells following the addition of crude oil and dispersant mixtures in the LDOil and HDOil treatments (Fig. 5.2). Compared to the control treatment, Dalby *et al*. (2008) reported an approximately ≥ 7 fold increase in the bacterial cell density in a bottle incubation with the addition crude oil and emulsifier (100 ppm and 10 ppm, respectively) while the addition of crude oil alone did not trigger an increase in bacterial cells. They argued that the addition of emulsifier enhanced the bioavailability and biodegradation of the oil hydrocarbons and thus might be used as carbon and energy sources by the bacteria. Though we used a lower oil:dispersant concentration ratio than that used in Dalby *et al*. (2008), it is believed that the volume ratio of 20:1 is high enough to increase the bioavailability and biodegradation rate of petroleum hydrocarbons (Almeda *et al*, 2014b; Bacosa *et al*., 2015).

The lack of increase in the bacterial cells could be due to factors such as other bottom-up mechanisms or top-down controls. Apart from a carbon source, bacterial growth requires the supply of major nutrients such as nitrogen (N) and phosphorus (P). For instance, Apple *et al*. (2004) showed a persistent response pattern of bacterioplankton to the enrichment of nutrients on a system wide scale in Chesapeake Bay. Considering that seawater from the Ship Channel of Port Aransas (Texas), an coastal estuarine region with relatively high inorganic nutrient levels (Evans *et al*., 2012), was collected for our

experiment, we did not amend the seawater with N or P nutrients to the microcosms as a measure to directly reflect the effects of the addition of crude oil and dispersant on the abundance and community composition of the bacteria and nanoplankton (Tremaine & Mills, 1987; del Campo *et al*., 2013). However, our results suggest that the addition of as high as 8 μL L^{-1} final nominal concentration of chemically dispersed crude oil to the coastal seawater without the addition of major inorganic nutrients may not be enough to trigger increases in bacterial abundance (Fig. 5.2), although increase in the cell densities of hydrocarbon-degrading bacteria phylotypes was observed in the LDOil and HDOil treatment (Fig. 5.12). It therefore suggested that bacterial growth in our microcosms could be nutrient-limited, even though the bottom-up control of nutrient availability on bacterial abundance is more likely to occur in oligotrophic than in eutrophic environments (Sanders *et al*, 1992). Further, inorganic nutrients data (retrieved from http://cdmo.baruch.sc.edu/get/landing.cfm; the Ship Channel station) in March from 2010-2014 revealed that the ratio of N (NO_2^- and NO_3^-) to P (PO_4^{3-}) was ~1.8:1 on average in local water, which was much lower than the 16:1 Redfield ratio (Redfield, 1934). It suggested that N limitation could have been limiting the bacterial growth.

Although we did not distinguish the cell densities between phototrophic and heterotrophic nanoplankton, it is presumed that with the light intensities ≤ 6 μE m^{-2} s^{-1} throughout the whole experiment (Fig. 5.1), most of the nanoplankton were phagotrophic heterotrophs or mixotrophs. The absence of sharp increases in the bacterial abundance co-occurred with the relatively steady levels of nanoplankton (Fig. 5.2). The overall ratio of the cell densities of bacteria:nanoplankton averaged ~860:1 for all samples (Ctrl: 829:1; LDOil: 891:1; and HDOil: 860:1; data not shown). These ratios were close to the reported ratio between bacteria and nanoplanktonic protozoa of ~1000:1 from the euphotic zones of various marine and freshwater environments (Sanders *et al*., 1992).

Nanoplankton (2-20 μm) are the main predators of bacterial cells. Heterotrophic nanoflagellates, particularly < 5 μm, are believed to be responsible for the majority of bacterivory (Fenchel, 1982; Landry *et al.*, 1984; Sherr & Sherr, 1994; Unrein *et al*, 2007; Mansano *et al*, 2014). Our results revealed that bacterivory (reflected by the coefficient

of grazing mortality of bacteria) by nanoplankton ranged from 0.38 d^{-1} to 1.65 d^{-1} in the Ctrl treatment, which were not obviously different from those in the LDOil (0.27-1.03 d^{-1}) and HDOil (0.55-1.49 d^{-1}) treatments (Fig. 5.3). The regression between coefficients μ and g revealed that grazing mortality accounted for most of the population loss of bacterial cells (82-133% based on the slope of the linear regression, Fig. 5.5), though the relationships were not statistically significant in the Ctrl (P = 0.06) and LDOil (P = 0.34) treatments. Admittedly, the *in situ* nutrient limitation of seawater in the microcosms and the absence of nutrient addition to the incubation containers in the dilution experiments could have violated the assumption of the dilution experiment that prey growth is not affected by the presence of other prey cells (Landry & Hassett, 1982). This violation could have led to an exaggerated negative slope of the linear regression and thus the grazing mortality rates, g, of bacterioplankton since the net growth rate of bacteria in the high dilution fraction (i.e. 100% < 20 μm seawater) was lowered. Consequently, with the exaggerated negative slope, the y-intercept of the linear regression, μ, would likely be overestimated as well since the regression line was tilted downward on the other end (i.e. the 100% dilution fraction). Though further confirmation is needed, it is believed that the comparison between coefficients μ and g in the forms of a linear regression (Fig. 5.5), the estimated %PP (Fig. 5.4) or the g:μ ratio (data not shown) are still valid to a certain degree.

Bacterivory by nanoplankton was shown to have grazing selectivity based on the cell traits of bacteria including size, motility, cell wall structure, morphology, toxin production, and exopolymer formation (Monger *et al*., 1999; Jurgens & Matz, 2002; Pernthaler, 2005). Hahn & Hofle (2001) revealed that pelagic bacterial cells < 0.4 μm and > 1.6 μm were less susceptible to nanoplankton grazing than cells in the size of 0.4-1.6 μm. Our dilution experiment focused on bacterial cells of 0.2-1.0 μm size, which were believed to be highly susceptible to nanoplankton grazing. This may explain the tight coupling between the population growth and grazing mortality of the bacteria in our experiments.

Biodegradation of petroleum hydrocarbons by marine bacteria

The concentrations of petroleum hydrocarbons such as the *n*-alkanes and polycyclic aromatic hydrocarbons (PAHs) were expected to be at the highest on Day 0 and decrease gradually to a baseline level during the 14-day incubation as bacterial degradation progresses. Unfortunately, we did not observe the expected results. Instead, the concentration of total PAH (TPAH) and total *n*-alkanes hydrocarbon (TNAH) reached the highest levels on Day 7 and Day 3, respectively (Fig. 5.6). The increase in TPAH on Day 7 was mainly caused by abnormal spikes in the concentration of individual PAHs (i.e. Benz[a]anthracene, Benzo[b]fluoranthene, Benzo[k]fluoranthene, Indeno[1,2,3-cd]fluoranthene, and Benzo[g,h,i]perylene) that were not detected on the previous sampling days or on Day 14 in the treatments of LDOil, HDOil, abLDOil, and abHDOil (Fig. 5.8). Similarly, the increase in the concentrations of TNAH on Day 3 were caused by sudden spikes in concentration of individual *n*-alkanes that were non-detectable or at very low levels in the previous sampling days, particularly in the abHDOil treatment (Fig. 5.7). The spikes in hydrocarbon concentrations in the middle of the experiment were suspected to be related to sample collection where oil adhered to the inner wall of the carboy microcosms or the siphon handpump and was subsequently released during the sampling events on Days 1, 3 or 7. This mechanism could be the reason for the cases of the LDOil and HDOil treatments. However, since Teflon bags were used to contain the oil-loaded seawater in the abLDOil and abHDOil treatments and once-only autoclaved pipette tips were used for the sampling, the adhesion-and-released-later mechanism could not explain the observed spikes in the concentration of hydrocarbons in the abiotic controls (Fig. 5.7 & 5.8). This suggests that mechanisms other than sampling errors could have also contributed to the abnormal temporal pattern of concentrations of the hydrocarbons.

Using the same crude oil and dispersant source as ours, Bacosa *et al*. (2015) found that *n*-alkanes were readily degraded by microbes with the degradation rate constants of C9-C21 *n*-alkanes ranged approximately from 0.07 d^{-1} to 0.22 d^{-1} in the dark+oil+disp treatment (i.e. chemically dispersed oil in darkness). While the rate constants of PAHs

naphthalene, fluorene and phenanthrene were high (ranged 0.22-0.39 d^{-1}) in the same treatment, they discovered a lag period of about 10 days in the biodegradation of the PAHs. Unexpectedly, we found negative degradation constants of C9 *n*-alkane for all the oil-loaded treatments in our experiment while those of C12, C14 and C15 *n*-alkanes in the abHDOil treatment were higher than previously reported (Table 5.1). The degradation constants of PAH naphthalene ranged from 0.08-0.20 d^{-1}, which were close to the reported values (Bacosa *et al*., 2015) but lower than those determined in our mesocosm study (Dissertation Chapter 4, Table 4.2). The mesocosms in our study were exposed to natural sunlight and were not sealed, and the rates of weathering and degradation of PAHs were expected to be higher than those in this study.

Even though increases in TPAH and TNAH concentrations were detected in the middle of the 14-day experiment, high abundances of hydrocarbon-degrading bacteria were present in the LDOil and HDOil treatments. Relatively high abundance of *Cycloclasticus* was found on Days 3, 7, and 14 in the LDOil and HDOil (Fig. 5.12) treatments. Similarly, high abundance of *Alcanivorax* was found on Days 7 and 14 in the LDOil and HDOil treatments (Fig. 5.12). These two genera are believed to be important and widespread oil-consuming bacteria (Prince *et al*., 2018). *Cycloclasticus pugetii* described by Dyksterhouse *et al*. (1995) is an aerobic gram-negative bacterium that can utilize aromatic compounds such as biphenyl, naphthalene, phenanthrene, anthracene and toluene as carbon sources for growth. The *Alcanivorax* bacterium described by Yakimov *et al*. (1998) is an aerobic gram-negative prokaryote that can metabolize aliphatic hydrocarbons (e.g. *n*-alkanes) and produce active biosurfactants. The detection of these bacteria in the LDOil and HDOil treatments indicated that biodegradation of PAHs and *n*-alkanes occurred, especially during the later stage of the experiment (Days 7-14). Interestingly, *Alcanivorax* was detected in low abundance in the Ctrl treatment throughout the whole experiment (Fig. 5.12) and *Marinobacterium*, a bacterial genus believed to be an aerobic degrader of crude oil (Pham *et al*., 2009; Prince *et al*., 2018), was consistently detected in the Ctrl, LDOil and HDOil treatments throughout the entire experiment, with relatively high abundances on Days 0 and 1 (Fig. 5.9-5.11). The

detection of these two hydrocarbon-degrading bacterial genera in the Ctrl treatment suggested that they are common in local seawater. It further implies that the local water of the Ship Channel may have been subjected to chronic baseline pollution of crude oil.

The role of nanoplankton grazing in the bacterial biodegradation of petroleum hydrocarbons

The role of nanoplankton grazing in the biodegradation of hydrocarbons is still controversial, some studies showed a stimulating effect of the protozoan grazers (Tso & Taghon, 2006) while others showed an inhibiting effect of the grazers on the biodegradation process (Kota *et al*, 1999). It was unfortunate that the abnormal changes in the concentrations of PAHs and *n*-alkanes in our results hindered the quantitative analysis of the degree of bacterivory on the degradation rates of the petroleum hydrocarbons.

Metabarcoding of the 16S rRNA genes did reveal the changed community composition of the bacteria in our treatments. For instance, the Shannon's diversity (quantitative measurement of the within sample species richness) and Pielou's evenness indices increased from Day 0 to Day 3 and remained high in the Ctrl, LDOil, HDOil treatments (Fig. 5.13). They indicated that the bacterial communities changed to be more diverse in terms of the total number of phylotypes and more even in terms of the relative abundance of each phylotype of a sample. However, such changes did not indicate that the communities in each treatment are more similar. On the contrary, as the PCoA of the unweighted UniFrac phylogenetic distance revealed, while the community compositions of bacteria in the LDOil and HDOil become more similar towards the end of the experiment, those in the Ctrl treatment tended to differentiate from the oil-loaded treatments (Fig. 5.13), even though the pairwise comparison of the PERMANOVA tests did not reveal a statistically significant difference ($P > 0.05$, Table 5.3) between the treatments. The changes in the community composition of bacteria could be contributed by nanoplankton grazing and (or) the addition of petroleum hydrocarbons.

In the perspective of top-down control from nanoplankton grazing on the bacterial communities, the degree of bacterivory by nanoplankton did not differ among the treatments. The percentage of standing stock grazed (%SS) were 30-80% in the Ctrl treatment, 31-58% in the LDOil treatment and 40-75% in the HDOil treatment (Fig. 5.4). The potential percentage of net production grazed (%PP) were 37-156%, 62-98% and 67-96% in the Ctrl, LDOil and HDOil treatment, correspondingly (Fig. 5.4). One-way ANOVA (data not shown) revealed that there was no significant difference ($P > 0.05$) among the treatments in terms of the %SS or %PP. This suggests that the addition of dispersed oil in the LDOil and HDOil treatments did not affect the degree of bacterivory of nanoplankton when compared to the Ctrl treatment.

There are not many of studies documenting the grazing selectivity of nanoplankton towards hydrocarbon-degrading bacteria. However, bacterial engulfment rates by grazers were shown to be related to the differential digestion of bacterial cells and the digestion of gram-positive cells is more time-consuming than that of gram-negative cells (reviewed in Pernthaler, 2005). While most of the hydrocarbon-degrading bacteria belong to Gamma-proteobacteria that are gram-negative organisms (Prince *et al*., 2018), we did not observe direct evidence that nanoplankton grazed selectively towards these bacteria. In the LDOil and HDOil treatments, the increases in the mean percentage abundance and the estimated cell densities of hydrocarbon-degrading bacteria *Alcanivorax* and *Cycloclasticus* during the later stage of the experiment were accompanied by decreases in both the percentage abundance and cell densities of the predominating bacteria HIMB11 and *Actinomarina* (Fig. 5.10, 5.11 & 5.12). Meanwhile, the total bacterial cell densities did not experience obvious increase in LDOil and HDOil treatments (Fig.5.2) and the linear regression between the population growth and grazing mortality of bacterial cells indicated tight couplings between nanoplankton grazing and bacterial growth in the Ctrl (marginally significant, $P = 0.06$) and HDOil treatment (Fig. 5.5). Therefore, it was likely that while nanoplankton grazing in oil-polluted seawater was not affected by the pollutants and kept the standing stock of bacterioplankton steady, there were changes in the community composition of the bacterial cells. These

compositional changes were likely caused by the addition of petroleum hydrocarbons rather than by nanoplankton grazing.

CONCLUSION

Results of the dilution experiments revealed similar degrees of bacterivory of nanoplankton in the Ctrl, LDOil and HDOil treatments, indicating the grazing on bacteria was not affected by the addition of chemically dispersed crude oil at the investigated concentrations. Even though the abnormal changes in the concentrations of PAHs and *n*-alkanes hindered the quantitative measurement of the degradation of petroleum hydrocarbons, the relatively high abundance of oil-degrading bacteria including *Cycloclasticus*, *Alcanivorax* and *Marinobacterium* indicated the occurrence of biodegradation of crude oil in the LDOil and HDOil treatments. While the bacterial population growth was tightly coupled with the grazing mortality by nanoplankton grazing and the total abundance of bacterial cells were steady throughout the experiment in the HDOil treatment, changes in the community composition of bacteria was more likely related to the addition of dispersed crude oil rather than the top-down control from nanoplanktonic grazers.

ACKNOWLEDGEMENTS

The authors are thankful to Dr. Deana Erdner for the use of her laboratory and the equipment for the samples and DNA processing. This research was made possible by a grant from The Gulf of Mexico Research Initiative. Data are publicly available through the Gulf of Mexico Research Initiative Information & Data Cooperative (GRIIDC) at https://data.gulfresearchinitiative.org.

Treatments	*n*-alkanes	Day 0 concentration ($\mu g\ L^{-1}$)	k (SE) (d^{-1})	R^2
HDOil	C9	0.84±0.14	**-0.09** (0.02)	0.62
	C14	0.10±0.09	0.03 (0.09)	0.03
LDOil	C9	0.94±0.24	**-0.12** (0.02)	0.75
abHDOil	C9	1.15±0.59	**-0.09** (0.03)	0.52
	C12	1.75±0.23	**0.13** (0.04)	0.70
	C14	3.15±0.72	**0.57** (0.07)	0.96
	C15	3.33±1.19	**0.38** (0.15)	0.57
abLDOil	C9	0.93±0.19	-0.07 (0.04)	0.41

Table 5.1 Mean concentrations (±1 S.D.) of individual *n*-alkanes on Day 0 and the rate constants (k, with S.E. in parenthesis) of degradation in the treatments. R^2 value represents the determination coefficient of the linear regression. Bold k value denotes $P < 0.05$ of the linear regression.

Treatments	PAHs	Day 0 concentration ($\mu g\ L^{-1}$)	k (SE) (d^{-1})	R^2
HDOil	Fluorene	0.12±0.10	0.00 (0.04)	0.00
	Naphthalene	0.50±0.09	**0.20** (0.05)	0.59
	Phenanthrene	0.16±0.15	0.03 (0.07)	0.03
LDOil	Fluorene	0.17±0.02	0.00 (0.02)	0.00
	Naphthalene	0.34±0.03	**0.08** (0.02)	0.53
	Phenanthrene	0.09±0.15	0.02 (0.10)	0.00
abHDOil	Fluorene	0.51±0.08	**0.09** (0.03)	0.69
	Naphthalene	1.12±0.14	**0.19** (0.07)	0.54
	Phenanthrene	0.43±0.08	0.03 (0.09)	0.02
abLDOil	Fluorene	0.19±0.02	0.01 (0.05)	0.02
	Naphthalene	0.31±0.04	0.17 (0.07)	050

Table 5.2 Mean concentrations (±1 S.D.) of individual PAHs on Day 0 and the rate constants (k, with S.E. in parenthesis) of degradation in the treatments. R^2 value represents the determination coefficient of the linear regression. Bold k value denotes $P < 0.05$ of the linear regression.

		Day 0	Day 7	Day 14
Overall	Sample size	9	7	7
	Test statistic	0.80	2.23	1.81
	P value	0.94	0.04	0.02
Pairwise (*P* value)	Ctrl:HDOil	1.00	0.34	0.11
	Ctrl:LDOil	0.81	0.10	0.33
	HDOil:LDOil	1.00	0.40	0.20

Table 5.3 Results of the PERMANOVA pseudo-*F* statistics of the unweighted UniFrac distance of the bacterial communities among the 3 treatments on Days 0, 7 and 14 (number of permutations = 9,999).

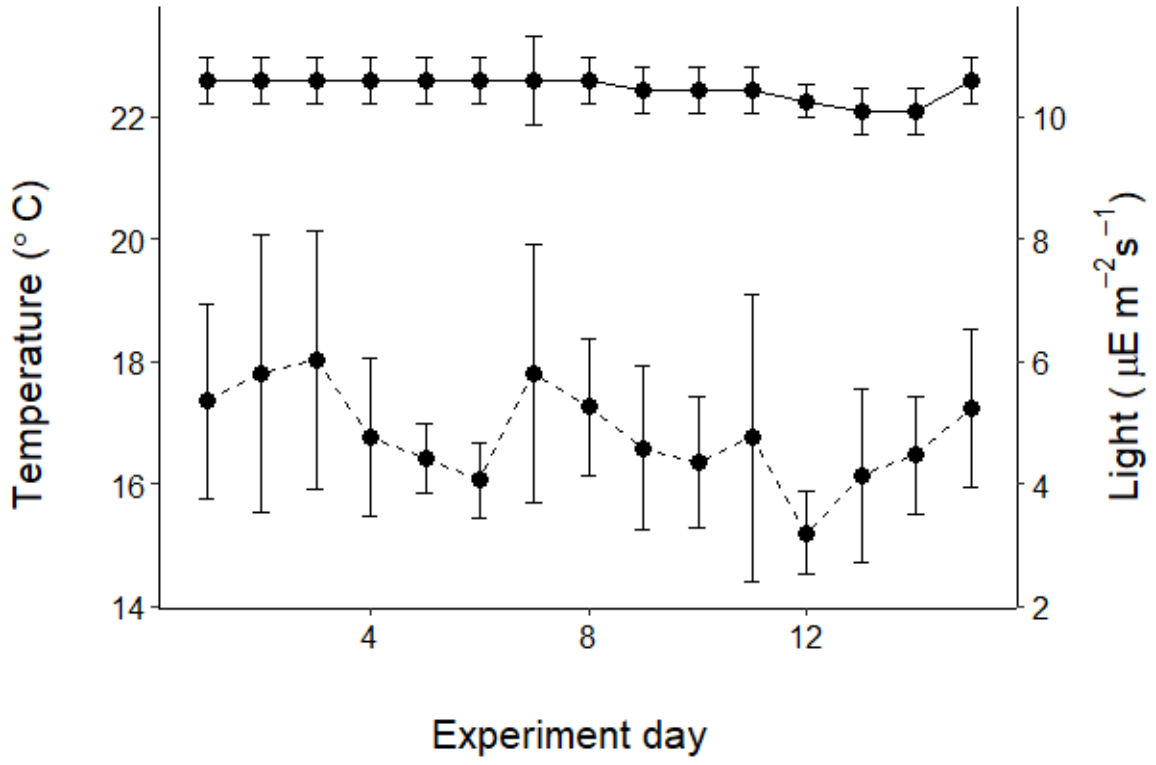

Figure 5.1 Mean temperatures (±1 S.D., solid line, left y-axis) and light intensities (±1 S.D., dashed line, right y-axis) on different experiment days.

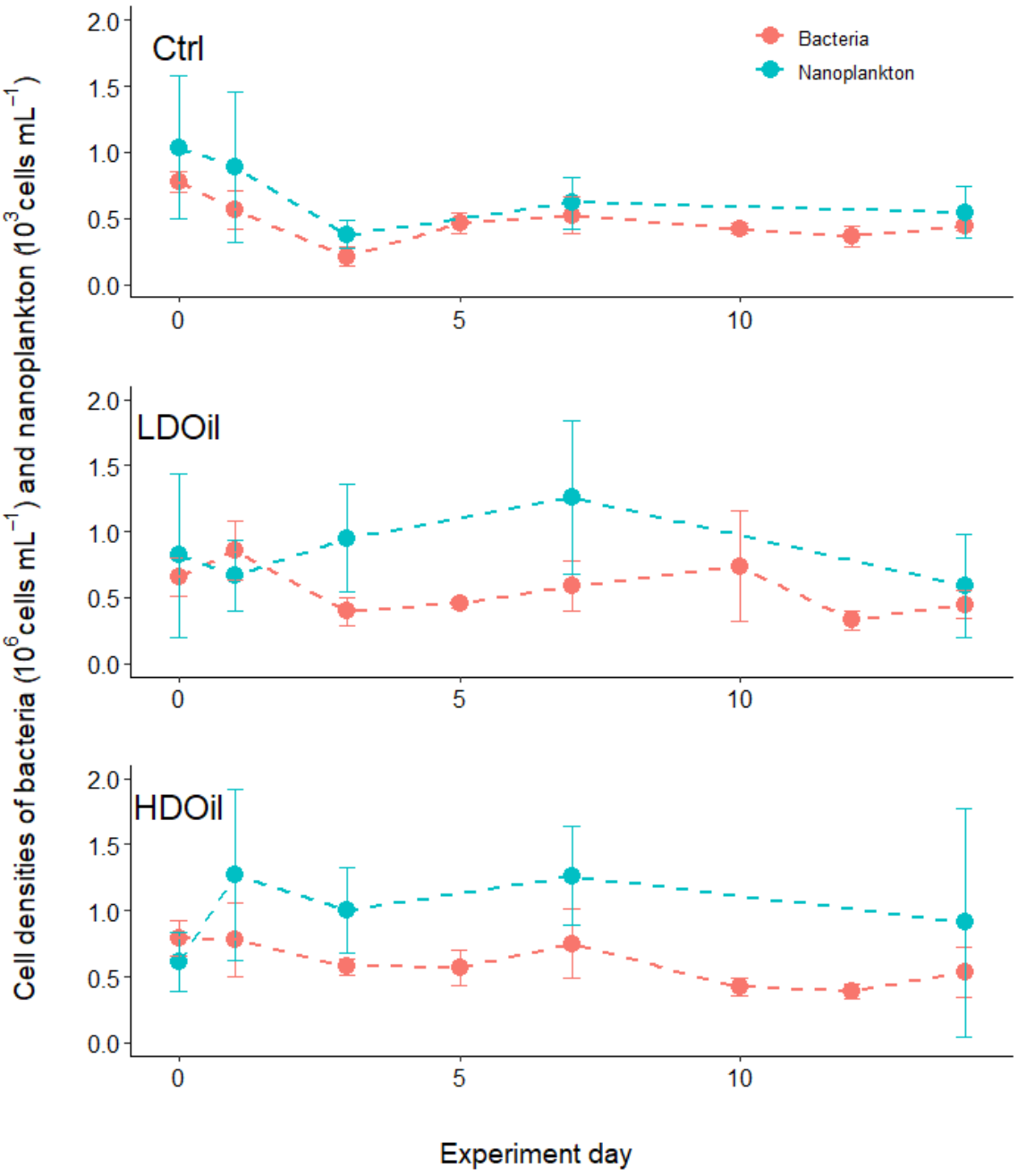

Figure 5.2 Mean cell densities (±1 S.D.) of bacteria (0.2-1.0 μm) and nanoplankton (1.0-20 μm) in the treatments throughout the experiment.

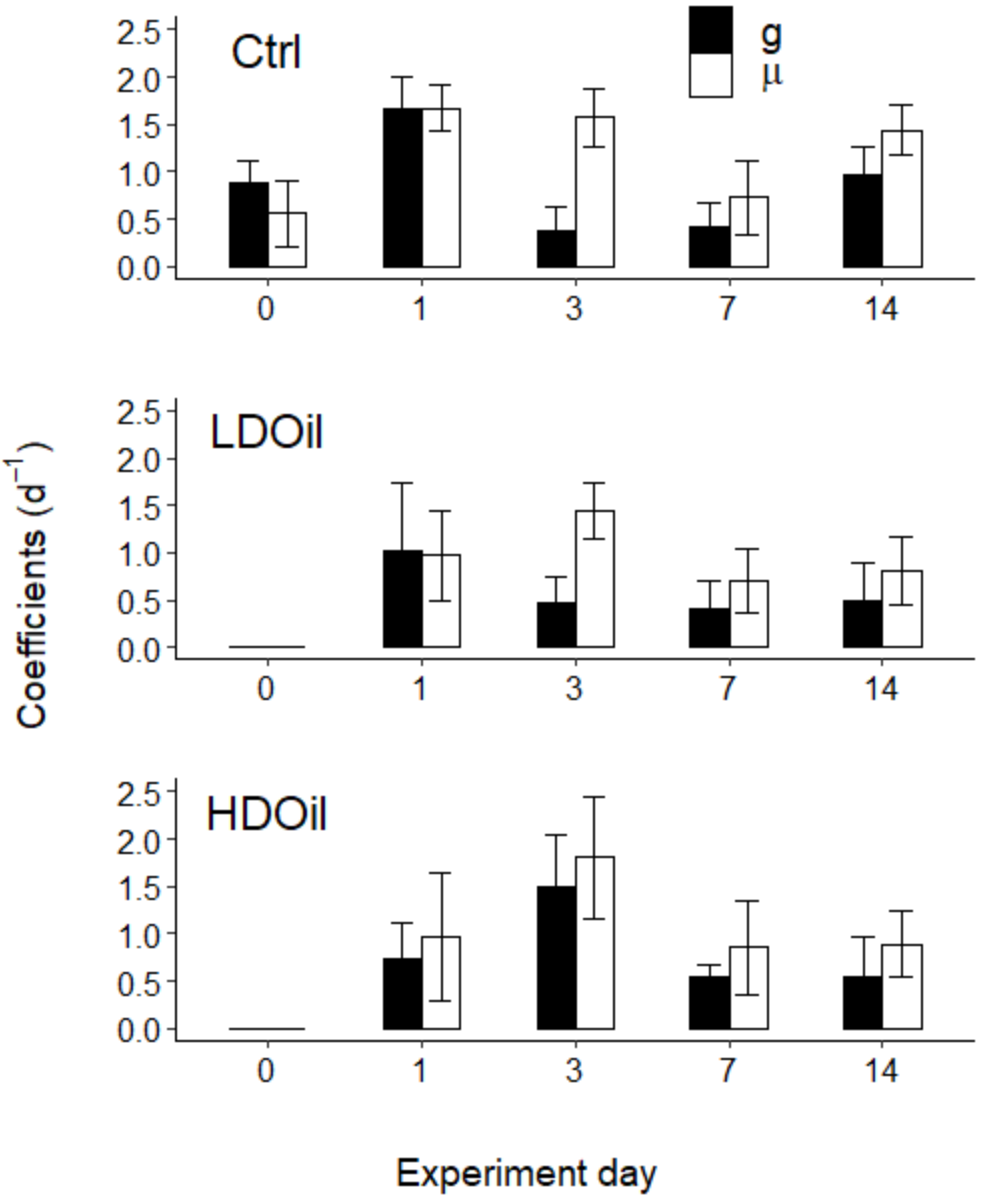

Figure 5.3 Mean coefficients (±1 S.D.) of grazing mortality (g) and population growth (μ) of bacteria on different experiment days. Error bar represents standard error of estimation of the coefficients.

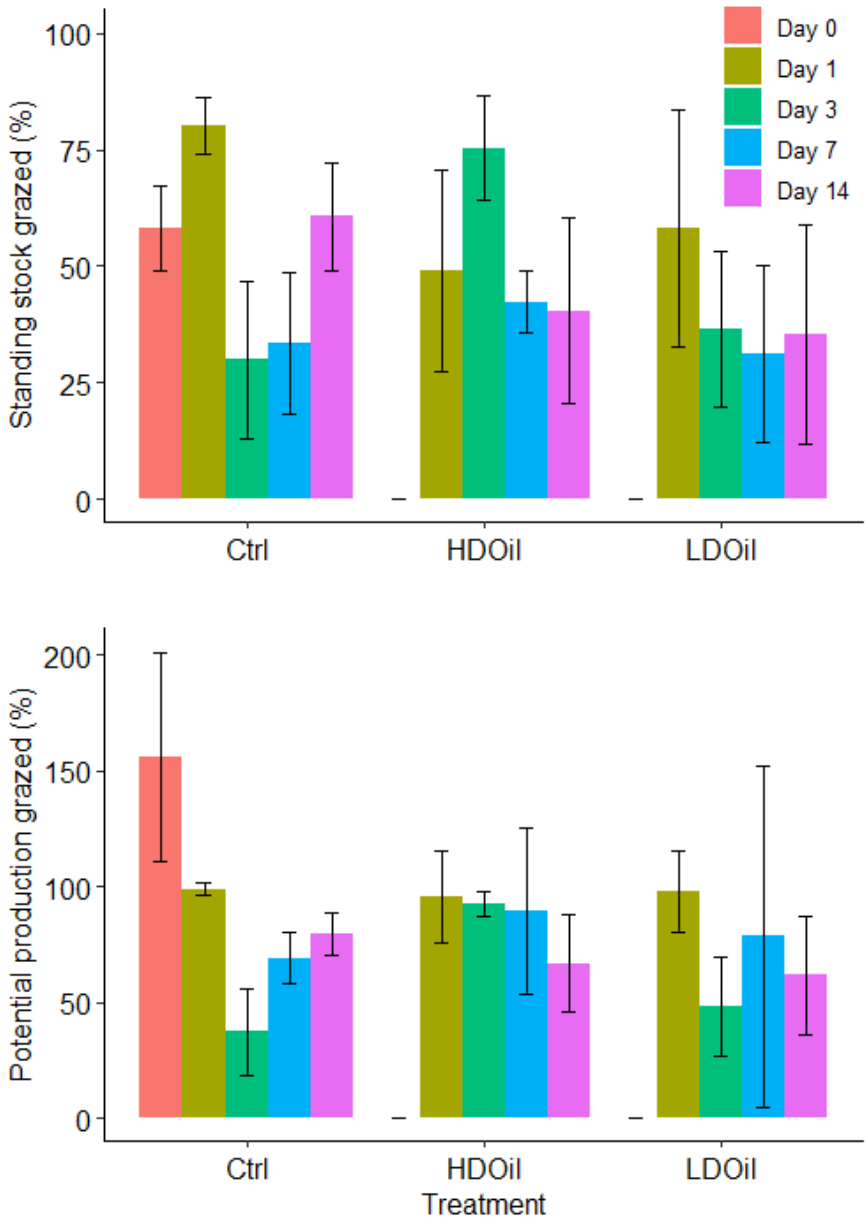

Figure 5.4 Mean percentages (±1 S.D.) of the standing stock grazed and the net production grazed of bacterial cells in the Ctrl, HDOil and LDOil treatments.

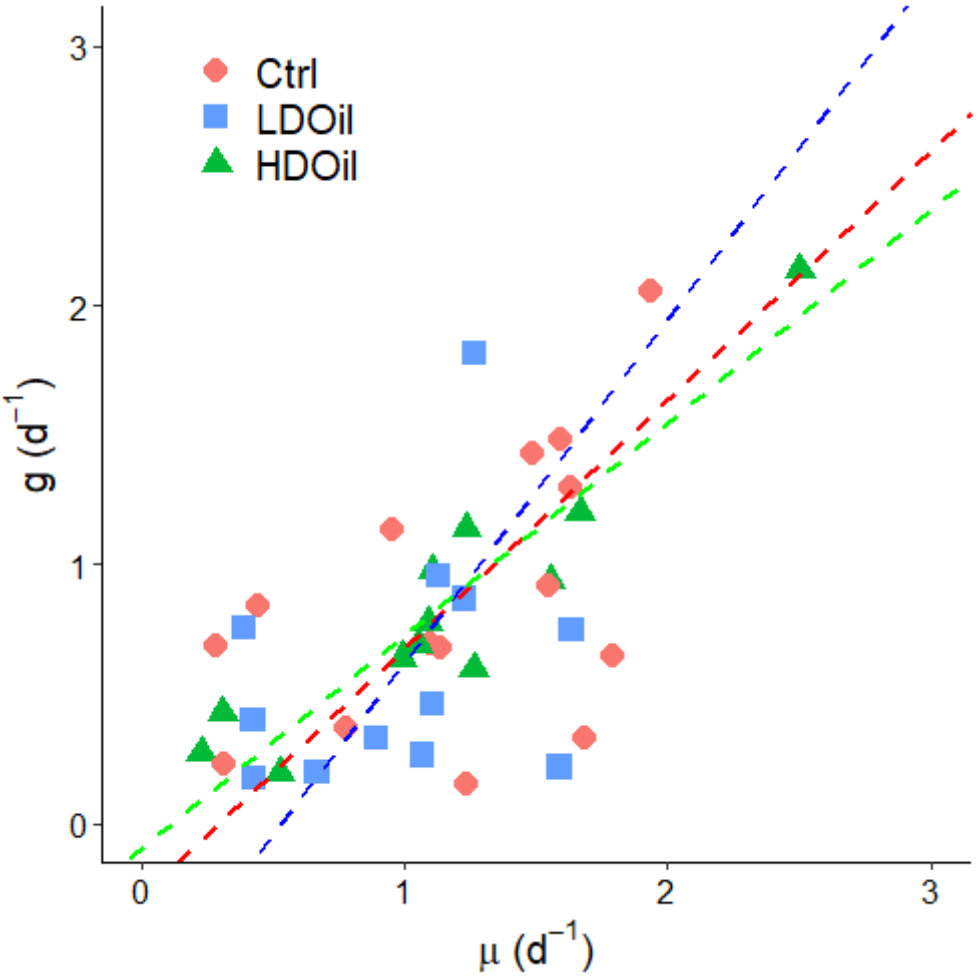

Figure 5.5 Model II linear regression (major axis) between population growth and grazing mortality of bacteria in the treatments. Red line represents the relationship of the Ctrl treatment ($g = 0.96\mu - 0.29$; $R^2 = 0.24$; $P = 0.06$), blue line represents that of the LDOil treatment ($g = 1.33\mu - 0.71$; $R^2 = 0.09$; $P = 0.34$) and green line presents that of the HDOil treatment ($g = 0.82\mu - 0.10$; $R^2 = 0.86$; $P < 0.001$).

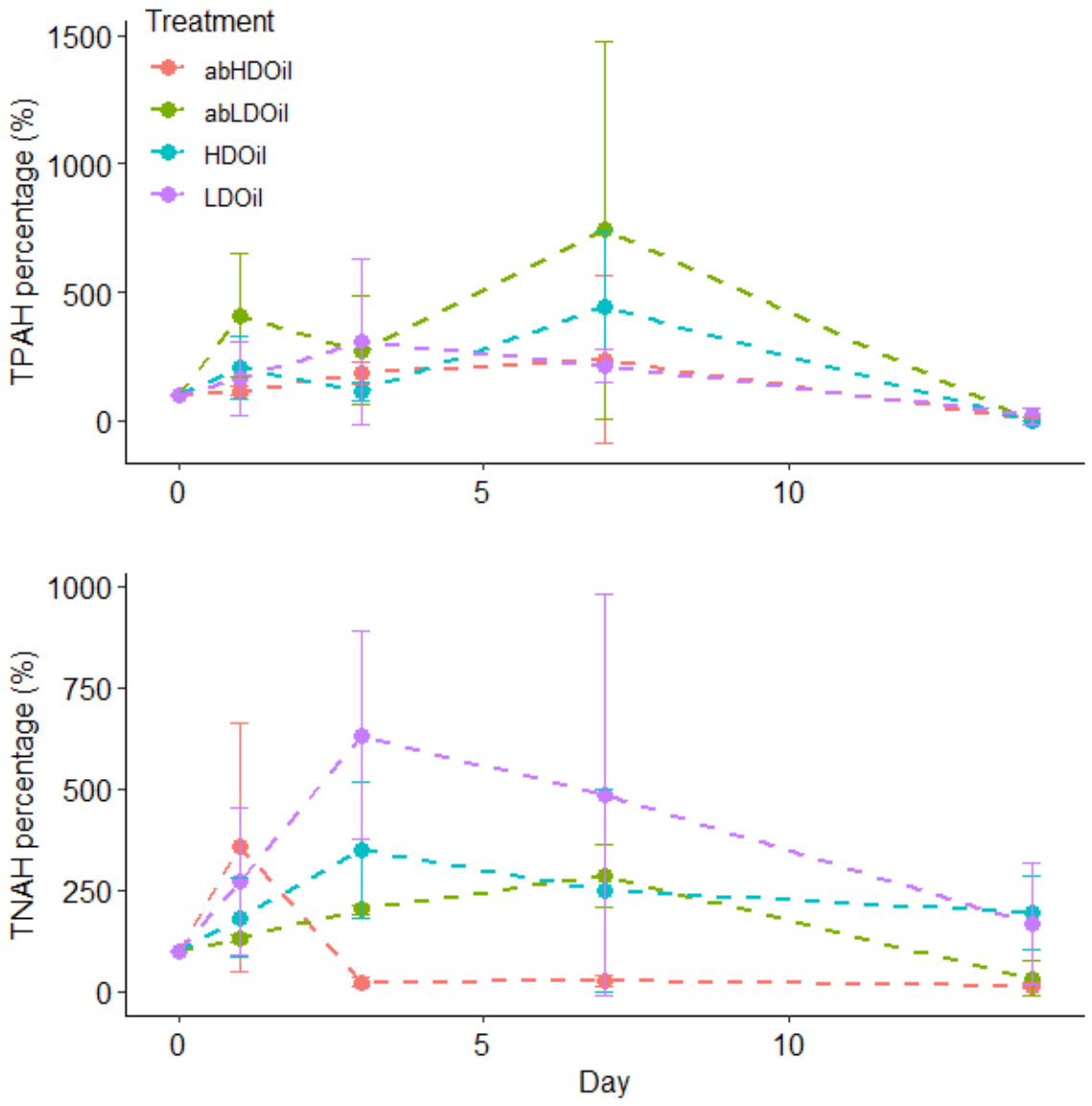

Figure 5.6. Mean percentage changes (±1 S.D.) of TPAH and TNAH compared to the concentrations on Day 0 in the treatments.

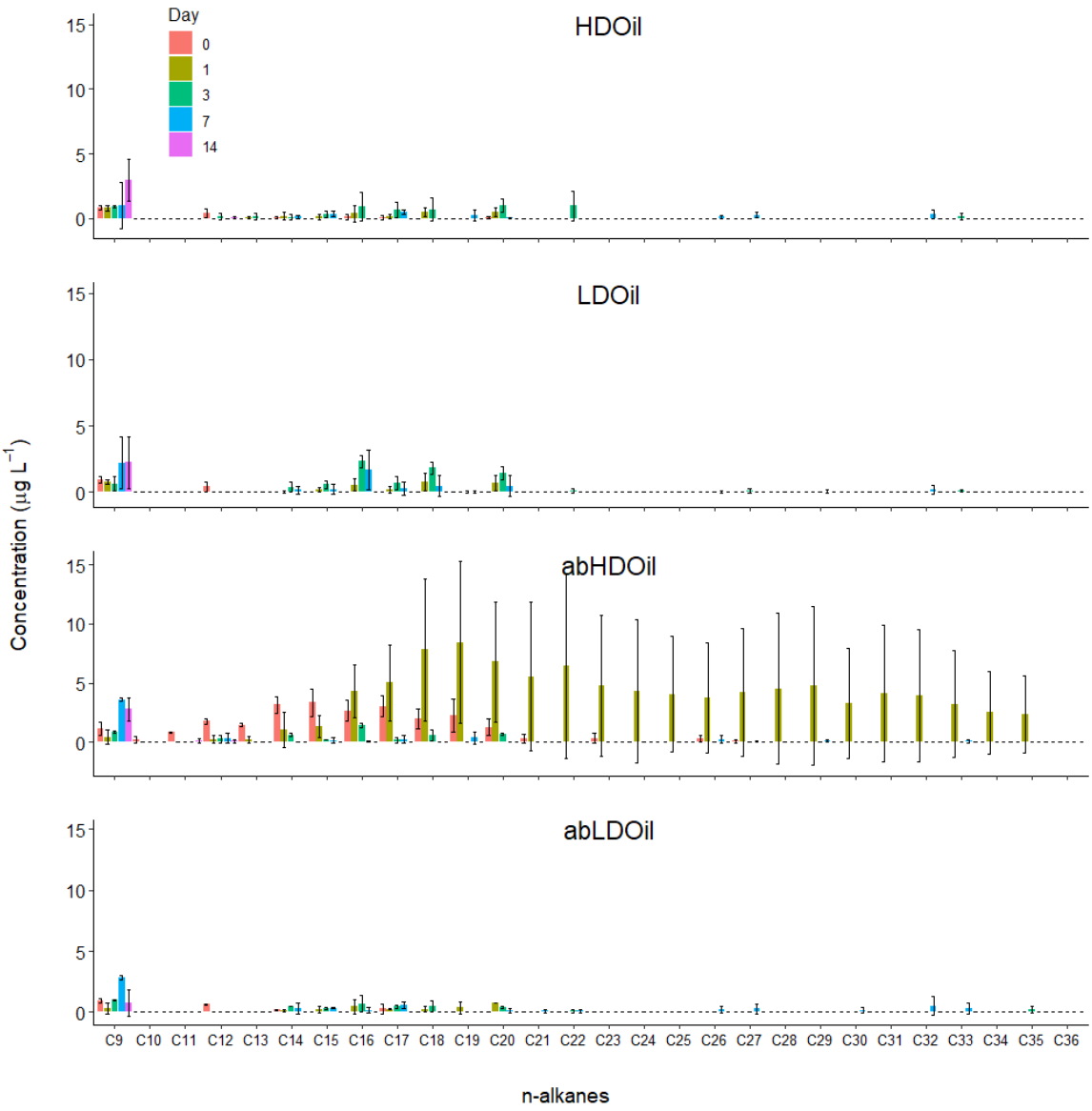

Figure 5.7 Mean concentrations (±1 S.D.) of *n*-alkanes (C9-C36) in the microcosms of HDOil, LDOil, abHDOil, and abLDOil on Day 0 through Day 14.

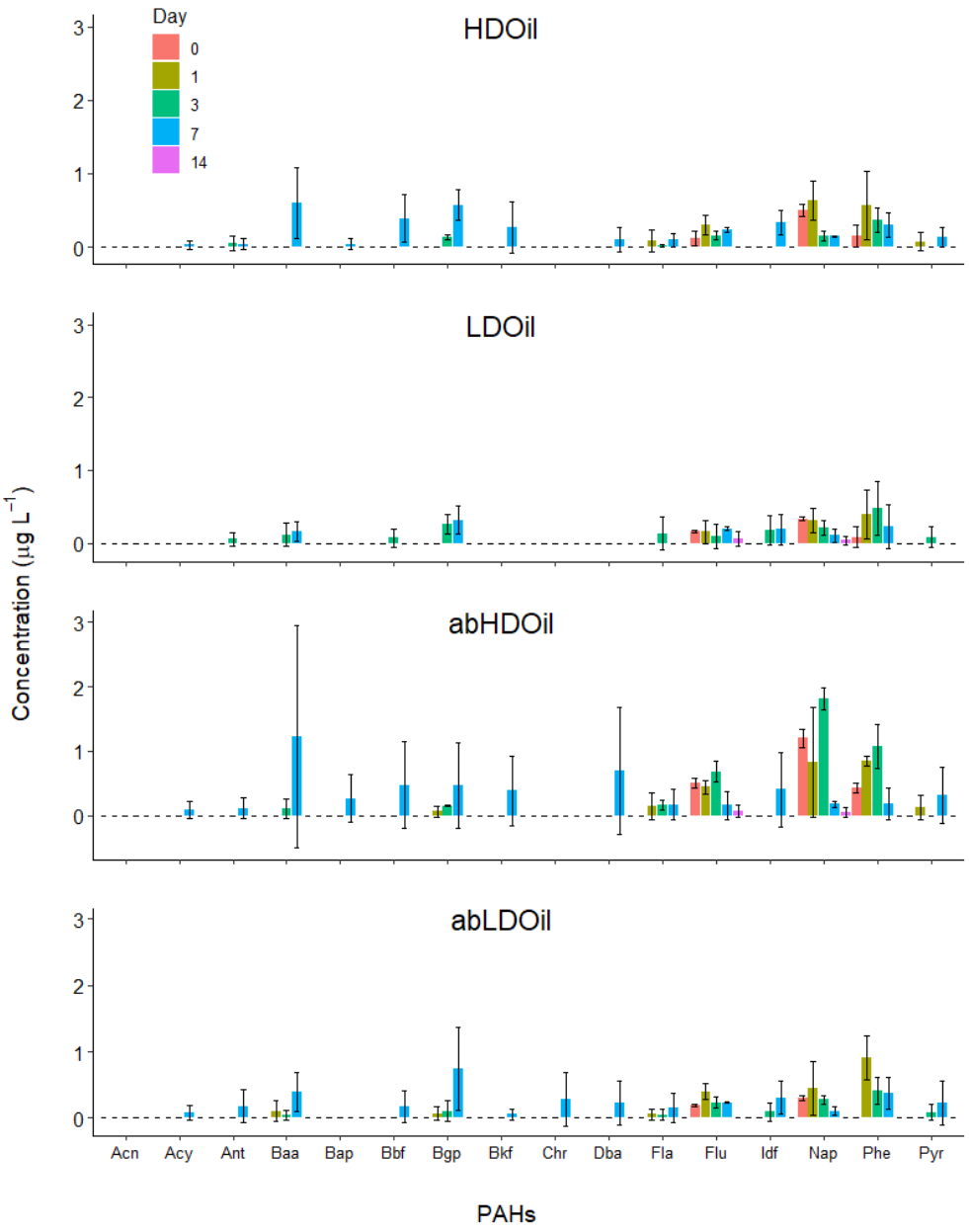

Figure 5.8 Mean concentrations (±1 S.D.) of PAHs in the microcosms of HDOil, LDOil, abHDOil, and abLDOil on Day 0 through Day 14. Acn: acenaphthene; Acy acenaphthylene; Ant: anthracene; Baa: benz[a]anthracene; Bap: benzo[a]pyrene; Bbf: benzo[b]fluoranthene; Bgp: benzo[g,h,i]perylene; Bkf: benzo[k]fluoranthene; Chr: chrysene; Dba: diben[a,h]anthracene; Fla: fluoranthene; Flu: fluorene; Idf: indeno[1,2,3-cd]fluoranthene; Nap: naphthalene; Phe: phenanthrene; and Pyr: pyrene.

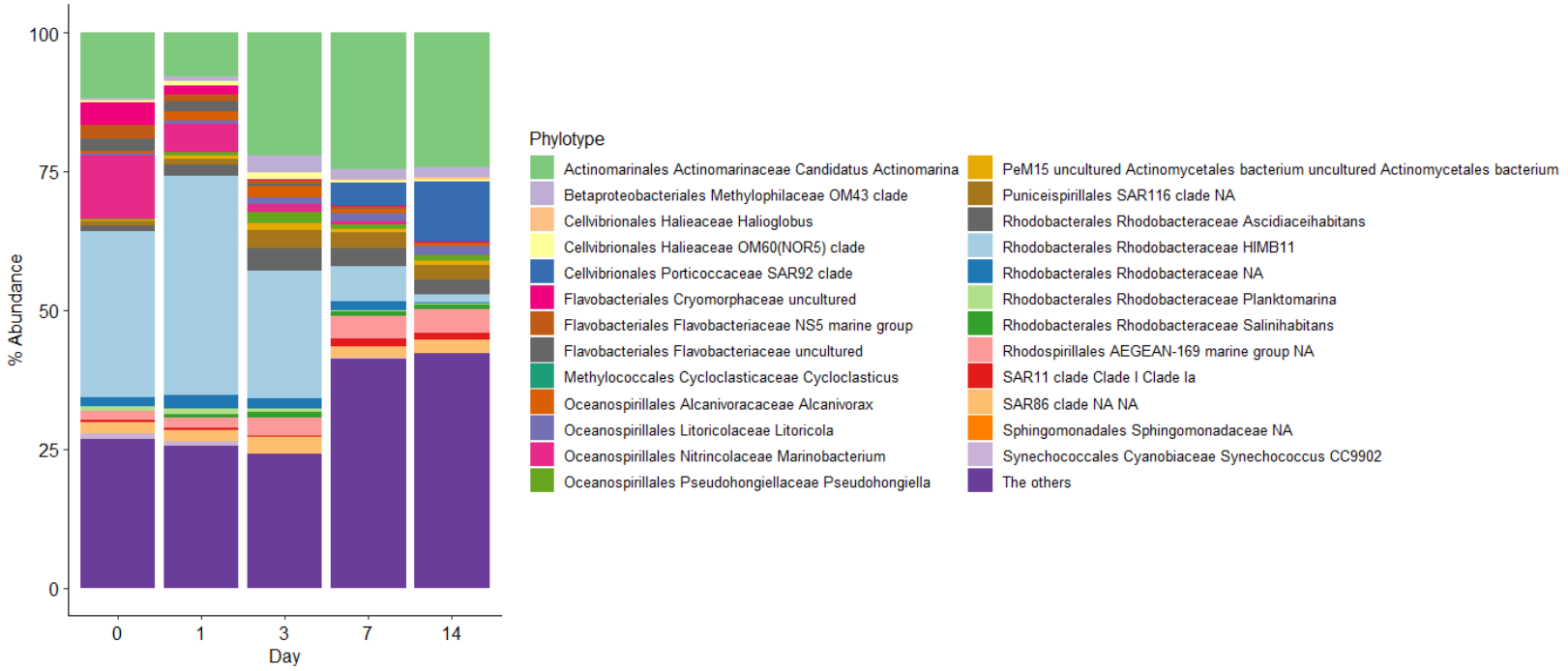

Figure 5.9 Mean percentage abundances of the 25 most abundant phylotypes (Genus) of microbial community in the Ctrl treatment.

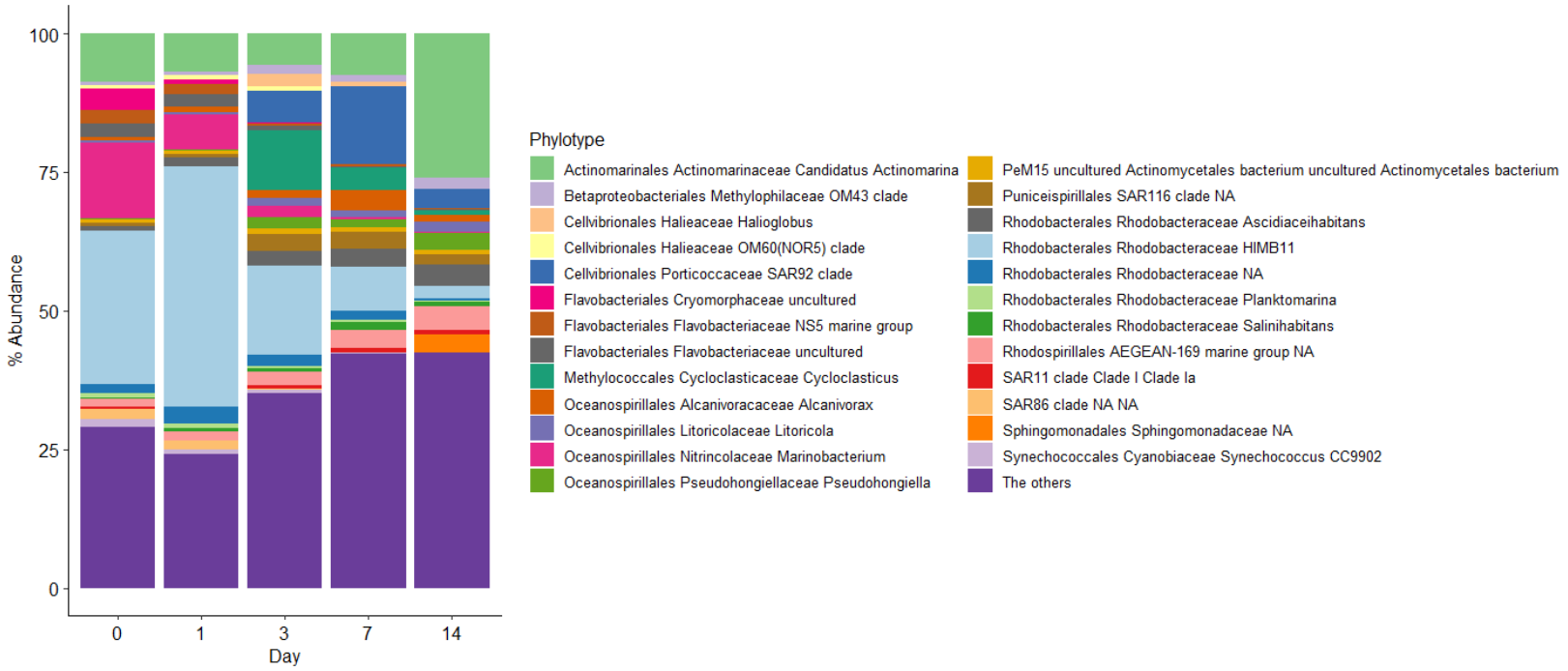

Figure 5.10 Mean percentage abundances of the 25 most abundant phylotypes (Genus) of microbial community in the LDOil treatment.

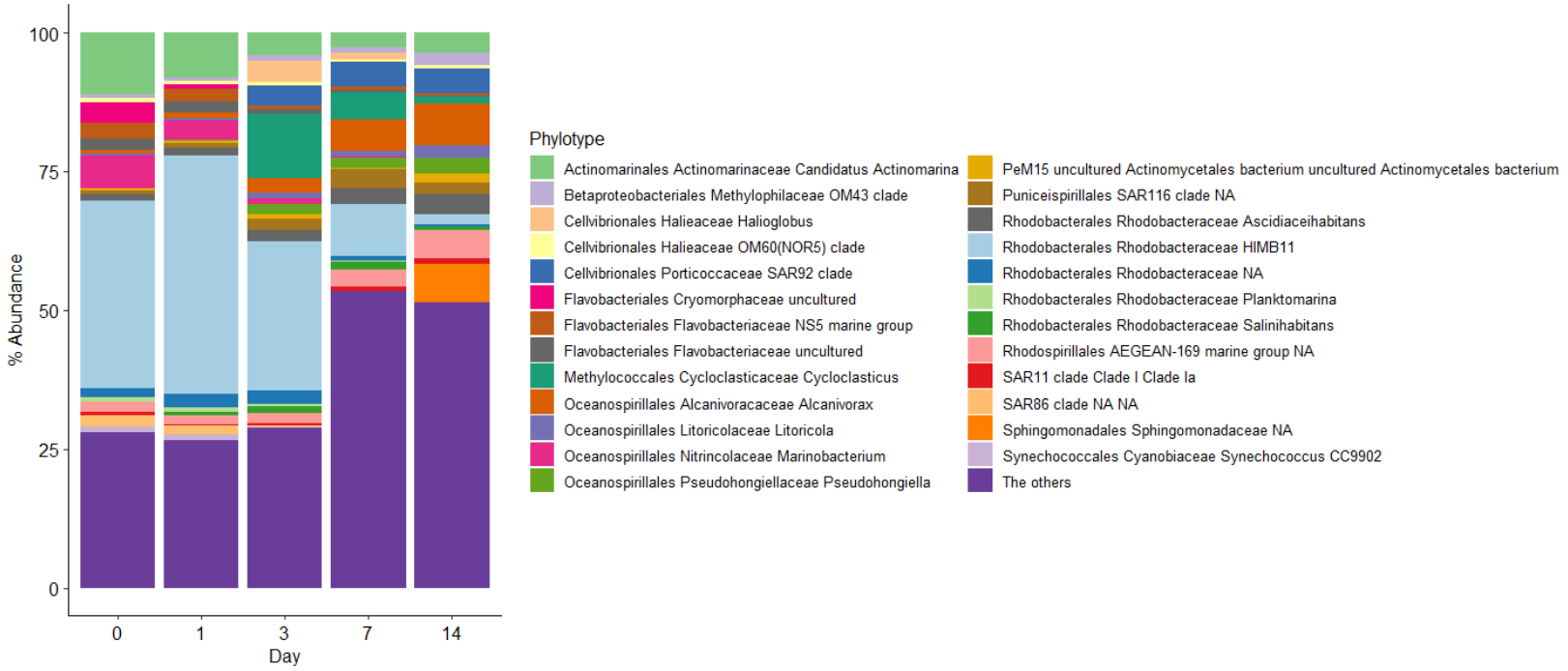

Figure 5.11 Mean percentage abundances of the 25 most abundant phylotypes (Genus) of microbial community in the HDOil treatment.

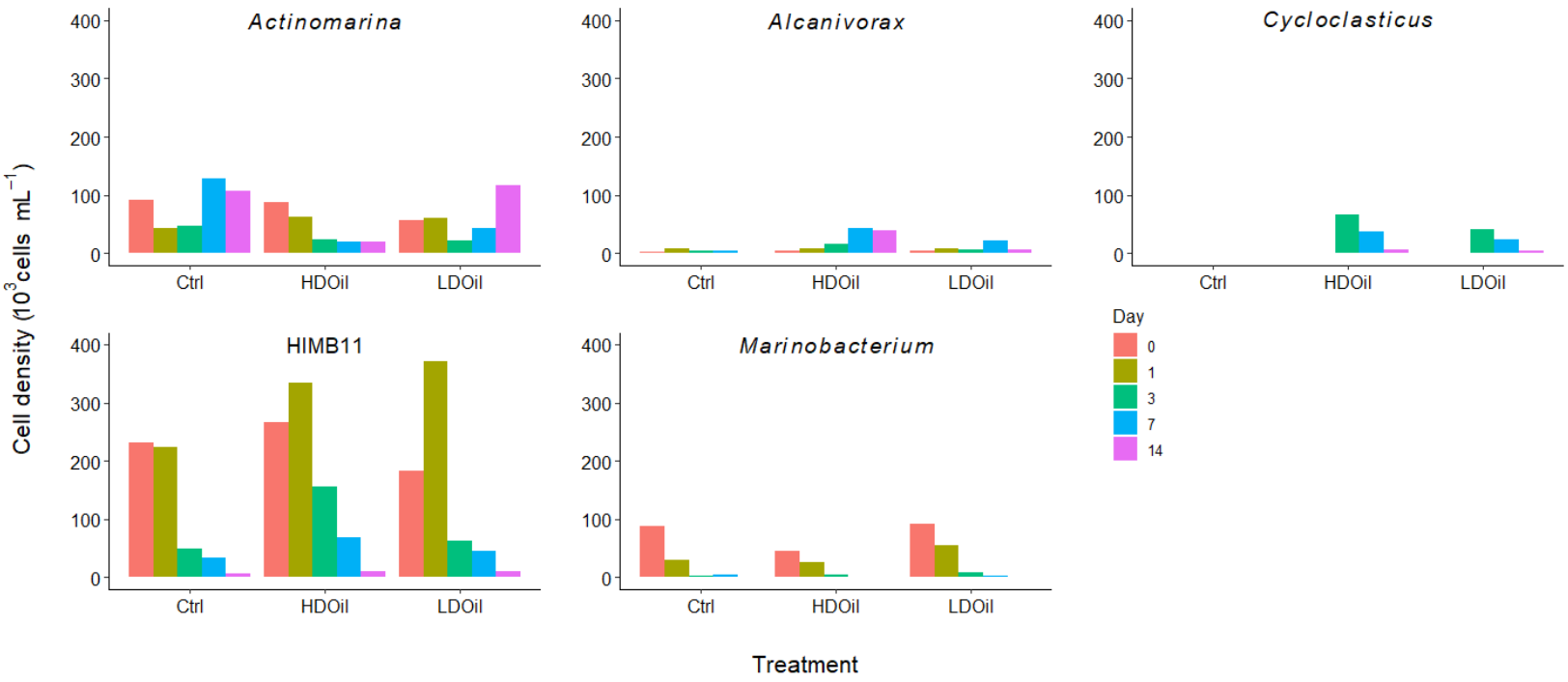

Figure 5.12 The estimated cell densities of bacterial phylotypes *Actinomarina*, *Alcanivorax*, *Cycloclasticus*, HIMB11 and *Marinobacterium* in the Ctrl, HDOil, and LDOil treatments throughout the experiment.

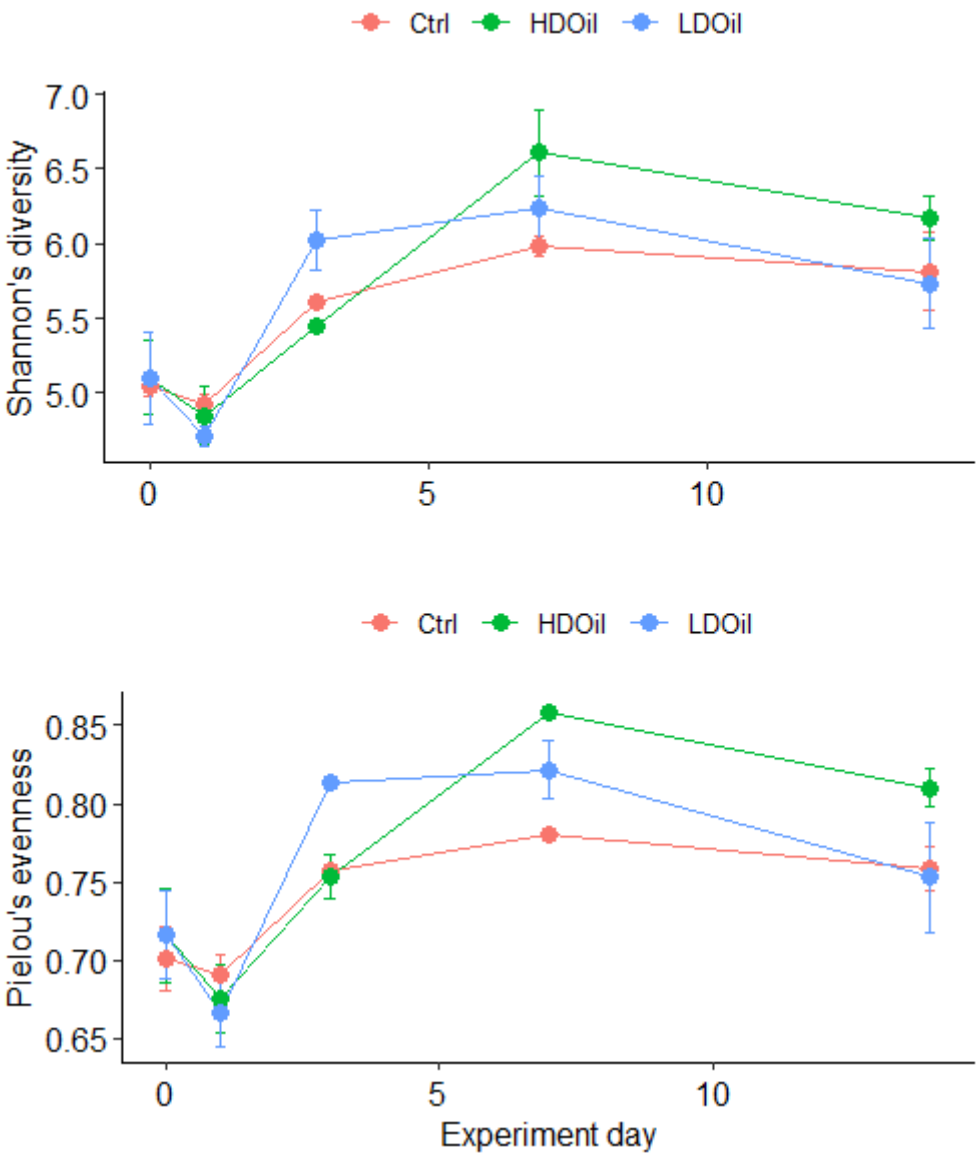

Figure 5.13 Mean (± S.E.) values of Shannon's diversity and Pielou's evenness indices of the bacterial community on Days 0, 1, 3, 7 and 14 in the Ctrl, LDOil and HDOil treatments.

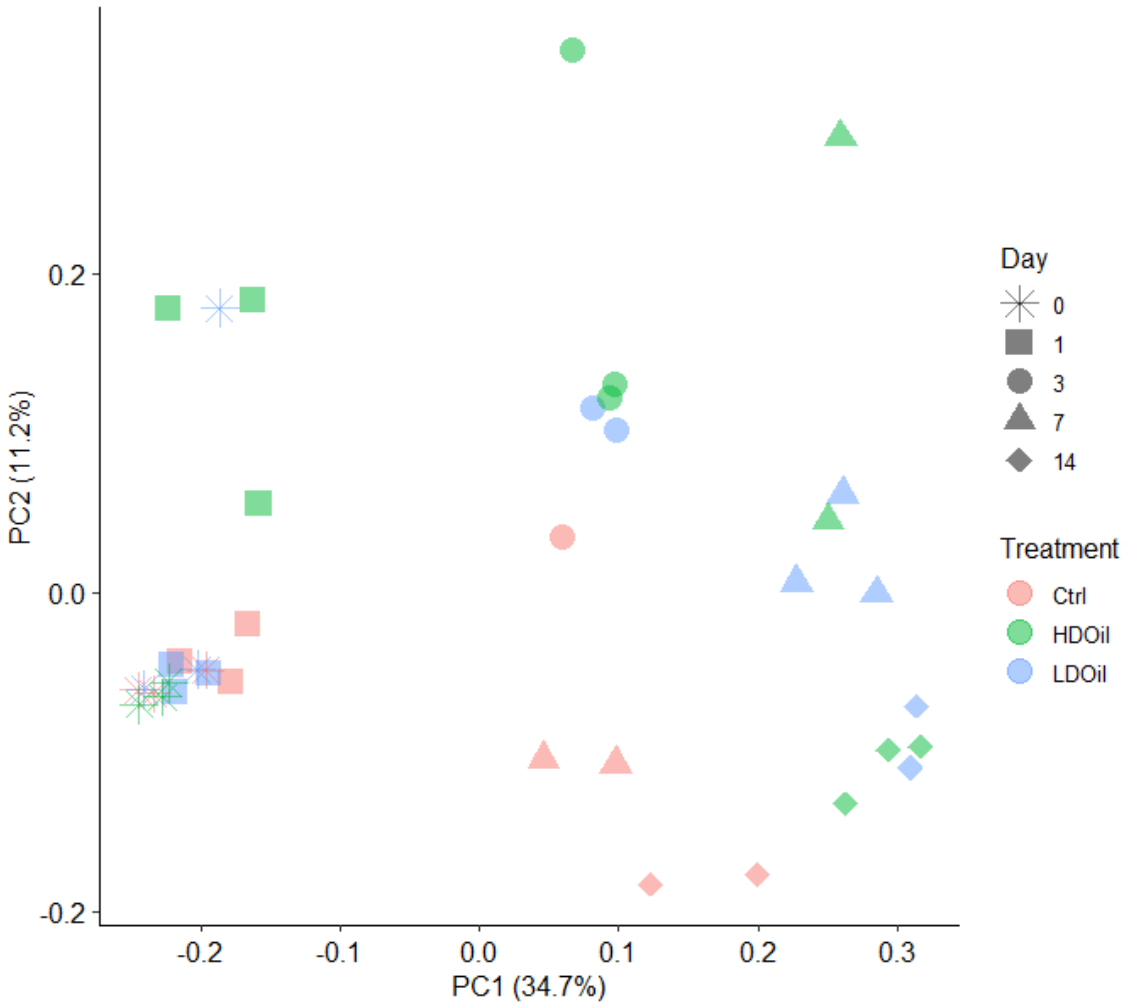

Figure 5.14 Results of PCoA of the unweighted UniFrac distance of the bacterial communities.

Chapter 6: General Conclusion

Marine protists, consisting of both microscopic producers and consumers, are the most important components at the base of the food web. At the community level, a simulated 7-day oil spill experiment at the nominal concentration of 10 μL L^{-1} of crude oil in 500 L mesocosms revealed a disrupted coupling between phytoplankton growth and microzooplankton grazing. While microzooplankton grazing accounted for approximately 50% of the phytoplankton growth in the control treatment, the microzooplankton grazing impacts in the oil-loaded treatment was negligible. The lack of microzooplankton grazing reduces the top-down control on phytoplankton and could potentially lead to algal blooms in the natural environment during oil spill events under certain conditions.

The bacterivory by nanoplankton assembly in seawater added with chemically dispersed crude oil at 2 μL L^{-1} and 8 μL L^{-1} concentrations in the 20 L microcosms was examined in a 14-day experiment. The grazing on bacteria by nanoplankton seemed not affected by the addition of hydrocarbons and it was tightly coupled with the bacterial growth and kept the bacterial abundance relatively steady throughout the entire experiment. The community composition of bacteria shifted during the experiment, with the compositions in the oil-loaded treatments becoming more similar to one another and more differentiated from those in the control treatment towards the end of the experiment. The relatively high abundance of hydrocarbon-degrading bacteria *Cycloclasticus* and *Alcanivorax* in the oil-loaded treatments indicated the presence of biodegradation of crude oil. Given that the degrees of bacterivory did not differ among the three treatments, the compositional changes in the bacterial community is believed to be related to bottom-up control of carbon and inorganic nutrient availabilities rather than top-down control by nanoplankton grazing.

At the species level, the vulnerabilities of the heterotrophic dinoflagellates *Oxyrrhis marina*, *Protoperidinium* sp., ciliates *Euplotes* sp. and *Metacylis* sp., and their algal prey species to the water accommodated fraction of petroleum hydrocarbons and dispersant were tested. All the protistan species showed species-specific response to the

pollutants. Their cell volume and taxonomic grouping did not explain their variations in their vulnerability to toxicants. Most of the grazer species experienced reduced population grazing impacts or *per capita* ingestion rates in the treatments of crude oil alone and chemically dispersed crude oil at a certain concentration.

Mixotrophic dinoflagellates and ciliates are thought to be capable of dominating the plankton grazer community. However, the mixotrophic dinoflagellate *Fragilidium subglobosum* tested did not grow well in media with *Tripos tripos* as added prey when separately maintained at 19°C and 23°C. While its maximum photosynthetic efficiencies were higher at 19°C, *F. subglobosum* did not show obvious feeding at both temperatures. The negligible prey ingestion could be due to prey selectivity, triggering mechanisms of phagotrophy or intra-specific strain variations. It is suspected that this Florida strain of *F. subglobosum* is not mixotrophic. The hypothesis that it becomes more heterotrophic at elevated seawater temperature is therefore not proved or disapproved.

Overall, the herbivory by microzooplankton was reduced while the bacterivory by nanoplankton was not affected in the presence of chemically dispersed crude oil at the tested concentrations. The tested marine protists reacted differently to the changed environments of the elevated seawater temperature and the addition of petroleum hydrocarbon pollutants.

References

Abed, R.M.M. (2010). Interaction between cyanobacteria and aerobic heterotrophic bacteria in the degradation of hydrocarbons. *International Biodeterioration & Biodegradation 64*, 58-64.

Akimov, A.I., Solomonova, E.S. (2019). Characteristics of growth and fluorescence of certain types of algae during acclimation to different temperatures under culture conditions. *Oceanology 59*, 316-326.

Alexander, M.A., Scott, J.D., Friedland, K.D., Mills, K.E., Nye, J.A., Pershing, A.J., et al. (2018). Projected sea surface temperature over the 21st century: changes in the mean, variability and extremes for large marine ecosystem regions of Northern Oceans. *Elementa Science of the Anthropocene 6*, 9.

Allen, A.P., Gillooly, J.F., Brown, J.H. (2005). Linking the global carbon cycle to individual metabolism. *Functional Ecology 19*, 202-213.

Almeda, R., Connelly, T.L., Buskey, E.J. (2014a). Novel insight into the role of heterotrophic dinoflagellates in the fate of crude oil in the sea. *Scientific Reports 4*, 7560.

Almeda, R., Cosgrove, S., Buskey, E.J. (2018). Oil spills and dispersants can cause the initiation of potentially harmful dinoflagellate blooms ("red tides"). *Environmental Science & Technology 52*, 5718-5724.

Almeda, R., Hyatt, C., Buskey, E.J. (2014b). Toxicity of dispersant Corexit 9500A and crude oil to marine microzooplankton. *Ecotoxicology and Environmental Safety 106*, 76-85.

Almeda, R., Wambaugh, Z., Chai, C., Wang, Z., Liu, Z., Buskey, E.J. (2013). Effects of crude oil exposure on bioaccumulation of polycyclic aromatic hydrocarbons and survival of adult and larval stages of gelatinous zooplankton. *PLoS One 8*, e74476.

Anderson, M.J. (2001). A new method for non-parametric multivariate analysis of variance. *Austral Ecology 26*, 32-46.

Anderson, R.A. (2005). (Ed.). *Algal Culturing Techniques*. Burlington, MA: Elsevier Academic Press. Pp. 578.

Andrews, A.R., Floodgate, G.D. (1974). Some observations on the interactions of marine protozoan and crude oil residues. *Marine Biology 25*, 7-12.

Apple, J.K., del Giorgio P.A., Newell, R.I.E. (2004). The effects of system-level nutrient enrichment on bacterioplankton production in a tidally-influenced estuary. *Journal of Coastal Research SI 45*, 110-133.

Atkinson, D., Ciotti, B.J., Montagnes, D.J.S. (2003). Protists decrease in size linearly with temperature: ca. 2.5% $°C^{-1}$. *Proceedings of the Royal Society B: Biological Sciences 270*, 2605-2611.

Avila, T.R., Bersano, J.G.F., Fillmann, G. (2010). Lethal and sub-lethal effects of the water-soluble fraction of a light crude oil on the planktonic copepod *Acartia tonsa*. *Journal of the Brazilian Society of Ecotoxicology 5*, 19-25.

Azam, F.A., Fenchel, T., Field, J.G., Gray, J.S., Meyer-Reil, L.A., Thingstad, F. (1983). The ecological role of water-column microbes in the sea. *Marine Ecology Progress Series 10*, 257-263.

Bacosa, H.P., Erdner, D.L., Liu, Z. (2015). Differentiating the roles of photooxidation and biodegradation in the weathering of Light Louisiana Sweet crude oil in surface water from the Deepwater Horizon site. *Marine Pollution Bulletin 95*, 265-272.

Bamdad, M., Reader, S., Groliere, C.A., Bohatier, J., Denizeau, F. (1997). Uptake and efflux of polycyclic aromatic hydrocarbons by *Tetrahymena pyriformis*: evidence for a resistance mechanism. *Cytometry 28*, 170-175.

Banse, K. (1982). Cell volumes, maximal growth rates of unicellular algae and ciliates, and the role of ciliates in the marine pelagial. *Limnology and Oceanography 27*, 1059-1071.

Barron, M.G. (2017). Photochemical toxicity of petroleum to aquatic invertebrates and fish. *Achieves of Environmental Contamination and Toxicity 73*, 40-46.

Beaufort, L., Probert, I. de Garidel-Thoron, T., Bendif, E.M., Ruiz-Pino, D. Metzl, N., et al. (2011). Sensitivity of coccolithophores to carbonate chemistry and ocean acidification. *Nature 476*, 80-83.

Bisanz, J.E. (2018). qiime2R: importing QIIME2 artifacts and associated data into R sessions.

Bode, A., Gonzalez, N., Lorenzo, J., Valencia, J., Varela, M.M., Varela, M. (2006). Enhanced bacterioplankton activity after the '*Prestige*' oil spill off Galicia, NW Spain. *Aquatic Microbial Ecology 43*, 33-41.

Boehm, P.D., Page, D.S. (2007). Exposure elements in oil spill risk and natural resource damage assessments: A review. *Human and Ecological Risk Assessment 13,* 418 – 448.

Boenigk, J., Arndt, H. (2002). Bacterivory by heterotrophic flagellates: community structure and feeding strategies. *Antonie van Leeuwenhoek 81,* 465-480.

Bokulich N.A., Kaehler, B.D., Rideout, J.R., Dillon, M., Bolyen E., Knight, R., et al. (2018). Optimizing taxonomic classification of marker-gene amplicon sequences with QIIME 2's q2-feature-classifier plugin. *Microbiome 6,* 90.

Bolyen, E., Rideout, J.R., Dillon, M.R., Bokulich, N.A., Abnet, C.C., Al-Ghalith, G.A., et al. (2019). Reproducible, interactive, scalable and extensible microbiome data science using QIIME 2. *Nature Biotechnology 37,* 848-857.

Bonnet, J.L., Guiraud, P., Dusser, M., Kadri, M., Laffosse, J., Steinman, R., et al. (2005). Assessment of anthracene toxicity toward environmental eukaryotic microorganisms: *Tetrahymena pyriformis* and selected micromycetes. *Ecotoxicity and Environmental Safety 60,* 87-100.

Brown, J.H., Gilloly, J.F., Allen, A.P., Savage, V.M., West, G.B. (2004). Toward a metabolic theory of ecology. *Ecology 85,* 1771-1789.

Burgherr, P. (2007). In-depth analysis of accidental oil spills from tankers in the context of global spill trends from all sources. *Journal of Hazardous Materials 40,* 245-256.

Burkholder, J.M., Glibert, P.M., Skelton, H.M. (2008). Mixotrophy, a major mode of nutrition for harmful algal species in eutrophic waters. *Harmful Algae 8,* 77-93.

Buskey, E.J. (1997). Behavioral components of feeding selectivity of the heterotrophic dinoflagellate *Protoperidinium pellucidum*. *Marine Ecology Progress Series 153,* 77-89.

Buskey, E.J., Coulter, C.J., Brown, S.L. (1994). Feeding, growth and bioluminescence of the heterotrophic dinoflagellate *Protoperidinium huberi*. *Marine Biology 121,* 373-380.

Buskey, E.J., Deyoe, H., Jochem, F.J., Villareal, T.A. (2003). Effects of mesozooplankton removal and ammonium addition on planktonic trophic structure during a bloom of the Texas 'brown tide': a mesocosm study. *Journal of Plankton Research 25,* 215-228.

Buskey, E.J., Montagna, P.A., Amos, A.F., Whiteledge, T.E. (1997). Disruption of grazer populations as a contributing factor to the initiation of the Texas brown tide algal bloom. *Limnology and Oceanography 42*, 1215-1222.

Cabreizo, M.J., Gonzalez-Olalla, J.M., Hinojosa-Lopez, V., Peralta-Cornejo, F.J., Carrillo, P. (2019). A shifting balance: responses of mixotrophic marine algae to cooling and warming under UVR. *New Phytologist 221*, 1317-1327.

Calbet, A. (2008). The trophic role of microzooplankton in marine systems. *ICES Journal of Marine Science 65*, 325-331.

Calbet, A., Bertos, M., Fuentes-Grunewald, C., Alacid, E., Figueroa, R., Renom, B., Garces, E. (2011). Intraspecific variability in *Karlodinium veneficum*: Growth rates, mixotrophy, and lipid composition. *Harmful Algae 10*, 654-667.

Calbet, A., Landry, M.R. (2004). Phytoplankton growth, microzooplankton grazing, and carbon cycling in marine systems. *Limnology and Oceanography 49*, 51-57.

Calbet, A., Saiz, E. (2005). The ciliate-copepod link in marine ecosystems. *Aquatic Microbial Ecology 38*, 157-167.

Calbet, A., Saiz, E., Barata, C. (2007). Lethal and sublethal effects of naphthalene and 1,2-dimethylnaphthalene on the marine copepod *Paracartia grani*. *Marine Biology 151*, 195-204.

Callahan B.J., McMurdie P.J., Rosen, M.J., Han, A.W., Johnson, A.J., Holmes, S.P. (2016). DADA2: High-resolution sample inference from Illumina amplicon data. *Nature Methods 13*, 581-583.

Carstensen, J., Conley, D.J., Henriksen, P. (2004). Frequency, composition, and causes of summer phytoplankton blooms in a shallow coastal ecosystem, the Kattegat. *Limnology & Oceanography 49*, 190-201.

Cermeno, P., Estevez-Blanco, P., Maranon, E., Fernandez, E. (2005). Maximum photosynthetic efficiency of size-fractionated phytoplankton assessed by ^{14}C uptake and fast repetition rate fluorometry. *Limnology & Oceanography 50*, 1438-1446.

Chen, B., Liu, H., Landry, M.R., Dai, M., Huang, B., Sun, J. (2009). Close coupling between phytoplankton growth and microzooplankton grazing in the western South China Sea. *Limnology and Oceanography 54*, 1084-1097.

Chisholm, S.W. (1992). Phytoplankton size. In P.G. Falkowski, A.D. Woodhead (Eds.) *Primary Productivity and Biogeochemical Cycles in the Sea.* (pp. 213-237). New York: Plenum Press.

Clough, J., Strom, S. (2005). Effects of *Heterosigma akashiwo* (Raphidophyceae) on protist grazers: laboratory experiments with ciliates and heterotrophic dinoflagellates. *Aquatic Microbial Ecology 39*, 121-134.

Cohen, J.H., McCormick, L.R., Burkhardt, S.M. (2014). Effects of dispersant and oil on survival and swimming activity in a marine copepod. *Bulletin of Environmental Contamination and Toxicology 92*, 381-387.

Connell, D.W., Miller, G.J., Farrington, J.W. (1981). Petroleum hydrocarbons in aquatic ecosystems-behavior and effects of sublethal concentrations: Part 2. *Critical Reviews in Environmental Science and Technology 11*, 105-162.

Corner, E.D.S., Harris, R.P., Kilvington, C.C., O'Hara, S.C.M. (1976). Petroleum compounds in the marine food web: short-term experiments on the fate of naphthalene in *Calanus*. *Journal of the Marine Biological Association of the United Kingdom 56*, 121-133.

Dabestani, R., Ivanov, I.N. (1999). A compilation of physical, spectroscopic and photophysical properties of polycyclic aromatic hydrocarbons. *Photochemistry and Photobiology 70*, 10-34.

Dahl, E., Laake, M., Tjessem, K., Eberlein, K., Bohle, B. (1983). Effects of Ekofisk crude oil on an enclosed planktonic ecosystem. *Marine Ecology Progress Series 14*, 81-91.

Dalby, A.P., Kormas, K.A., Christaki, U., Karayanni, H. (2008). Cosmopolitan heterotrophic microeukaryotes are active bacterial grazers in experimental oil-polluted systems. *Environmental Microbiology 10*, 47-56.

del Campo, J., Balague, V., Forn, I., Lukunberri I., Massana, R. (2013). Culturing bias in marine heterotrophic flagellates analyzed through seawater enrichment incubations. *Microbial Ecology 66*, 489-499.

del Giorgio, P.A., Gasol, J.M., Vaque, D., Mura, P., Agusti, S., Duarte, C.M. (1996). Bacterioplankton community structure: protists control net production and the production of active bacteria in a coastal marine community. *Limnology and Oceanography 41*, 1169-1179.

DeLong, S.P., Vasseur, D.A. (2012). Size-density scaling in protists and the links between consumer-resource interaction parameters. *Journal of Animal Ecology 81*, 1193-1201.

Dickman, E.M., Vanni, M.J., Horgan, M.J. (2006). Interactive effects of light and nutrients on phytoplankton stoichiometry. *Oecologia 149*, 676-689.

Dong, J., Zhou, W., Song, L., Li, G. (2015). Responses of phytoplankton functional groups to simulated winter warming. *Annales de Limnologie – International Journal of Limnology 51*, 199-210.

Dunstan, W.M., Atkinson, L.P., Natoli, J. (1975). Stimulation and inhibition of phytoplankton growth by low molecular weight hydrocarbons. *Marine Biology 31*, 305-310.

Dyksterhouse, S.E., Gray, J.P., Herwig, R.P., Lara, J.C., Staley, J.T. (1995). *Cycloclasticus pugetii* gen. nov., sp. nov., an aromatic hydrocarbon-degrading bacterium from marine sediments. *International Journal of Systemic Bacteriology 45*, 116-123.

Echeveste, P., Agusti, S., Dachs, J. (2010a). Cell size dependent toxicity thresholds of polycyclic aromatic hydrocarbons to natural and cultured phytoplankton populations. *Environmental Pollution 158*, 299-307.

Echeveste, P., Agusti, S., Dachs, J. (2011). Cell size dependence of additive versus synergetic effects of UV radiation and PAHs on oceanic phytoplankton. *Environmental Pollution 159*, 1307-1316.

Echeveste, P., Dachs, J., Berrojalbiz, N., Agusti, S. (2010b). Decrease in the abundance and viability of oceanic phytoplankton due to trace levels of complex mixtures of organic pollutants. *Chemosphere 81*, 161-168.

Edwards, K.F. (2019). Mixotrophy in nanoflagellates across environmental gradients in the ocean. *The Proceedings of the National Academy of Science 116*, 6211-2220.

Edwards, K.F., Thomas, M.K., Klausmeier, C.A., Litchman, E. (2016). Phytoplankton growth and the interaction of light and temperature: a synthesis at the species and community level. *Limnology and Oceanography 61*, 1232-1244.

El-Sheekh, M.M., El-Naggar, A.H., Osman, M.E.H., Haieder, A. (2000). Comparative studies on the green algal *Chlorella homosphaera* and *Chlorella vulgaris* with respect to oil pollution in the river Nile. *Water, Air, and Soil Pollution 124*, 187-204.

Eppley, R.W. (1972). Temperature and phytoplankton growth in the sea. *Fishery Bulletin 70,* 1063-1085.

Evans, A., Madden, K., Palmer, S.M. (2012). (Eds.) *The Ecology and Sociology of The Mission-Aransas Estuary-An Estuarine and Watershed Profile*. Pp. 183.

Farrelly, V., Rainey, F.A., Stackebrandt, E. (1995). Effect of genome size and rrn gene copy number on PCR amplification of 16S rRNA genes from a mixture of bacterial species. *Applied and Environmental Microbiology 61,* 2798-2801.

Fenchel, T. (1982). Ecology of heterotrophic microflagellates. IV. Quantitative occurrence and importance as bacterial consumers. *Marine Ecology Progress Series 9,* 35-42.

Feng, Y., Warner, M.E., Zhang, Y., Sun, J., Fu, F.X., Rose, J.M., et al. (2008). Interactive effects of increased pCO_2, temperature and irradiance on the marine coccolithophore *Emiliania huxleyi* (Prymnesiophyceae). *European Journal of Phycology 43,* 87-98.

Fiocco, R.J., Lewis, A. (1999). Oil spill dispersants. *Pure and Applied Chemistry 71,* 27-42.

Flynn, K.J., Mitra, A., Glibert, P.M., Burkholder, J.M. (2018). Mixotrophy in harmful algal blooms: by whom, on whom, when, why, and what next. In P.M. Glibert, E. Berdalet, M.A. Burford, G.C. Pitcher, M. Zhou (Eds.) *Global Ecology and Oceanography of Harmful Algal Blooms*. (pp. 113-132). Cham, Switzerland: Springer.

Flynn, K., Stoecker, D.K., Mitra, A., Raven, J.A., Glibert, P.M., Hansen, P.J., et al. (2013). Misuse of the phytoplankton-zooplankton dichotomy: the need to assign organisms as mixotrophs within plankton functional types. *Journal of Plankton Research 35,* 3-11.

Forth, H.P., Mitchelmore, C.L., Morris, J.M., Lay, C.R., Lipton, J. (2017a). Characterization of dissolved and particulate phases of water accommodated fractions used to conduct aquatic toxicity testing in support of the Deepwater Horizon natural resource damage assessment. *Environmental Toxicology and Chemistry 36,* 1460-1472.

Forth, H.P., Mitchelmore C.L., Morris, J.M., Lipton, J. (2017b). Characterization of oil and water accommodated fractions used to conduct aquatic toxicity testing in

support of the Deepwater Horizon oil spill natural resource damage assessment. *Environmental Toxicity and Chemistry 36*, 1450-1459.

Franze, G., Lavrentyev, P.J. (2014). Microzooplankton growth rates examined across a temperature gradient in the Barents Sea. *PLoS One 9*, e86429.

Frost, B.W. (1972). Effects of size and concentration of food particles on the feeding behavior of the marine planktonic copepod *Calanus pacificus*. *Limnology & Oceanography 17*, 805-815.

Fussmann, K.E., Rosenbaum, B., Brose, U., Rall, B.C. (2017). Interactive effects of shifting body size and feeding adaptation drive interaction strengths of protist predators under warming. *bioRxiv* Preprint. (doi: https://doi.org/10.1101/101675).

Gaines, G., Elbrachter, M. (1987). Heterotrophic nutrition. In F.J.R. Taylor (Ed.) *The Biology of Dinoflagellates*. (pp. 224-268). Oxford: Blackwell.

Gallegos, C.L., Vant, W.N. Safi, K.A. (1996). Microzooplankton grazing of phytoplankton in Manukau Harbor, New Zealand. *New Zealand Journal of Marine and Freshwater Research 30*, 423-434.

Garcia-Soto, C. (2004). '*Prestige*' oil spill and Navidad flow. *Journal of the Marine Biological Association of the United Kingdom 84*, 297-300.

Geel, C., Versluis, W., Snel, J.F.H. (1997). Estimation of oxygen evolution by marine phytoplankton from measurement of the efficiency of Photosystem II electron flow. *Photosynthesis Research 51*, 61-70.

George-Ares, A., Clark, J.R. (2000). Aquatic toxicity of two Corexit dispersants. *Chemosphere 40*, 897-906.

Gertler, C., Nather, D.J., Gerdts, G., Malpass, M.C., Golyshin, P.N. (2010). A mesocosm study of the changes in marine flagellate and ciliate communities in a crude oil bioremediation trail. *Microbial Ecology 60*, 180–191.

Gilde, K., Pinckney, J.L. (2012). Sublethal effects of crude oil on the community structure of estuarine phytoplankton. *Estuaries and Coasts 35*, 853-861.

Glibert, P.M., Burkholder, J.M., Kana, T.M., Alexander, J., Skelton, H., Shilling, C. (2009). Grazing by *Karenia brevis* on *Synechococcus* enhances its growth rate and may help to sustain blooms. *Aquatic Microbial Ecology 55*, 17-30.

Gomez, F. (2013). Reinstatement of the dinoflagellate genus *Tripos* to replace *Neoceratium*, marine species of *Ceratium* (Dinophyceae, Alveolata). *CICIMAR Oceanides 28*, 1-22.

Gomiero, A., Sforzini, S., Dagnino, A., Nasci, C., Viarengo, A. (2012). The use of multiple endpoints to assess cellular responses to environmental contaminants in the interstitial marine ciliate *Euplotes crassus*. *Aquatic Toxicology 114-115*, 206-216.

Gonzalez, J., Figueiras, F.G., Aranguren-Gassis, M., Crespo, B.G., Fernandez, E., Moran, X.A.G., et al. (2009). Effect of a simulated oil spill on natural assemblages of marine phytoplankton enclosed in microcosms. *Estuarine, Coastal and Shelf Science 83*, 265-276.

Gonzalez, J.J., Vinas, L., Franco, M.A., Fumega, J., Soriano, J.A., Grueiro, G., et al. (2006). Spatial and temporal distribution of dissolved/dispersed aromatic hydrocarbons in seawater in the area affected by the *Prestige* oil spill. *Marine Pollution Bulletin 53*, 250-259.

Graham, S.L., Strom, S.L. (2010). Growth and grazing of microzooplankton in response to the harmful algal *Heterosigma akashiwo* in prey mixtures. *Aquatic Microbial Ecology 59*, 111-124.

Guillard, R.R.L. (1975). Culture of phytoplankton for feeding marine invertebrates. In W.L. Smith, M.H. Chanley (Eds.) *Culture of Marine Invertebrate Animals*. (pp. 29-60). New York: Plenum Press.

Guo, Z., Zhang, H., Liu, S., Lin, S. (2013). Biology of the marine heterotrophic dinoflagellate *Oxyrrhis marina*: current status and future directions. *Microorganisms 1*, 33-57.

Hahn, M.W., Hofle, M.G. (2001). Grazing of protozoa and its effect on populations of aquatic bacteria. *FEMS Microbiology Ecology 35*, 113-121.

Han, J., Park, J.C., Kang, H.M., Byeon, E., Yoon, D.S., Lee, M.C., et al. (2019). Adverse effects, expression of defense-related genes, and oxidative stress-induced MAPK pathway in the benzo[α]pyrene-exposed rotifer *Brachionus rotundiformis*. *Aquatic Toxicology 210*, 188-195.

Hansen, B.H., Altin, D., Olsen, A.J., Nordtug, T. (2012). Acute toxicity of naturally and chemically dispersed oil on the filter-feeding copepod *Calanus finmarchicus*. *Ecotoxicology and Environmental Safety 86*, 38-46.

Hansen, B., Fotel, F.L., Jensen, N.J., Wittrup, L. (1997). Physiological effects of the detergent linear alkylbenzene sulphonate on blue mussel larvae (*Mytilus edulis*) in laboratory and mesocosm experiments. *Marine Biology 128*, 627-637.

Hansen, P.J. (1989). The red tide dinoflagellate *Alexandrium tamarense*: effects on behavior and growth of a tintinnid ciliate. *Marine Ecology Progress Series 53*, 105-116.

Hansen, P.J. (2011). The role of photosynthesis and food uptake for the growth of marine mixotrophic dinoflagellates. *The Journal of Eukaryotic Microbiology 58*, 203-214.

Hansen, P.J., Bjornsen, P.K., Hansen, B.W. (1997). Zooplankton grazing and growth: scaling within the 2-2000-µm body size range. *Limnology and Oceanography 42*, 687-704.

Hansen, P.J., Calado, A.J. (1999). Phagotrophic mechanisms and prey selection in free-living dinoflagellates. *Journal of Eukaryotic Microbiology 46*, 382-389.

Hansen, P.J., Nielsen, T.G. (1997). Mixotrophic feeding of *Fragilidium subglobosum* (Dinophyceae) on three species of *Ceratium*: effects of prey concentration, prey species and light intensity. *Marine Ecology Progress Series 147*, 187-196.

Hansen, P.J., Skovgaard, A., Glud, R.N., Stoecker, D.K. (2000). Physiology of the mixotrophic dinoflagellate *Fragilidium subglobosum*. II. Effects of time scale and prey concentration on photosynthetic performance. *Marine Ecology Progress Series 201*, 137-146.

Hassanshahian, M., Cappello, S. (2013). Crude oil biodegradation in the marine environments. In R. Chamy, F. Rosenkranz (Eds.) *Biodegradation - Engineering and Technology*. (doi: 10.6772/55554).

Head, I.M., Jones, D.M., Rolling, W.F.M. (2006). Marine microorganisms make a meal of oil. *Nature Reviews 4*, 173-182.

Heinbokel, J.F. (1978). Studies on the functional role of tintinnids in the Southern California Bight. I. Grazing and growth rates in laboratory cultures. *Marine Biology 47*, 177-189.

Heinze, A.W., Truesdale, C.L., DeVaul, S.B., Swinden, J., Sanders, R.W. (2013). Role of temperature in growth, feeding, and vertical distribution of the mixotrophic chrysophyte *Dinobryon*. *Aquatic Microbial Ecology 71*, 155-163.

Hemmer, M.J., Barron, M.G., Greene, R.M. (2011). Comparative toxicity of eight oil dispersants, Louisiana sweet crude oil (LSC), and chemically dispersed LSC to two aquatic test species. *Environmental Toxicology and Chemistry 30*, 2244-2252.

Hermens, J.L.M. (1989). Quantitative structure-activity relationships of environmental pollutants. In J. Hermens, A. Opperhuizen, D.T.H.M. Sijim, R.P. Wayne, B.L. Worobey (Eds.) *Reactions and Processes*. (pp. 111-162). Berlin: Springer-Verlag.

Hinder, S.L., Hays, G.C., Edwards, M., Roberts, E.C., Walne, A.W., Gravenor, M.B. (2012). Changes in marine dinoflagellate and diatom abundance under climate change. *Nature Climate Change 2*, 271-275.

Hjorth, M., Forbes, V.E., Dahllof, I. (2008). Plankton stress responses from PAH exposure and nutrient enrichment. *Marine Ecology Progress Series 363*, 121-130.

Hook, S.E., Osborn, H.L. (2012). Comparison of toxicity and transcriptomic profiles in a diatom exposed to oil, dispersants, dispersed oil. *Aquatic Toxicology 124-125*, 139-151.

Hu, C., Weisberg, R.H., Liu, Y., Zheng, L., Daly, K.L., English, D.C., et al. (2011). Did the northeastern Gulf of Mexico become greener after the Deepwater Horizon oil spill? *Geophysical Research Letters 38*, L09601.

Huang, Y.J., Jiang, Z.B., Zeng, J.N., Chen, Q.Z., Zhao, Y., Liao, Y., et al. (2011). The chronic effects of oil pollution on marine phytoplankton in a subtropical bay, China. *Environmental Monitoring and Assessment 176*, 517-530.

Irigoien, X., Flynn, K.J., Harris, R.P. (2005). Phytoplankton blooms: a 'loophole' in microzooplankton grazing impact? *Journal of Plankton Research 27*, 313-321.

Jacobson, D.M., Anderson, D.M. (1996). Widespread phagocytosis of ciliates and other protists by marine mixotrophic and heterotrophic thecate dinoflagellates. *Journal of Phycology 32*, 279-285.

Jeong, H.J., Latz, M.I. (1994). Growth and grazing rates of the heterotrophic dinoflagellates *Protoperidinium* spp. on red tide dinoflagellates. *Marine Ecology Progress Series 106*, 173-185.

Jeong, H.J., Lee, C.W., Yih, W.H., Kim, J.S. (1997). *Fragilidium* cf. *mexicanum*, a thecate mixotrophic dinoflagellate which is prey for and a predator on co-occurring thecate heterotrophic dinoflagellate *Protoperidinium* cf. *divergens*. *Marine Ecology Progress Series 151*, 299-305.

Jeong, H.J., Lee, K.H., Yoo, Y.D., Kang, N.A., Song, J.Y., Kim, T.H., et al. (2018). Effects of light intensity, temperature, and salinity on the growth and ingestion rates of the red-tide mixotrophic dinoflagellate *Paragymnodinium shiwhaense*. *Harmful Algae 80*, 46-54.

Jeong, H.J., Yoo, Y.D., Park, J.Y., Song, J.Y., Kim, S.T., Lee, S.H., et al. (2005). Feeding by phototrophic red-tide dinoflagellates: five species newly revealed and six species previously known to be mixotrophic. *Aquatic Microbial Ecology 40*, 133-150.

Jiang, Z., Huang, Y., Chen, Q., Zeng, J., Xu, X. (2012). Acute toxicity of crude oil water accommodated fraction on marine copepod: the relative importance of acclimatization temperature and body size. *Marine Environmental Research 81*, 12-17.

Johansson, S., Larsson, U., Boehm, P. (1980). The *Tsesis* oil spill impact on the pelagic ecosystem. *Marine Pollution Bulletin 11*, 284-293.

Johnson, M.D. (2015). Inducible mixotrophy in the dinoflagellate *Prorocentrum minimum*. *The Journal of Eukaryotic Microbiology 62*, 431-443.

Jung, S.W., Kwon, O.Y., Joo, C.K., Kang, J.H., Kim, M., Shim, W.J., et al. (2012). Stronger impact of dispersant plus crude oil on natural plankton assemblages in short-term marine mesocosms. *Journal Hazardous Materials 217-218*, 338-349.

Jurgen, K., Massana, R. (2008). Protist grazing on marine bacterioplankton. In D.L. Kirchman (Ed.) *Microbial Ecology of the Oceans* 2nd Edition. (pp. 383-441). Wilmington, DE: John Wiley & Sons.

Jurgen, K., Matz, C. (2002). Predation as a shaping force for the phenotypic and genotypic composition of planktonic bacteria. *Antonie van Leeuwenhoek 81*, 413-434.

Kamiyama, T., Tsuijino, M., Matsuyama, Y., Uchida, T. (2005). Growth and grazing rates of the tintinnid ciliate *Favella taraikaensis* on the toxic dinoflagellate *Alexandrium tamarense*. *Marine Biology 147*, 989-997.

Karydis, M., Fogg, G.E. (1980). Physiological effects of hydrocarbons on the marine diatom *Cyclotella cryptica*. *Microbial Ecology 6*, 281-290.

Katoh, K., Misawa, K., Kuma, K., Miyata, T. (2002). MAFFT: a novel method for rapid multiple sequence alignment based on fast Fourier transform. *Nucleic Acids Research 30*, 3059-3066.

Kerr, R.A. (2010). A lot of oil on the loose, not so much to be found. *Science 329*, 734-735.

Kim, S.H., Kim, S.J., Lee, J.S., Lee, Y.M. (2014). Acute effects of heavy metals on the expression of glutathione-related antioxidant genes in the marine ciliate *Euplotes crassus*. *Marine Pollution Bulletin 85*, 455-462.

Kim, H., Yim, B., Kim, J., Kim, H., Lee, Y.M. (2017). Molecular characterization of ABC transporters in marine ciliates, *Euplotes crassus*: Identification and responses to cadmium and benzo[a]pyrene. *Marine Pollution Bulletin 124*, 725-735.

Klappenbach, J.A., Dunbar, J.M., Schmidt, T.M. (2000). rRNA operon copy number reflects ecological strategies of bacteria. *Applied and Environmental Microbiology 66*, 1328-1333.

Koshikawa, H., Xu, K.Q., Liu, Z.L., Kohata, K., Kawachi, M., Maki, H., et al. (2007). Effect of the water-soluble fraction of diesel oil on bacterial and primary production and the trophic transfer to mesozooplankton through a microbial food web in Yangtze, China. *Estuarine, Coastal and Shelf Science 71*, 68-80.

Kota, S., Borden, R.C., Barlaz, M.A. (1999). Influence of protozoan grazing on contaminant biodegradation. *FEMS Microbiology Ecology 29*, 179-189.

Kvenvolden, K.A., Cooper, C.K. (2003). Natural seepage of crude oil into the marine environment. *Geo-Marine Letters 23*, 140-146.

Landry, M.R., Haas, L.W., Fagerness, V.L. (1984). Dynamics of microbial plankton communities: experiments in Kaneohe Bay, Hawaii. *Marine Ecology Progress Series 16*, 127-133.

Landry, M.R., Hassett, R.P. (1982). Estimating the grazing impact of marine micro-zooplankton. *Marine Biology 67*, 283-288.

Lavrentyev, P.J., McCarthy, M.J., Klarer, D.M., Jochem, F., Gardner, W.S. (2004). Estuarine microbial food web patterns in a Lake Erie coastal wetland. *Microbial Ecology 48*, 567-577.

Lee, K.W., Choi, Y.U. (2016). Population growth of a tropical tintinnid, *Metacylis tropica* on different temperature, salinity and diet. *Journal of the Korea Academia-Industrial Cooperation Society 17*, 322-328.

Legendre, P. (2018). lmode2: Model II Regression. R package version 1.7-3.

Legrand, C., Graneli, E., Carlsson, P. (1998). Induced phagotrophy in the photosynthetic dinoflagellate *Heterocapsa triquetra*. *Aquatic Microbial Ecology 15*, 65-75.

Leles, S.G., Mitra, A., Flynn, K.J., Stoecker, D.K., Hansen, P.J., Calbet, A., et al. (2017). Oceanic protists with different forms of acquired phototrophy display contrasting biogeographies and abundance. *Proceedings of the Royal Society B 284*, 20170664.

Leles, S.G., Mitra, A., Flynn, K.J., Tillman, U., Stoecker, D., Jeong, H.J., et al. (2018). Sampling bias misrepresents the biogeographical significance of constitutive mixotrophs across global oceans. *Global Ecology and Biogeography 28*, 418-428.

Lenth, R. (2019). emmeans: Estimated marginal means, aka least-squares means. R package version 1.4.6.

Lesser, M.P. (2006). Oxidative stress in marine environments: biochemistry and physiological ecology. *Annual Review of Physiology 68*, 253-278.

Li, C., Xu, K., Lei, Y. (2011). Growth and grazing responses to temperature and prey concentration of *Condylostoma spatiosum*, a large benthic ciliate, feeding on *Oxyrrhis marina*. *Aquatic Microbial Ecology 64*, 97-104.

Lindmark, D.G. (1981). Activation of polynuclear aromatic hydrocarbons to mutagens by the marine ciliate *Parauronema acutum*. *Applied and Environmental Microbiology 41*, 1238-1242.

Liu, T., Chen, Z., Shen, Y., Gan, L., Cao, L., Zi-zhong, L.V. (2007). Monitoring bioaccumulation and toxic effects of hexachlorobenzene using the polyurethane foam unit method in the microbial communities of the Fuhe River, Wuhan. *Journal of Environmental Sciences 19*, 738-744.

Liu, K., Chen, B., Zhang, S., Sato, M., Shi, Z., Liu, H. (2019). Marine phytoplankton in subtropical coastal waters showing lower thermal sensitivity than microzooplankton. *Limnology and Oceanography 64*, 1103-1119.

Liu, Z, Liu, J., Zhu, Q., Wu, W. (2012). The weathering of oil after the Deepwater Horizon oil spill: insights from the chemical composition of the oil from the sea surface, salt marshes and sediments. *Environmental Research Letters 7*, 035302.

Liu, X., Tang, C.H., Wong, C.K. (2014). Microzooplankton grazing and selective feeding during bloom periods in the Tolo Harbour area as revealed by HPLC pigment analysis. *Journal of Sea Research 90*, 83-94.

Lomas, M.W., Glibert, P.M. (1999). Interactions between NH_4^+ and NO_3^- uptake and assimilation: comparison of diatoms and dinoflagellates at several growth temperatures. *Marine Biology 133*, 541-551.

Louca, S., Doebeli, M., Parfrey, L.W. (2018). Correcting for 16S rRNA gene copy numbers in microbiome surveys remains an unresolved problem. *Microbiome 6*, 41.

Lozupone, C., Knight, R. (2005). UniFrac: a new phylogenetic method for comparing microbial communities. *Applied and Environmental Microbiology 71*, 8228-8235.

Mansano, A.S., Hisatugo, K.F., Hayashi, L.H., Regali-Seleghim, M.H. (2014). The importance of protozoan bacterivory in a subtropical environment (Lobo-Broa Reservoir, SP, Brazil). *Brazilian Journal of Biology 74*, 569-578.

Margesin, R., Labbe, D., Schinner, F., Greer, C.W., Whyte, L.G. (2003). Characterization of hydrocarbon-degrading microbial populations in contaminated and pristine alpine soils. *Applied and Environmental Microbiology 69*, 3085-3092.

Marinov, I., Doney, S.C., Lima, I.D. (2010). Response of ocean phytoplankton community structure to climate change over the 21st century: partitioning the effects of nutrients, temperature and light. *Biogeosciences 7*, 3941-3959.

Matsubara, T., Nagasoe, S., Yamasaki, Y., Shikata, T., Shimasaki, Y., Oshima, Y., et al. (2007). Effects of temperature, salinity, and irradiance on the growth of the dinoflagellates *Akashiwo sanguinea*. *Journal of Experimental Marine Biology and Ecology 342*, 226-230.

McDonald, D., Vazquez-Baeza, Y., Koslicki D., McClelland, J., Reeve, N., Xu, Z., et al. (2018). Striped UniFrac: enabling microbiome analysis at unprecedented scale. *Nature Methods 15*, 846-848.

McGenity, T.J., Folwell, B.D., McKew, B.A., Sanni, G.O. (2012). Marine crude-oil biodegradation: a central role for interspecies interactions. *Aquatic Biosystems 8*, 10.

Menden-Deuer, S., Lessard, E.J. (2000). Carbon to volume relationship for dinoflagellates, diatoms and other protist plankton. *Limnology & Oceanography 45*, 569-579.

Menden-Deuer, S., Lessard, E.J., Satterberg, J. (2001). Effects of preservation on dinoflagellate and diatom cell volume and consequences for carbon biomass predictions. *Marine Ecology Progress Series 222*, 41-50.

Menden-Deuer, S., Lessard, E.J., Satterberg, J., Grunbaum, D. (2005). Growth rates and starvation survival of three species of the pallium-feeding, thecate dinoflagellate genus *Protoperidinium*. *Aquatic Microbial Ecology 41*, 145-152.

Mishamandani, S., Gutierrez, T., Berry, D., Aitken, M.D. (2016). Responses of the bacterial community associated with a cosmopolitan marine diatom to crude oil shows a preference for the biodegradation of aromatic hydrocarbons. *Environmental Microbiology 18*, 1817-1833.

Mitra, A., Flynn, K.J., Tillmann, U., Raben, J.A., Caron, D., Stoecker, D.K., et al. (2016). Defining planktonic protists functional groups on mechanisms for energy and nutrient acquisition: incorporation of diverse mixotrophic strategies. *Protist 167*, 106-120.

Mock, T., Hoch, N. (2005). Long-term temperature acclimation of photosynthesis in steady-state cultures of the polar diatom *Fragilariopsis cylindrus*. *Photosynthesis Research 85*, 307-317.

Monger, B.C., Landry, M.R., Brown, S.L. (1999). Feeding selection of heterotrophic marine nanoflagellates based on the surface hydrophobicity of their picoplankton prey. *Limnology & Oceanography 44*, 1917-1927.

Montagnes, D.J.S., Barbosa, A.B., Boenigk, J., Davidson, K., Jurgens, K., Macek, M., et al. (2008). Selective feeding behavior of key free-living protists: avenues for continued study. *Aquatic Microbial Ecology 53*, 83-98.

Montagnes, D.J.S., Franklin, D.J. (2001). Effect of temperature on diatom volume, growth rate, and carbon and nitrogen content: reconsidering some paradigms. *Limnology and Oceanography 46*, 2008-2018.

Montagnes, D.J.S., Lessard, E.J. (1999). Population dynamics of the marine planktonic ciliate *Strombidinopsis multiauris*: its potential to control phytoplankton blooms. *Aquatic Microbial Ecology 20*, 167-181.

Montagnes, D.J.S., Lowe, C.D., Roberts, E.C., Breckels, M.N., Boakes, D.E., Davison, K., et al. (2011). An introduction to the special issue: *Oxyrrhis marina*, a model organism? *Journal of Plankton Research 33*, 549-554.

Moore, M.N., Allen, J.I., McVeigh, A. (2006). Environmental prognostics: an integrated model supporting lysosomal stress responses as predictive biomarkers of animal health status. *Marine Environmental Research 61*, 278-304.

Muren, U., Berglund, J., Samuelsson, K., Andersson, A. (2005). Potential effects of elevated sea-water temperature on pelagic food webs. *Hydrobiologia 545*, 153-166.

National Research Council. (2003). *Oil in the Sea III: Inputs, Fates, and Effects*. Washington, DC: The National Academies Press. Pp. 265.

National Research Council. (2005). *Oil Spill Dispersants: Efficacy and Effects*. Washington DC: The National Academies Press. Pp. 377.

Nejstgaard, J.C., Gismervik, I., Solberg, P.T. (1997). Feeding and reproduction by *Calanus finmarchicus*, and microzooplankton grazing during mesocosm blooms of diatoms and the coccolithophore *Emiliania huxleyi*. *Marine Ecology Progress Series 147*, 197-217.

Nielsen, T.G. (1991). Contribution of zooplankton grazing to the decline of a *Ceratium* bloom. *Limnology & Oceanography 36*, 1091-1106.

Nogueira, D.J., Mattos, J.J., Dybas, P.R., Flores-Nunes, F., Sasaki, S.T., Taniguchi, S., et al. (2017). Effects of phenanthrene on early development of the Pacific oyster *Crassostrea gigas* (Thunberg, 1789). *Aquatic Toxicology 191*, 50-61.

O'Connor, M.I., Piehler, M.F., Leech, D.M., Anton, A., Bruno, J.F. (2009). Warming and resource availability shift food web structure and metabolism. *PLoS Biology 7*, e1000178.

Ohman, M.D., Snyder, R.A. (1991). Growth kinetics of the omnivorous oligotrich ciliate *Strombidium* sp. *Limnology & Oceanography 36*, 922-935.

Okamura, T., Mori, Y., Nakano, S., Kondo, R. (2012). Abundance and bacterivory of heterotrophic nanoflagellates in the meromictic Lake Suigetsu, Japan. *Aquatic Microbial Ecology 66*, 149-158.

Ortmann, A.C., Anders, J., Shelton, N., Gong, L., Moss, A.G., Condon, R.H. (2012). Dispersed oil disrupts microbial pathways in pelagic food webs. *PLoS One 7*, e42548.

Othman, H.B., Lanouguere, E., Got, P., Hlaili, A.S., Leboulanger, C. (2018). Structural and functional responses of coastal marine phytoplankton communities to PAH mixtures. *Chemosphere 209*, 908-919.

Othman, H.B., Leboulanger, C., Floc'h, E.L., Mabrouk, H.H., Hlaili, A.S. (2012). Toxicity of benz(a)anthracene and fluoranthene to marine phytoplankton in culture: Does cell size really matter? *Journal of Hazardous Materials 243*, 204-211.

Ozhan, K., Bargu, S. (2014a). Distinct responses of Gulf of Mexico phytoplankton communities to crude oil and the dispersant Corexit EC9500A under different nutrient regimes. *Ecotoxicology 23*, 370-384.

Ozhan, K., Bargu, S. (2014b). Responses of sympatric *Karenia brevis*, *Prorocentrum minimum*, and *Heterosigma akashiwo* to the exposure of crude oil. *Ecotoxicology 23*, 1387-1398.

Ozhan, K., Bargu, S. (2014c). Can crude oil toxicity on phytoplankton be predicted based on toxicity data on benzo(a)pyrene and naphthalene? *Bulletin of Environmental Contamination and Toxicology 92*, 225-230.

Ozhan, K., Miles, S.M., Gao, H., Bargu, S. (2014). Relative phytoplankton growth responses to physically and chemically dispersed South Louisiana sweet crude oil. *Environmental Monitoring and Assessment 186*, 3941-3956.

Ozhan, K., Zahraeifard, S., Smith, A.P., Bargu, S. (2015). Induction of reactive oxygen species in marine phytoplankton under crude oil exposure. *Environmental Science and Pollution Research 22*, 18874-18884.

Pedersen, T.L. (2020). ggforce: Accelerating "ggplot2". R package version 0.3.2.

Pelletier, E., Sargian, P., Payet, J., Demers, S. (2006). Ecotoxicological effects of combined UVB and organic contaminants in coastal waters: a review. *Photochemistry and Photobiology 82*, 981-993.

Perez, P., Fernandez, E., Beiras, R. (2010). Fuel toxicity on *Isochrysis galbana* and a coastal phytoplankton assemblage: growth rate vs. variable fluorescence. *Ecotoxicology and Environmental Safety 73*, 254-261.

Pernthaler, J. (2005). Predation on prokaryotes in the water column and its ecological implications. *Nature Reviews Microbiology 3*, 537-546.

Pham, V.D., Hnatow, L.L., Zhang, S., Fallon, R.D., Jackson, S.C., Tomb, J.F., et al. (2009). Characterizing microbial diversity in production water from an Alaskan mesothermic petroleum reservoir with two independent molecular methods. *Environmental Microbiology 11*, 176-187.

Pielou, E.C. (1966). The measurement of diversity in different types of biological collections. *Journal of Theoretical Biology 13*, 131-144.

Pillai, M.C., Vines, C.A., Wikramanayake, A.H., Cherr, G.N. (2003). Polycyclic aromatic hydrocarbons disrupt axial development in sea urchin embryos through a β-catenin dependent pathway. *Toxicology 186*, 93-108.

Pitcher, G.C., Probyn, T.A. (2011). Anoxia in southern Benguela during the autumn of 2009 and its linkage to a bloom of the dinoflagellate *Ceratium balechii*. *Harmful Algae 11*, 23-32.

Pomeroy, L.R. (1974). The ocean's food web. A changing paradigm. *BioScience 24*, 499-504.

Price M.N., Dehal, P.S., Arkin, A.P. (2010). FastTree2 – Approximately maximum-likelihood trees for large alignments. *PLoS One 5*, e9490.

Prince, R.C. (2010). Bioremediation of marine oil spills. In K.N. Timmis, T. McGenity, J.R. van der Meer, V. de Lorenzo (Eds.) *Handbook of Hydrocarbon and Lipid Microbiology*. (pp. 1671-1692). Berlin: Springer-Verlag.

Prince, R.C., Amande, T.J., McGenity, T.J. (2018). Prokaryotic hydrocarbon degraders. In T.J. McGenity (Ed.) *Taxonomy, Genomics and Ecophysiology of Hydrocarbon-Degrading Microbes, Handbook of Hydrocarbon and Lipid Microbiology*. (pp. 1-41). Cham: Springer.

Prince, R.C., Butler, J.D., Redman, A.D. (2017). The rate of crude oil biodegradation in the sea. *Environmental Science & Technology 51*, 1278-1284.

Princiotta, S.D., Smith, B.T., Sanders, R.W. (2016). Temperature-dependent phagotrophy and phototrophy in a mixotrophic chrysophyte. *Journal of Phycology 52*, 432-440.

Putt, M., Stoecker, D.K. (1989). An experimental determined carbon:volume ratio for marine “oligotrichous” ciliates from estuarine and coastal waters. *Limnology & Oceanography 34*, 1097-1103.

Quigg, A., Nunnally, C.C., McInnes, A.S., Gay, S., Rowe, G.T., Dellapenna, T.M., et al. (2013). Hydrographic and biological controls in two subarctic fjords: an environmental case study of how climate change could impact phytoplankton communities. *Marine Ecology Progress Series 480*, 21-37.

R Core Team (2019). R: A language and environment for statistical computing. R Foundation for Statistical Computing, Vienna, Austria.

Raven, J.A., Geider, R.J. (1988). Temperature and algal growth. *New Phytology 110*, 441-461.

Redfield, A.C. (1934). On the proportions of organic derivatives in sea water and their relation to the composition of plankton. In *James Johnstone Memorial Volume: 176*. (pp. 176-192).

Riaux-Gobin, C. (1985). Long-term changes in microphytobenthos in a Brittany estuary after the ‘*Amoco Cadiz’* oil spill. *Marine Ecology Progress Series 24*, 51-56.

Rico-Martinez, R., Snell, T.W., Shearer, T.L. (2013). Synergistic toxicity of Macondo crude oil and dispersant Corexit 9500A to the *Brachionus plicatilis* species complex (Rotifera). *Environmental Pollution 173*, 5-10.

Ritz, C., Baty, F., Streibig, J.C., Gerhard, D. (2015). Dose-response Analysis using R. *PLoS One 10*, e0146021.

Rodriguez, F., Riobo, P., Rial, P., Reguera, B., Franco, J.M. (2014). Feeding of *Fragilidium* cf. *duplocampanaeforme* and *F. subglobosum* on four *Dinophysis* species: prey selectivity, local adaptation and fate of toxins. *Aquatic Microbial Ecology 72*, 241-253.

Rogerson, A., Berger, J. (1981). The toxicity of the dispersant Corexit 9527 and oil-dispersant mixtures to ciliate protozoa. *Chemosphere 10*, 33-39.

Rose, J.M., Feng, Y., DiTullio, G.R., Dunbar, R.B., Hare, C.E., Lee, P.A., et al. (2009). Synergistic effects of iron and temperature on Antarctic phytoplankton and microzooplankton assemblages. *Biogeosciences 6*, 3131-3147.

Saco-Alvarez, L., Bellas, J., Nieto, O., Bayona, J.M., Albaiges, J., Beiras, R. (2008). Toxicity and phototoxicity of water-accommodated fraction obtained from

Prestige fuel oil and Marine fuel oil evaluated by marine bioassays. *Science of Total Environment 394*, 275-282.

Safi, K.A., Griffiths, F.B., Hall, J.A. (2007). Microzooplankton composition, biomass and grazing rates along the WOCE SR3 line between Tasmania and Antarctica. *Deep-Sea Research I 54*, 1025-1041.

Safi, K.A., Hall, J.A. (1999). Mixotrophic and heterotrophic nanoflagellate grazing in the convergence zone east of New Zealand. *Aquatic Microbial Ecology 20*, 83-93.

Saiz, E., Calbet, A. (2011). Copepod feeding in the ocean: scaling patterns, composition of their diet and the bias of estimates due to microzooplankton grazing during incubations. *Hydrobiologia 666*, 181-196.

Saiz, E., Movilla, J., Yebra, L., Barata, C., Calbet, A. (2009). Lethal and sublethal effects of naphthalene and 1,2-dimethlynaphthalene on naupliar and adult stages of the marine cyclopoid copepod *Oithona davisae*. *Environmental Pollution 157*, 1219-1226.

Sanders R.W., Caron, D.A., Berninger, U.G. (1992). Relationship between bacteria and heterotrophic nanoplankton in marine and fresh waters: an inter-ecosystem comparison. *Marine Ecology Progress Series 86*, 1-14.

Sanders, R.W., Gast, R.J. (2012). Bacterivory by phototrophic picoplankton and nanoplankton in Artic waters. *FEMS Microbiology Ecology 82*, 242-253.

Sargian, P., Mostajir, B., Chatila, K., Ferreyra, G.A., Pelletier, E., Demers, S. (2005). Non-synergistic effects of water-soluble crude oil and enhanced ultraviolet-B radiation on a natural plankton assemblage. *Marine Ecology Progress Series 294*, 63-77.

Selosse, M.A., Charpin, M., Not, F. (2017). Mixotrophy everywhere on land and in waters: the *grand ecart* hypothesis. *Ecology Letters 20*, 246-263.

Severin, T., Erdner, D.L. (2019). The phytoplankton taxon-dependent oil response and its microbiome: correlation but not causation. *Frontiers in Microbiology 10*, 385.

Shannon, C.E., Weaver, W. (1964). *The Mathematical Theory of Communication*. Urbana, IL: The University of Illinois Press. Pp. 125.

Sheng, Y., Tang, D., Pang, G. (2011). Phytoplankton blooms over the Northwest Shelf of Australia after the *Montara* oil spill in 2009. *Geomatics, Natural Hazards and Risk 2*, 329-347.

Sherr, E.B., Sherr, B.F. (1987). High rates of consumption of bacteria by pelagic ciliates. *Nature 325*, 710-711.

Sherr, E.B., Sherr, B.F. (1988). Role of microbes in pelagic food webs: A revised concept. *Limnology and Oceanography 33*, 1225-1227.

Sherr, E.B., Sherr, B.F. (1994). Bacterivory and herbivory: Key roles of phagotrophic protists in pelagic food webs. *Microbial Ecology 28*, 223-235.

Sherr, E.B., Sherr, B.F. (2002). Significance of predation by protists in aquatic microbial food webs. *Antonie van Leeuwenhoek 81*, 293-308.

Sherr, E.B., Sherr, B.F. (2009). Capacity of herbivorous protists to control initiation and development of mass phytoplankton blooms. *Aquatic Microbial Ecology 57*, 253-262.

Sherr, B.F., Sherr, E.B., Rassoulzadegan, F. (1988). Rates of digestion of bacteria by marine phagotrophic protozoa: temperature dependence. *Applied and Environmental Microbiology 54*, 1091-1095.

Sieburth, J.M., Smetacek, V., Lenz, J. (1978). Pelagic ecosystem structure: Heterotrophic compartments of the plankton and their relationship to plankton size fractions. *Limnology and Oceanography 23*, 1256-1263.

Singer, M.M., Aurand, D., Bragin, G.E., Clark, J.R., Coelho, G.M., Sowby, M.L., et al. (2000). Standardization of the preparation and quantitation of water-accommodated fractions of petroleum for toxicity testing. *Marine Pollution Bulletin 40*, 1007-1016.

Singer, M.M., Aurand, D.V., Coelho, G.M., Bragin, G.E., Clark, J.R., Sowby, M., et al. (2001). Making measuring and using water-accommodated fractions of petroleum for toxicity testing. *International Oil Spill Conference Proceedings 2001*, 1269-1274.

Skovgaard, A. (1996a). Engulfment of *Ceratium* spp. (Dinophyceae) by the thecate photosynthetic dinoflagellate *Fragilidium subglobosum*. *Phycologia 35*, 490-499.

Skovgaard A. (1996b). Mixotrophy in *Fragilidium subglobosum* (Dinophyceae): growth and grazing responses as functions of light intensity. *Marine Ecology Progress Series 143*, 247-253.

Skovgaard, A., Hansen, P.J., Stoecker, D.K. (2000). Physiology of the mixotrophic dinoflagellate *Fragilidium subglobosum*. I. Effects of phagotrophy and irradiance on photosynthesis and carbon content. *Marine Ecology Progress Series 201*, 129-136.

Smalley, G.W., Coats, D.W., Stoecker, D.K. (2003). Feeding in the mixotrophic dinoflagellate *Ceratium furca* is influenced by intracellular nutrient concentrations. *Marine Ecology Progress Series 262*, 137-151.

Smalley, G.W., Coats, D.W., Stoecker, D.K. (2012). Influence of inorganic nutrients, irradiance, and time of day on food uptake by the mixotrophic dinoflagellate *Neoceratium furca*. *Aquatic Microbial Ecology 68*, 29-41.

Smith, M., Hansen, P.J. (2007). Interaction between *Mesodinium rubrum* and its prey: importance of prey concentration, irradiance and pH. *Marine Ecology Progress Series 338*, 61-70.

Sokal, R.R., Rohlf, F.J. (2012). (Eds.). *Biometry: the Principles and Practice of Statistics in Biological Research*. New York: WH Freeman. Pp. 937.

Sommer, U., Hansen, T., Blum, O., Holzner, N., Vadstein, O., Stibor, H. (2005). Copepod and microzooplankton grazing in mesocosms fertilized with different Si:N ratios: no overlap between food spectra and Si:N influence on zooplankton trophic level. *Oecologia 142*, 274-283.

Stibor, H., Sommer, U. (2003). Mixotrophy of a photosynthetic flagellate viewed from an optimal foraging perspective. *Protist 154*, 91-98.

Stoecker, D.K., Capuzzo, J.M. (1990). Predation on protozoa: its importance to zooplankton. *Journal of Plankton Research 12*, 891-908.

Stoecker, D.K., Hansen, P.J., Caron, D.A., Mitra, A. (2017). Mixotrophy in the marine plankton. *Annual Review of Marine Science 9*, 311-335.

Stoecker, D.K., Silver, M.W., Michaels, A.E., Davis, L.H. (1988). Obligate mixotrophy in *Laboea strobila*, a ciliate which retained chloroplasts. *Marine Biology 99*, 415-423.

Stoecker, D.K., Taniguchi, A., Michaels, A.E. (1989). Abundance of autotrophic, mixotrophic and heterotrophic planktonic ciliates in shelf and slope of waters. *Marine Ecology Progress Series 50*, 241-254.

Stoecker, D.K., Thessen, A.E., Gustafson, D.E. (2008). “Windows of opportunity” for dinoflagellate blooms: Reduced microzooplankton net growth coupled to eutrophication. *Harmful Algae 8*, 158-166.

Stoecker, D.K., Tillmann, U., Graneli, E. (2006). Phagotrophy in harmful algae. In E. Graneli, J.T. Turner. (Eds.) *Ecology of Harmful Algae*. (pp. 177-187). Berlin: Springer.

Straile, D. (1997). Gross growth efficiencies of protozoan and metazoan zooplankton and their dependence on food concentration, predator-prey weight ratio, and taxonomic group. *Limnology and Oceanography 42*, 1375-1385.

Strom, S.L. (2002). Novel interactions between phytoplankton and microzooplankton: their influence on the coupling between growth and grazing rates in the sea. *Hydrobiologia 480*, 41-54.

Strom, S.L., Brainard, M.A., Holmes, J.L., Olson, M.B. (2001). Phytoplankton blooms are strongly impacted by microzooplankton grazing in coastal North Pacific waters. *Marine Biology 138*, 355-368.

Strom, S.L., Morello, T.A. (1998). Comparative growth rates and yields of ciliates and heterotrophic dinoflagellates. *Journal of Plankton Research 20*, 571-584.

Suffrian, K., Simonelli, P., Nejstgaard, J.C., Putzeys, S., Carotenuto, Y., Antia, A.N. (2008). Microzooplankton grazing and phytoplankton growth in marine mesocosms with increased CO_2 levels. *Biogeosciences 5*, 1145-1156.

Sun, J., Liu, D. (2003). Geometric models for calculating cell biovolume and surface area for phytoplankton. *Journal of Plankton Research 25*, 1331-1346.

Suzuki, K., Tsuda, A., Kiyosawa, H., Takeda, S., Nishioka, J., Saino, T., et al. (2002). Grazing impact of microzooplankton on a diatom bloom in a mesocosm as estimated by pigment-specific dilution technique. *Journal of Experimental Marina Biology and Ecology 271*, 99-120.

Tang, D., Sun, J., Zhou, L., Wang, S., Singh, R.P., Pan, G. (2019). Ecological response of phytoplankton to the oil spills in the oceans. *Geomatics, Natural Hazards and Risk 10*, 853-872.

The Federal Interagency Solutions Group, Oil Budget Calculator Science and Engineering Team. (2010). *Oil Budget Calculator - Deepwater Horizon*. Pp. 217.

The Intergovernmental Panel on Climate Change. (2018). Summary for policymakers. In V. Masson-Delmotte, P. Zhai, H.O. Portner, D. Roberts, J. Skea, P.R. Shukla, et al. (Eds.) *Global Warming of 1.5°C. An IPCC Special Report on the impacts of global warming of 1.5°C above pre-industrial levels and related global greenhouse gas emission pathways, in the context of strengthening the global response to the threat of climate change, sustainable development, and efforts to eradicate poverty*.

Thompson, H., Angelova, A., Bowler, B., Jones, M., Gutierrez, T. (2017). Enhanced crude oil biodegradative potential of natural phytoplankton-associated hydrocarbonoclastic bacteria. *Environmental Microbiology 19*, 2843-2861.

Tomas, C.R. (1996). (Ed.). *Identifying Marine Diatoms and Dinoflagellates*. San Diego, CA: Academic Press, Inc. Pp. 598.

Tremaine, S.C., Mills, A.L. (1987). Tests of the critical assumption of the dilution methods for estimating bacterivory by microeukaryoties. *Applied and Environmental Microbiology 53*, 2914-2921.

Trielli, F., Amorali, A., Sifredi, F., Marchi, B., Falugi, C., Corrado, M.U.D. (2007). Effects of xenobiotic compounds on the cell activities of *Euplotes crassus*, a single-cell eukaryotic test organism for the study of the pollution of marine sediments. *Aquatic Toxicology 83*, 272-283.

Tso, S.F., Taghon, G.L. (1998). Factors affecting predation by *Cyclidium* sp. and *Euplotes* sp. on PAH-degrading and nondegrading bacteria. *Microbial Ecology 37*, 3-12.

Tso, S.F., Taghon, G.L. (2006). Protozoan grazing increases mineralization of naphthalene in marine sediment. *Microbial Ecology 51*, 460-469.

Unrein, F., Massana, R., Alonso-Saez, L., Gasol, J.M. (2007). Significant year-round effect of small mixotrophic flagellates on bacterioplankton in an oligotrophic coastal system. *Limnology and Oceanography 52*, 456-469.

Verhaar, H.J.M., van Leeuwen, C.J., Hermens, J.L.M. (1992). Classifying environmental pollutants. 1: structure-activity relationships for prediction of aquatic toxicity. *Chemosphere 25*, 471-491.

Ward, B.A., Follows, M.J. (2016). Marine mixotrophy increases trophic transfer efficiency, mean organism size, and vertical carbon flux. *The Proceedings of National Academy of Science 113*, 2958-2963.

Wickham, H. (2016). ggplot2: Elegant Graphics for Data Analysis. New York: Springer-Verlag.

Wickham, H., Averick, M., Bryan, J., Chang, W., McGowan, L.D'A., Francois, R., et al. (2019). Welcome to the Tidyverse. *The Journal of Open Source Software 4*, 1686.

Wilken, S., Huisman, J., Naus-Wiezer, S., Donk, E.V. (2013). Mixotrophic organisms become more heterotrophic with rising temperature. *Ecology Letter 16*, 225-233.

Willis, A., Chuang, A.W., Orr, P.T., Beardall, J., Burford, M.A. (2019). Subtropical freshwater phytoplankton show a greater response to increased temperature than to increased pCO_2. *Harmful Algae 90*, 101705.

Wise, J., Wise Sr., J.P. (2011). A review of the toxicity of chemical dispersants. *Review of Environmental Health 26*, 281-300.

Wolfe, M.F., Schlosser, J.A., Schwartz, G.J.B., Singaram, S., Mielbrecht, E.E., Tjeerdema, R.S., et al. (1998). Influence of dispersant on the bioavailability and trophic transfer of petroleum hydrocarbons to primary levels of a marine food chain. *Aquatic Toxicology 42*, 211-227.

Yakimov, M.M., Golyshin, P.N., Lang, S., Moore, E.R.B., Abraham W.R., Lunsdorf, H., et al. (1998). *Alcanivorax borkumensis* gen. nov., sp. nov., a new hydrocarbon-degrading and surfactant-producing marine bacterium. *International Journal of Systemic Bacteriology 48*, 339-348.

Yamada, M., Takada, H., Toyoda, K., Yoshida, A., Shibata, A., Nomura, H., et al. (2003). Study on the fate of petroleum-derived polycyclic aromatic hydrocarbons (PAHs) and the effect of chemical dispersant using an enclosed ecosystem, mesocosm. *Marine Pollution Bulletin 47*, 105-113.

Yang, Z., Zhang, L., Zhu, X., Wang, J., Montagnes, D.J.S. (2016). An evidence-based framework for predicting the impact of differing autotroph-heterotroph thermal sensitivities on consumer-prey dynamics. *The ISME Journal 10*, 1767-1778.

Zhang, L., Gu, L., Wei, Q., Zhu, X., Wang, J., Wang, X., et al. (2017). High temperature favors elimination of toxin-producing *Microcystis* and degradation of microcystins by mixotrophic *Ochromonas*. *Chemosphere 172*, 96-102.

Zubkov, M.V., Tarran, G.A. (2008). High bacterivory by the smallest phytoplankton in the North Atlantic Ocean. *Nature 455*, 224-227.

Vita

Chi Hung Tang is a graduate student in Marine Science at the University of Texas at Austin. He received a master's degree in Biology in 2014 from The Chinese University of Hong Kong before joining Dr. Edward Buskey's zooplankton ecology laboratory in January 2016. He worked as a teaching assistant for the Department of Biology in the Fall 2015 semester and for the Department of Marine Science from 2016 to 2018. He was also a research scientist in the DROPPS consortium of the Gulf of Mexico Research Initiative.

Permanent address (or email): charles_tangchihung@hotmail.com

This dissertation was typed by Chi Hung Tang